Modelling primary proteolysis in cheddar cheese in commercial cool stores

A thesis presented in partial
fulfilment of the requirements
for the degree
of master of technology in Bioprocess Engineering at
Massey University

Richard Edmonds

2000

ABSTRACT

One issue identified as a possible problem during the manufacture of cheddar cheese is the possibility of producing a non-uniform product. It was proposed that a pallet of cheese experiencing different time-temperature histories, depending on the position within the pallet, could cause the heterogeneity. This work involved the investigation of that issue.

The level of primary proteolysis observed in cheese was measured over time in cheeses of different compositions, stored at different temperatures. The remaining intact α_{s1}casein was measured using reverse phase high performance liquid chromatography. Several trends were observed during maturation. High temperatures caused a faster rate of disappearance of α_{s1}casein. The temperature relationship followed Arrhenius law. High moisture content caused a faster rate of the disappearance of α_{s1}casein. The level of rennet added to the milk during production had a directly proportional effect on the rate of the disappearance of α_{s1}casein. Salt had no observable effect in the range investigated here. From the data a kinetic model was developed that described the rate of disappearance of α_{s1}casein in terms of the temperature, the moisture content, and the level of rennet in the cheese.

The heat transfer occurring in the commercial pallet of cheese was mathematically modelled and solved numerically. The heat transfer model was then applied to produce data describing the time-temperature profile throughout a pallet of cheese for a variety of possible industrial storage conditions. The kinetic model developed was then used to predict the extent of proteolysis in each case.

It was found that there would be significantly different levels of proteolysis within a pallet of cheese that had undergone chilling. A 10% difference in the level of proteolysis between the surface and the centre was observed after chilling for 40 days. During freezing the difference in the level of proteolysis after freezing was complete ranged from 10-25%. It was found that the heterogeneity was reduced during the thawing process and that the greatest reduction in non-uniformity was observed when thawed at lower temperatures.

ACKNOWLEDGEMENTS

It has been said that the search for knowledge is like a blind man searching for a black cat in a darkened room. I thought I heard it meow, but that may have been the walls closing in. As they say however: It's *all* good. It is true also, that this project would not have been possible without the help (and patience) of a number of people.

I would therefore like to thank the following:

- Dr J.E. Bronlund, Dr L.K. Creamer, C. Honoré for their supervision and guidance
- New Zealand Dairy Research Institute, for the research monies which made this work possible and for the use of their facilities in making and analysis of the cheese.
- Dave Alger, Don Otter, and Carmen Norris, without their assistance the HPLC work would have been impossible or least very much more time consuming and unsuccessful.
- Paul Mulligan, Hamish McCook, and Kiwi Dairies for providing industrial data collection opportunities.
- Harriet Gibbs for her input and assistance in experimental work
- Vanessa Schofield for her input and assistance in experimental work and analysis in particular her work involved in the creation of figure 3.3
- Tracy Loye, for her infinite patience and assistance in a great deal of the experimental sample preparations and support throughout the project.
- Last but not least (at least for some) family and friends, they know who they are and what they did. I haven't forgotten either... so watch it.

CONTENTS

PROJECT OVERVIEW

PROTEOLYSIS OF CHEDDAR CHEESE

HEAT TRANSFER

APPENDIX

LIST OF FIGURES

LIST OF TABLES

CHAPTER 1

PROJECT OVERVIEW

1.1 BACKGROUND AND PROBLEM DEFINITION

New Zealand produced approximately 245000 tonnes of cheese in the 1997/1998 season (Johnston, Luckman, Lilley, & Smale, 1998). As it is such a large part of New Zealand industry it is important that the process is understood and optimised.

Cheese making is a dehydration concentration process. Cheese curd is produced from standardised milk by destabilising the casein micelles present in the milk causing them to aggregate and precipitate out of solution. Destabilisation is carried out by acidulation or an enzymatic reaction transforming kappa casein proteins into non-stabilising para-kappa casein. The casein gel formed is then cut and cooked causing it to release water present in the gel as "whey". This leaves behind concentrated casein and milk fat that forms cheese curd. Once the whey is drained from the curd, it is dry salted to the desired level and cheddared. The curd is left until the pH reaches approximately 5.2 and then pressed. Once pressed, the cheese is put in chillers to mature, between 2-18 months for mild to tasty cheese respectively (Fox, 1989).

During maturation one of the reactions occurring is the proteolysis of α_{s1}-casein. As the protein is broken down this changes the functional properties of the cheese. The flavour and odour also change as breakdown products of the proteolysis process begin to appear. The rate at which the maturation occurs is a function of the cheeses composition. For example the salt content effects the rate at which enzymes can work. The rate is also a function of temperature (Law et al. 1979). In some applications the functional properties of the cheese are important. (e.g. processed cheese). As an ingredient some of the cheese used is required to have a low level of α_{s1}-casein breakdown in order to provide the desired functionality.

Production of cheese that has a low level of proteolysis is possible by manipulation of those factors that effect the rate of proteolysis. That is; adjusting the composition or temperature at which the cheese is stored. In addition to this, when

cheese is made it is packed into $\cong 1m^3$ pallets and then chilled or frozen. This leads to the possibility of non-homogeneous time-temperature histories depending on the position in the pallet. It is not known whether this could cause a significantly non-homogeneous product in terms of the level of proteolysis or functionality.

The challenge therefore is twofold. Firstly, to determine a method that can be used to estimate the ripeness of cheese given different compositions and chilling regimes. Secondly, characterise the extent of and offer possible solutions to the problem of a non-uniform cheddar cheese after storage.

1.2 PROJECT OBJECTIVES

The solution to the problem outlined above is the development of a method to control the rate of proteolysis in cheddar cheese. This requires the understanding of a number of things including:

- The cheese composition. The influence of cheese composition and how this may effect the cheese and its ripening properties. (i.e. the aim of this work is to determine the impact of salt, rennet, and moisture on rate of proteolysis in the early stages of proteolysis).
- Low temperature during the early stages of proteolysis. This includes an understanding of the effects of low temperatures and freezing on the rate of proteolysis. This understanding would allow prediction of the level of proteolysis for any given cheese under any given time-temperature profile and would allow for the prediction of maximum storage times for these cheeses in terms of the amount of remaining intact α_{s1}-casein.
- The extent of the heterogeneity of the level of proteolysis throughout a pallet of cheese caused by variations in the temperature time history. This can be achieved through modelling the heat transfer through a pallet of cheese and combining this with the understanding of the rate of proteolysis.

1.2.1 SPECIFIC OBJECTIVES

To achieve the understanding outlined above the following objectives were proposed.

1) Experimentally measure the rate of proteolysis in cheddar cheese by measuring the rate of disappearance of α_{s1}-casein with time. The reaction rate was to be described mathematically in terms of temperature and composition. This work has been covered in chapter 2.

2) To collect data on the thermophysical properties of cheddar cheese in the chilling and freezing range 15°C to -40°C. The results of this investigation are given in chapter 3.

3) To construct and validate a mathematical model to predict the time temperature relationship with position in a pallet of cheese undergoing chilling or freezing. This would use the thermophysical properties described in chapter 3. The formulation and testing of that model is presented in chapter 4.

4) To combine the chilling/freezing model for a pallet of cheese produced in chapter 4 with the proteolysis work carried out in chapter 2. This was to allow the prediction of positional variability of the level of primary proteolysis in a pallet of commercial cheese and identification of possible ways to control this variability. This work is outlined in chapter 5.

CHAPTER 2

PROTEOLYSIS OF CHEDDAR CHEESE

2.1 INTRODUCTION

This chapter describes the current literature on the cheese making process and how it effects the product. Since proteolysis is a major flavour and texture development process in cheese making (Fox, 1989), it is important that all the processing factors, which effect it, are understood. Processing parameters that effect the proteolysis in cheese curd and final product include; fat/protein ratio standardisation, starter used, adjunct cultures used, rennet addition, set temperature, cut time, knife-cut size, cook temperature, run pH, cheddaring, mill pH, and salt addition (Fox, 1989; Grappin et al., 1985; O'Keeffe et al., 1976).

In general only a few factors effect proteolysis directly and most processing parameters effect proteolysis indirectly through these factors.

2.2 PROTEOLYSIS

2.2.1 PROTEOLYSIS AS AN INDICATOR OF RIPENESS

It is generally accepted that the major components of flavour and texture development in cheese are due to the proteolysis reactions which occur during maturation (Fox, 1989). During maturation the degree of ripening can be directly related to the level of proteolysis (Aston et al., 1983). Methods have been developed to correlate ripeness with the level of proteolysis in order to assess ripeness of cheddar type cheeses (Pham & Naki, 1984; Santa-Maria & Ramos, 1986). From this work it can be concluded that a model, which determines the level of proteolysis, could indicate the level of maturity. Unfortunately, the proteolysis process is complex. It involves the breakdown of the different proteins into large fragments, which can be further hydrolysed themselves, producing a multitude of different protein fragments each providing different flavour aspects to the cheese. Work has been carried out to some extent on correlation's between ripeness, age, taste, texture, and quality in general with respect to time and temperature factors (Bouzas et al., 1993). The level of ripening will

also be affected by process paramenters such as pH, moisture content, temperature, salt content, enzyme activity, and protein aggregation (Kelly et al., 1996).

To estimate the ripening of cheese, as a function of these parameters there is a need for a general model including all these factors. (Bouzas et al., 1993) produced a model of ripening and quality with respect to some of these parameters, however their investigations involved "normal" temperatures during maturation and the temperature range did not extend as low as some maturation temperatures used in industry. In addition to this, the models prepared cannot be extended to include temperatures below –5°C as freeze effects may become important.

2.2.2 TYPES OF PROTEOLYSIS

During the production of cheese, proteins from milk are aggregated into a curd, which constitutes the bulk of the final cheese. Proteins in the curd include: αs_1-casein, αs_2-casein, β-casein, and κ-casein. During the ripening of cheese these proteins are broken down into smaller proteins and finally into peptides and amino acids. The initial breakdown of the major proteins into smaller fractions is known as primary proteolysis (Fox, 1989). It is this stage of proteolysis that influences the texture of cheese.

The second stage or "secondary" proteolysis is where smaller proteins are broken down into peptides and amino acids. These reactions are partially responsible for the flavour development in cheese along with lipolysis and glycolysis. Flavour development is a complex process during which a large number of different compounds are produced and consumed (Bouzas, 1993). In terms of the production of cheese and its initial storage, the important parameter of ripeness is primary proteolysis. In particular the breakdown of α_{s1}casein has been correlated with textural changes in cheese (Hynes *et al.* 1999, Otte *et al.* 1996, Fox 1989). Therefore the investigation of primary proteolysis depends only on measuring the decay of those large initial proteins. Due to this simplification the measurement and analysis of primary proteolysis by measuring the level of α_{s1}casein is a feasible method of following the functional properties of cheeses in the initial stages of maturation.

2.2.3 MOISTURE CONTENT

One of the main factors that effect proteolysis is moisture content (Kelly et al., 1996). It has been observed that softer cheeses (higher moisture content) have faster rate of proteolysis (Folkertsma et al., 1996). This is possibly due to the availability of enzymes and proteins in the system and their relative mobility at different moisture contents. Some of the factors, which effect proteolysis, have an indirect effect through an alteration in moisture content or effective moisture content (McSweeney et al., 1993). The moisture content of the cheese resulting from the cheddar process is influenced by the method of coagulation. The cheese curd is first formed by the destabilisation of protein micelles once about 85% of the kappa casein present have been hydrolysed (McSweeney et al., 1993). The gel that forms contains all the water present from the milk. The gel network continues to develop over time. At some point during the cheese making process the milk gel is cut and cooked. When the gel is disturbed it begins to synerese. Syneresis is the process by which the cheese curd shrinks and expels liquid in the form of whey

(Johnston, 1987) lists some factors that effect syneresis:

- Cutting the curd finely. A fine cut produces smaller pieces of curd and therefore promotes syneresis. A thick cut will produce larger pieces of curd which would retard syneresis.
- pH, the lower the pH the greater the extent of syneresis.
- Calcium ions are required to be present for the coagulation process to proceed and help strengthen the curd and promote syneresis.
- The higher the cooking temperature the higher the level of syneresis.
- Protein to fat ratio; the greater the proportion of protein to fat, the greater the syneresis except at high protein levels where the gel is too firm.

It appears that there is a general qualitative understanding about the processing parameters affect on moisture content in cheese. Quantitative predictions can be made if the machinery in use is known (Johnston et al., 1998). The understanding of the effect of moisture content on proteolysis is limited to a qualitative understanding. That is, that higher moisture content leads to a more rapid rate of proteolysis and ripening.

Since the fat content would be expected to be inert in terms of the proteolysis reaction it should be noted that for the purpose of this investigation the value of the moisture content (x_w) is not considered to be as important as the weight percentage of moisture in non-fatty substance or MNFS.

2.2.4 STARTER USED

The purpose of the starter culture is to lower the pH, which aids in coagulation as described above. In addition to being an acidulant, the starter also has a part to play in the proteolysis of ripening. (O'Keeffe et al., 1976) showed that primary proteolysis is carried out predominantly by rennet but that the starter used contributes to the secondary breakdown of proteins and therefore the final make-up of peptides and amino acids that are produced. Although not directly responsible for the rate of primary proteolysis (apart from its acidification affect) the starter contributes to the final flavour of the cheese. They also propose that this applies to externally introduced flora (non-starter bacteria) which would include adjunct cultures. (Law et al., 1979) suggest that starter cultures should be selected such that the growth is restricted to coagulation of the curd and that their presence in the cheese in high numbers is detrimental to the flavour of the final cheese. They also suggest that in small numbers starter bacteria have only a small and passive effect on the flavour development in cheddar type cheeses.

2.2.5 RENNET AND ENZYMATIC PROTEOLYSIS

O'Keefe *et al.,* (1976) describe the three proteolytic agents in cheddar cheese. They are:

- Milk coagulants such as rennet (chymosin)
- Bacterial enzymes (Starter and non-starter bacteria)
- Indigenous milk proteases such as plasmin.

In a study on the proteolysis of cheese O'Keefe *et al* (1976) found that proteolysis, in particular primary proteolysis, was due to the action of rennet. They also found that the action of rennet alone did not impart all the flavours of cheddar cheese. The study showed that rennet does not fully degrade proteins to all the peptides and amino acids, which give cheddar its flavour, and these need to be produced through the action of bacteria in the cheese. This study, therefore, upholds the work discussed above with respect to bacteria providing only flavour components typical of cheddar cheese.

2.2.6 SALT CONTENT

Salt can be added either directly in dry form to the curd or alternatively by immersion in brine. Industry in New Zealand generally adds dry salt to the curd. The effect of salt on the ripening of cheese is twofold. Firstly there is a simple relationship between salt content and water activity. As salt concentration is increased the resulting water activity in the cheese is reduced. The water activity has a direct effect on the growth of micro-organisms. The growth of the microflora present in cheese are restricted by low water activity. The change in ionic strength of cheese results in a change in the aggregation status of protein substrates (Kelly et al., 1996).

Secondly the salt has a direct effect on enzyme activity. The most important enzyme involved in primary proteolysis is chymosin from rennet (Kosikowski & Mistry, 1997). (Kelly et al., 1996) found that primary proteolysis was inversely affected by salt concentration. They found that α_{s1}-casein proteolysis was slowed, and suggested that this effect was caused by the higher ionic strength. They also suggest that the inhibitory action of salt on chymosin breakdown of β-casein that was observed is caused by aggregation of the β-casein. This aggregation results in cleavage sites becoming inaccessible. In terms of break down products changing the salt content also changes the primary breakdown products, presumably because one cleavage site has a reduced availability while another's is increased (Kelly et al., 1996).

2.2.7 pH

Mulvihill and Fox (1977,1979) showed that while different proteolysis products can be correlated to a change in pH, this is due to the salt in moisture concentration which is associated with varying pH. (Hynes et al., 1999) found that a low pH has an effect on texture but not on proteolysis. They suggest that at low pH there is a loss of colloidal calcium and the binding capacity of the proteins decrease. This imparts a "gritty" or "crumbly" texture to the cheese. When they tested the cheeses for levels of proteolysis they found no significant difference in primary proteolysis, secondary proteolysis, nor proteolysis breakdown products.

2.2.8 TEMPERATURE

2.2.8.1 GENERAL EFFECT OF TEMPERATURE ON PROTEOLYSIS

Law *et al.,* (1979) suggest that temperature is the most important factor in determining flavour intensity. Temperature effects the growth of microflora (Folkertsma et al., 1996). This has good and bad effects. The increase in growth rate of micro-flora involved in normal ripening (12°C), increases the general rate of ripening, thereby reducing storage time and capital costs. However the drawback of increased bacterial growth is the growth of non-starter bacteria. Some of these can cause off flavours or spoilage (Wilkinson., 1993).

Overall, Folkerstma *et al.* (1996) found that temperature has an additive effect on the ripening of cheese. Periods of high temperature correspond to periods of increased proteolysis and ripening (and vice versa, lower temperatures reducing the rate of proteolysis and ripening). In addition to this they found that higher temperatures also gave rise to different products of proteolysis, presumably due to the proteolytic action of alternative micro-organisms, which would have different affinities to protein binding sites. Secondly, temperature effects the enzymatic proteolysis reaction itself. In terms of quality, high temperature ripening (up to 16°C) produces higher grade cheese in the short term but after extended ripening the quality of flavour and especially texture decreases (Folkertsma et al., 1996).

2.2.8.2 THE EFFECT OF FREEZE CONCENTRATION

The reaction rate of a system below its initial freezing point depends on the extent of freeze concentration and the system temperature. The increase in concentration due to freezing will increase the rate of reaction for systems of order greater than zero. The drop in temperature, which drives the freezing process, will also decrease the reaction rate. Many real systems exhibit an increase in rate below freezing or at least a reduction in the rate of decline of reaction rate as the temperature falls. In the case of enzyme reactions the reaction rate is unlikely to be enhanced for non-cellular systems (Fennema, 1975). In the specific case of enzymatic degradation of casein the reaction exhibits only a decrease in rate (Fennema, 1975). This may be in part due to the depressing effects of salt concentration on the reaction out-weighing the freeze induced increase in enzyme concentration.

2.3 LITERATURE CONCLUSIONS

It can be seen from the review that some work has been carried out on the ripening of cheese under different process parameters and chilling conditions. The mechanism of proteolysis appears well understood. Each of the parameters, which show an effect on proteolysis, has been investigated. However it is apparent that these data need to be combined into an overall model of the process. To achieve the objective of producing a reliable mathematical model explaining the relationship between thermophysical properties of cheddar cheese and process parameters, a study needs to be undertaken that looks at all the important effects and combines them into a coherent model. This has been carried out up to a point in terms of temperature, salt and moisture (Bouzas et al., 1993). This work lacked investigation of a range of all the important process parameters. The temperature range did not include low or sub-freezing temperatures. Nor did the work include the effect of rennet level, which has been identified as a major contributor to primary proteolysis. It is suggested that different levels of the parameters: salt content (salt-in-moisture), moisture content, and rennet addition be added to a time-temperature investigation.

To achieve the objective of determining the effect of sub-freezing temperature on cheese proteolysis it will be necessary to investigate this directly. Some work has been done which generally states how reactions change under freezing conditions. In some cases quantitative equations are available (Miyawaki et al., 1998). It is known that lower temperatures reduce reaction rates, and the concentration due to freezing can cause an increase in reaction rate. However it was found that in the case of cheese ripening there is unlikely to be any noticeable effect. It is suggested that low and sub freezing temperature conditions be added to the investigation.

In order to determine the relationship between the important parameters a full factorial experiment is proposed where each of the parameters (moisture, salt in moisture, and rennet addition) are adjusted to at least two different levels and the rates of proteolysis compared. In addition to the processing parameters investigated the temperature can be investigated by taking each cheese produced above and subdividing them into different temperature-maturation conditions. From this the relationship of proteolysis with temperature can be included in the final analysis.

To achieve cheeses with varied compositions a number of things can be implemented as outlined above. Including:

For moisture content; Curd cut size (smaller curd pieces result in a lower moisture content), Cooking (cooking for longer time at a higher temperature results in a lower moisture content).

For salt content: Directly adjusting the salt addition will change the resulting salt levels, although it is expected that there will be an interaction effect where the level of salt added will effect the resulting moisture content and vice versa.

For rennet: The direct manipulation of the amount of rennet added will suffice.

2.4 METHOD DEVELOPMENT

The change in the textural (functional) properties of cheese can be estimated from the measurement of the intact casein levels remaining in the cheese. These can be measured using high performance liquid chromatography (HPLC). It was considered that salt, moisture, rennet addition, and temperature were the most important controllable factors that determine the rate at which cheese ripens.

2.4.1 METHODS AND MATERIALS

Salt, moisture, and rennet levels were adjusted to two different levels and the temperature, which is considered to be the most important factor, was applied at six levels. This resulted in a factorial design of eight different cheeses being ripened at six different temperatures.

These eight different cheeses were made with an additional four replicates. This produced in all 12 cheeses at 6 temperatures for a total of 72 samples. Where:

		Levels			Target Levels		
Treatment	Vat no.	moisture	rennet	salt/moisture	moisture wt%	rennet added	salt/moisture wt%
ABC	1	+1	+1	+1	37%	12 [ml/100l]	5.95%
abc	2	-1	-1	-1	33%	4.6 [ml/100l]	4.85%
aBC	3	-1	+1	+1	33%	12 [ml/100l]	5.95%
aBc	4	-1	+1	-1	33%	12 [ml/100l]	4.85%

ABC	5	+1	+1	+1	37%	12 [ml/100l]	5.95%
ABc	6	+1	+1	-1	37%	12 [ml/100l]	4.85%
Abc	7	+1	-1	-1	37%	4.6 [ml/100l]	4.85%
abc	8	-1	-1	-1	33%	4.6 [ml/100l]	4.85%
abc	9	-1	-1	-1	33%	4.6 [ml/100l]	4.85%
abC	10	-1	-1	+1	33%	4.6 [ml/100l]	5.95%
AbC	11	+1	-1	+1	37%	4.6 [ml/100l]	5.95%
ABC	12	+1	+1	+1	37%	12 [ml/100l]	5.95%

Table 2-1 Experimental design table

2.4.1.1 CHEESE MAKING METHOD

400 liter vats were filled with standardised milk and the appropriate amounts of starter and rennet were added. The starter was a cremoris triplet (2374/2340/2338) added at 1.5% for the low moisture cheeses and 2.5% for the high moisture cheeses. The rennet added was 4.6ml/100l for the low rennet cheeses and 12ml/100l for the high rennet cheeses. The curd was then set for 60 minutes at 32°C. The set curd was then cut to maximise or minimise the moisture content of the resulting cheese. A knife cut size of 9mm was used for low moisture cheeses and 12mm for high moisture cheeses. The curd was then cooked at 39°C for low moisture cheeses and 37°C for high moisture cheeses and mixed until the pH reached 6.2 . The whey was then drained from the curd and the curd was milled and salt was added; 32g/kg for high salt, 22g/kg for low salt. Finally the curds were pressed into approximately 20 kg blocks and left to set overnight at room temperature.

Each of the cheeses produced were tested for the characteristic properties, including moisture content, fat content, salt content, and total protein. A full table of all the results can be seen in the appendix section 7.1. Interactions during the production process mean that the resulting composition did not match exactly to the targets discussed above. In addition to this the level of residual rennet in the resulting cheese will also be a function of the cheese composition. For the purposes of analysis it is important that the level of rennet used is an accurate representation of the rennet present.

Rennet is soluble in water, and when whey is drained from the cheese it is expected that most of the rennet would be lost in this stream. The rennet would be expected to have the same concentration in the remaining moisture as was in the initial

water portion of the milk. Therefore the concentration calculated above can be normalised against the moisture content of the resulting cheese to provide an appropriate estimate of the residual rennet in the cheese. Finally the fat, which would be inert in terms of the proteolysis reaction, would alter the relative concentration of rennet in the cheese. As a truer representation of the available rennet, the rennet concentration can be normalised against the weight percent of remaining non fatty substance. This procedure outlined above has been carried out for this study. The procedure is summarised in Equation 2-1 below.

$$[\text{rennet}] = \frac{\text{rennet added(ml/100l)}}{(1 - \text{wt\%solids in milk})} \cdot \frac{\text{wt\%moisture in cheese}}{(1 - \text{wt\%fat})}$$

Equation 2-1

Since the milk used in this experiment was standardised and from the same batch it was not required to be normalised against the level of milk solids present. The equation that was used in this investigation to calculate the normalised rennet concentration, which was used in the proceeding data analysis, in given below:

$$[\text{rennet(normalised)}] = \frac{\text{rennet added(ml/100l)}}{} \cdot \frac{\text{wt\%moisture in cheese}}{(1 - \text{wt\%fat})}$$

Equation 2-2

The resulting levels of moisture in non fat substance (MNFS), salt/moisture in non fat substance and [rennet (normalised)] for each cheese produced is given below.

Final measured result				
Treatment	Vat no.	MNFS wt. fraction	Rennet (normalised)	salt/MNFS wt%
ABC	1	0.571	10.4	4.9%
abc	2	0.544	3.5	4.5%
aBC	3	0.561	9.7	5.6%
aBc	4	0.573	10.0	3.7%
ABC	5	0.571	10.4	4.9%
ABc	6	0.579	10.0	3.7%
Abc	7	0.573	3.8	3.6%
abc	8	0.544	3.5	4.5%
abc	9	0.551	3.5	4.4%
abC	10	0.524	3.3	6.5%
AbC	11	0.534	3.4	6.5%
ABC	12	0.576	9.9	4.1%

Table 2-2 Experimental design result levels

The day after manufacture, each cheese was cut into 500g sampling blocks, vacuum packed and placed in chillers or freezers at the appropriate temperature. The final cheese being divided equally amongst 6 different temperatures; -18, -10, -2, 2, 10, and 15 °C.

2.4.1.2 SAMPLING

One sample was taken from each cheese produced at each temperature every two weeks. The three warmer chillers (2, 10, 15 [°C]) were sampled on odd weeks and the three cooler chillers were sampled on even weeks. So each fortnight, one vacuum sealed block was taken for each cheese from each temperature chiller to make a total of 36 samples.

Each 500g block was opened with a knife and a 7mm diameter core sampling tube was used to take three core samples from each block. The first core sample was discarded to reduce the effect of cross contamination from the previous sample. The second sample was extracted and tested on the same day, using the extraction method outlined below. The sample measured here was subject to uncertainty due to deviations in the level of extraction, protein solubilisation, and mobile phase concentration between HPLC runs on the day. To reduce this uncertainty the third sample was placed in a labelled glass ¼ ounce bijou bottle and frozen in a –70°C freezer to quench the proteolysis reaction.

Due to availability of an auto-sampling HPLC the extraction and protein determination process carried out on the third sample was delayed until all the samples over a period of seven months had been collected. Then all of the samples collected for each of the twelve cheeses were tested at the same time; one cheese per HPLC run, a total of 60 samples per run. This reduced the uncertainties caused by deviations in the level of extraction, protein solubilisation, and mobile phase concentration between HPLC runs on the day.

Each 10g sample was thawed to room temperature and a $\cong 0.1$g slice was removed, weighed, placed in a labelled 1.5 ml graduated micro-centrifuge tube and tested for the level of remaining casein using the procedure outlined below.

2.4.1.3 EXTRACTION AND HPLC ANALYSIS

In order to quantitatively determine the casein level in each sample, the casein was extracted from 0.1g samples and measured using reverse phase HPLC. Each 0.1g sample was dissolved in a sample buffer of 0.1M tris buffer, 5mM sodium citrate, 8M urea, and 10% v/v β-mercaptoäthanol. After resting in a hot water bath for an hour the samples were centrifuged at 10000 rpm for 5 minutes. The fat was skimmed off the top and 0.1ml of the clear supernatant was taken and diluted in 0.9ml of dilution buffer. The dilution buffer was 8M Urea in 32% v/v acetonitrile. The 1ml HPLC preparation sample was transferred to a 1.5ml HPLC auto sampler vial. The HPLC program is given below.

	Time [min]	Flow [ml/min]	%A	%B	%C	Curve
1	0.01	1	65	35	0	6
2	22	1	51	49	0	6
3	24	1	51	49	0	6
4	25	1	0	100	0	6
5	28	1	0	100	0	6
6	29	1	65	35	0	6
7	36	1	65	35	0	6

Table 2-3 HPLC program

The HPLC program was carried out using a reverse phase jupiter 5μ C18 300A Phenomenex column with the two mobile phases being:

phase A: 94.9% Water, 5%Acetonitrile, 0.1% Tri-fluoro-acetic acid
phase B: 4.9% Water, 95%Acetonitrile, 0.1% Tri-fluoro-acetic acid

Curve 6 denotes a linear concentration gradient between time steps. Detection was carried out at 220 nm using a Waters UV detector.

2.4.2 CHROMATOGRAM RESULT

A typical HPLC chromatogram for a typical medium aged cheese (70 days) is shown below:

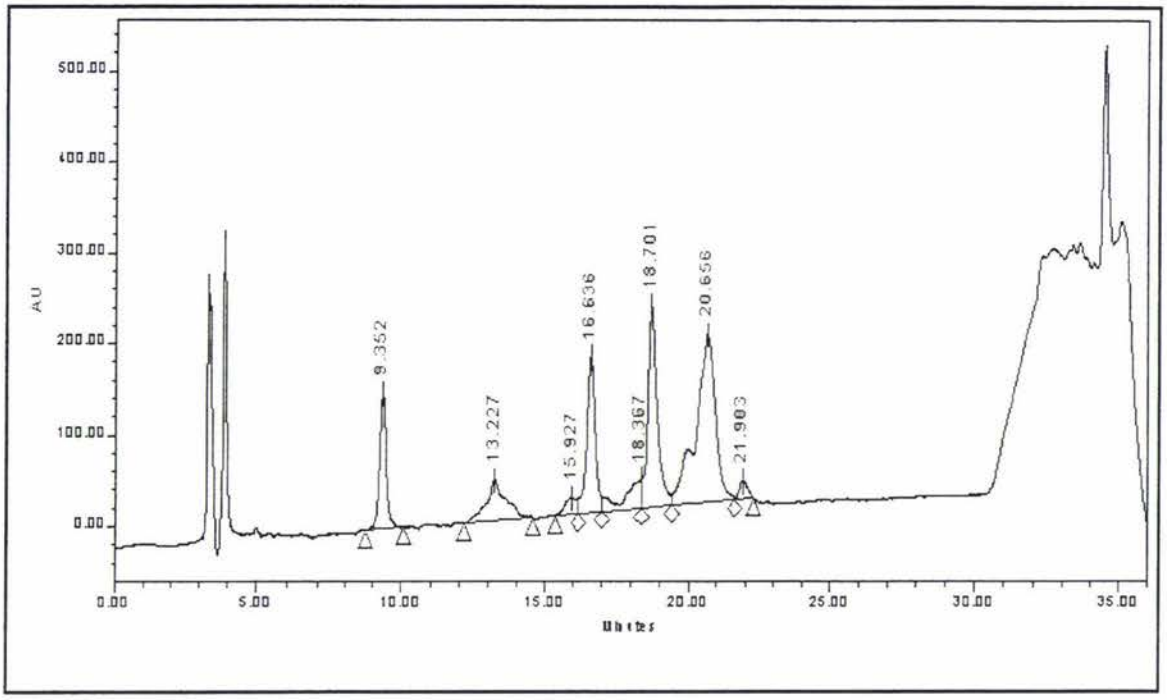

Figure 2.1 Typical chromatogram

Each peak represents one type of protein present in the sample. The peak areas were integrated using Millenium 32[tm] software. The complete data representing areas of each of the eight peaks marked here is extensive and has been included on the compact disk accompanying this thesis.

The level of proteolysis in cheese can be monitored by the degradation of proteins as measured by reverse phase HPLC. When a casein standard is put through the program above, the proteins present it show up as peaks 2,6,7. These peaks belong to para-$\varkappa$-casein, αs_1-casein, and β-casein. During the proteolysis of cheese proteins it is known that αs_1-casein is the first to be broken down; firstly into αs_1I-casein. αs_1I-casein is represented by peak 4. Throughout the initial part of this experiment it was observed that as peak 6 shrinks peak 4 grows. In order to quantify the level of proteolysis, each chromatogram was normalised against an unchanging factor consistent across all the chromatograms from one cheese. Para-$\varkappa$-casein remains intact well into the proteolysis of α_{s1}casein (Grappin *et al* , 1985). This could be seen in this study as it was observed to have an unchanging relative size on the chromatograms for any one cheese. As a

consequence it was decided to normalise the peak representing αs_1-casein against that of para-κ-casein.

When peak six was divided by peak two this gives an indication of the relative amount of α_{s1}-casein remaining in the sample. A table of all these values with respect to the cheese vat sampled from, the temperature at which the sample was matured, and the length of time matured for, is given in the CD ROM (see errata files) These data have also been plotted; A plot for each cheese investigated showing the casein remaining-time profile for each temperature are all given in the appendix section 7.2 Examples of the remaining casein for one high rennet cheese (vat 3) and one low rennet cheese (vat 7) are given below Figure 2.2 and Figure 2.3 respectively.

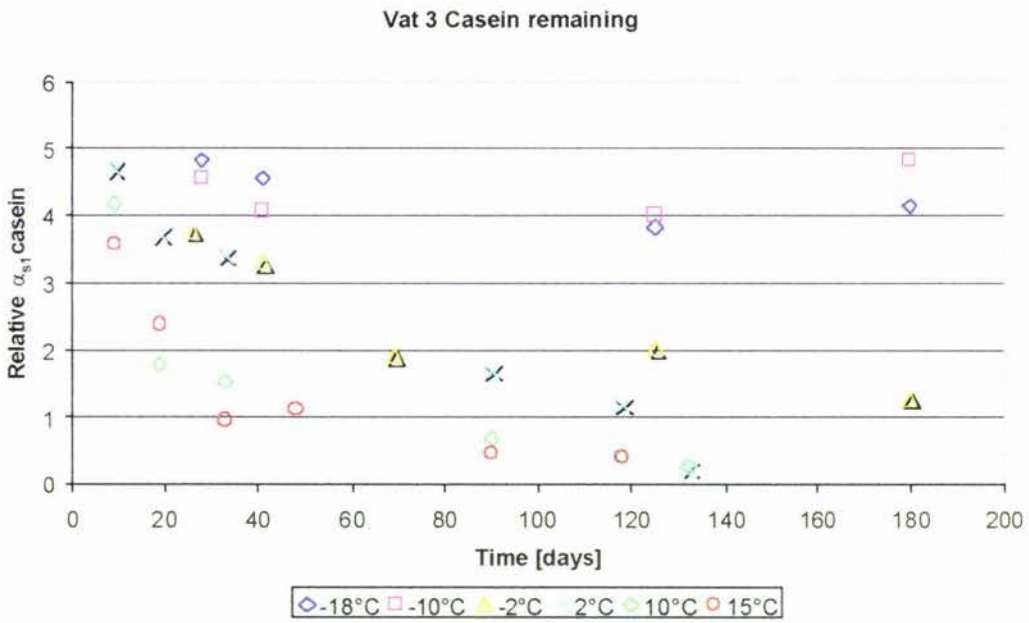

Figure 2.2 Example raw data for vat 3 (high rennet)

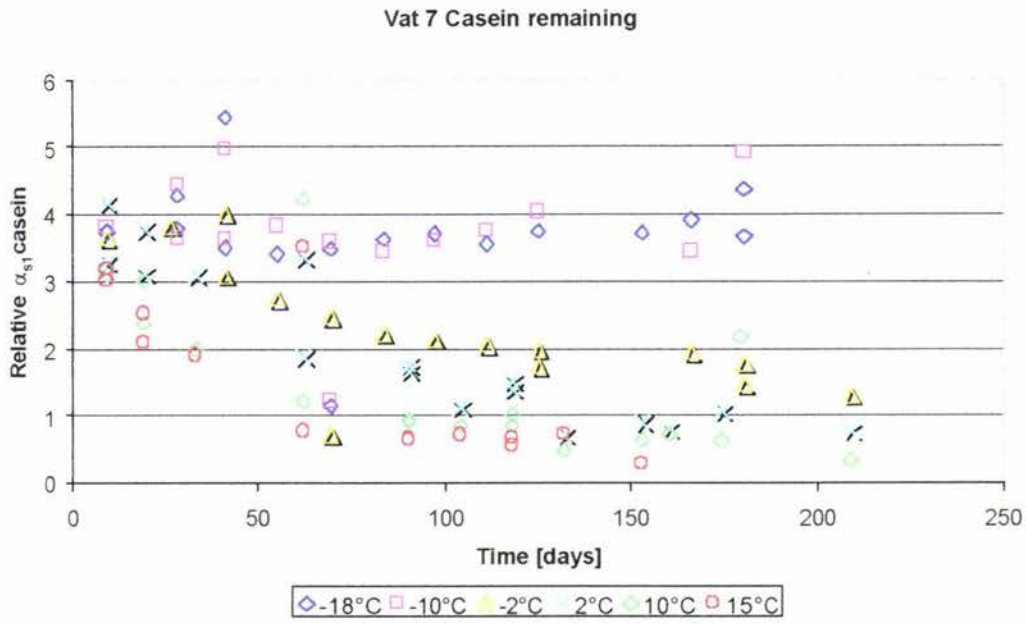

Figure 2.3 Example raw data for vat 7 (low rennet)

2.4.3 DATA DISCUSSION

It can be seen from the plots above that level of α_{s1} casein decays with time at different rates depending on the cheese and the temperature at which it is stored. There is some scatter in the data. This may be due to non-homogeneity in the cheese. Each cheese was made using a batch process that produced ≅ 40kg of cheese. Samples analysed were only 0.1g which represents only 0.00025% of the total cheese produced. In spite of the observed uncertainty in the level of proteolysis, some trends are clearly evident at this stage of maturation. Cheeses stored in temperatures in the frozen range do not appear to have experienced any significant proteolysis over the period of analysis. Cheeses stored at the higher temperatures have considerable degradation of α_{s1} casein over the 200 days investigated. In order to investigate the effects of composition and temperature on proteolysis, a further investigation of the reaction kinetics of the proteolysis process was carried out.

2.4.4 KINETIC DISCUSSION

If 1st order kinetics apply, the rate equation for the proteolysis of α_{s1} casein is given below:

$$-\frac{dC}{dt} = kC$$

Equation 2-3

Solving the rate equation gives:

$$\ln\left(\frac{C}{C_0}\right) = -kt$$

Equation 2-4

Therefore a plot of the natural log of the ratio of measured intact α_s-casein to initial intact α_s-casein vs time [days] should give a straight line of slope –k [days^{-1}]. These plots for all the cheeses studied are available in appendix section 7.2. The two examples from above (Vat 3-low rennet and vat 7-high rennet) have been displayed below in Figure 2.4 and Figure 2.5.

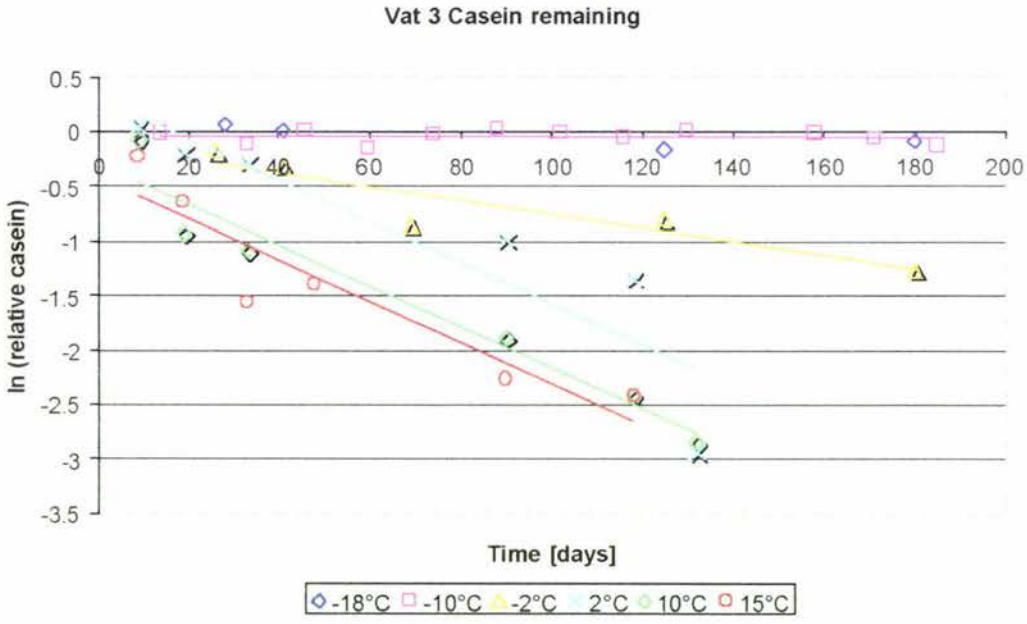

Figure 2.4 Example log plot vat 3 (high rennet)

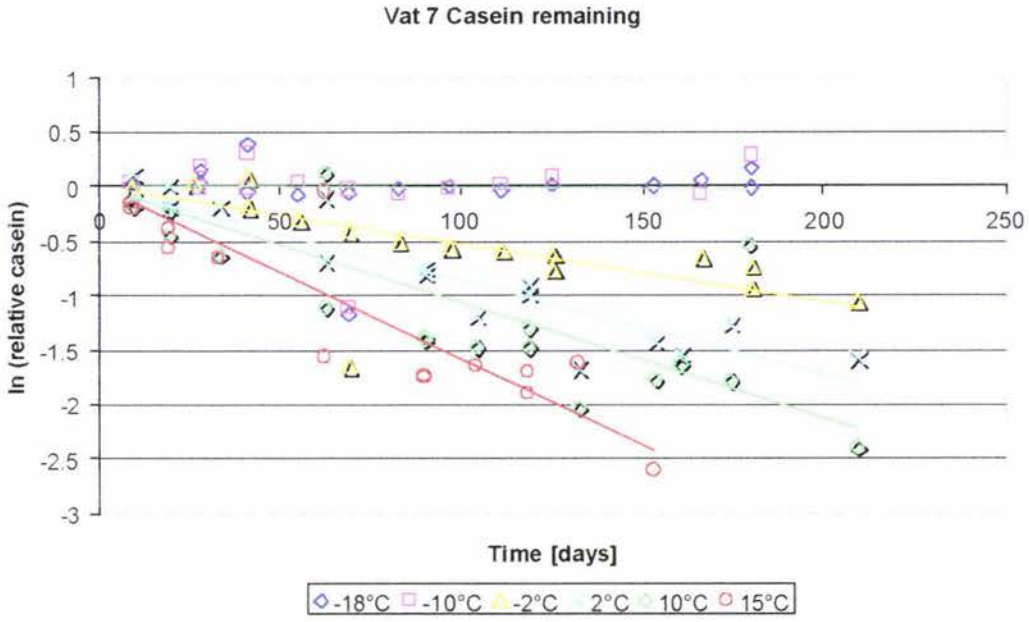

Figure 2.5 Example log plot vat 7 (low rennet)

It can be seen from these plots that the proteolysis of α_{s1} casein reaction, despite it's biochemical complexity, can be approximated with first order decay. When the level of uncertainty in the results, particularly at higher temperatures is considered it is clear that applying first order kinetics will suffice. There is no point in applying more complex systems for the removal of α_{s1} casein. The simple first order case will explain the results as well as any more advanced model. Although the data are not "perfect" it can be seen that these plots can give overall trend on the rate of proteolysis and how temperature and composition effect that rate.

The 1st order rate constants resulting from the regression of the experimental data have been tabulated below in Table 2-4 for all cheese-temperature combinations.

	Rate constant [days^{-1}] at Temperature given below					
Vat No.	-18 [°C]	-10 [°C]	-2 [°C]	2 [°C]	10 [°C]	15 [°C]
1	0.00010	0.00031	0.00600	0.01496	0.01774	0.03949
2	0.00015	0.00037	0.00232	0.00427	0.00885	0.01183
3	0.00066	0.00014	0.00734	0.01576	0.02155	0.02401
4	0.00022	0.00089	0.00866	0.01801	0.02281	0.02700
5	0.00052	0.00073	0.01189	0.01978	0.01403	0.01902
6	0.00052	0.00022	0.01093	0.01704	0.01486	0.01692
7	0.00021	0.00015	0.00526	0.00862	0.01065	0.01579
8	0.00061	0.00048	0.00330	0.00299	0.01873	0.01958
9	0.00033	0.00015	0.00244	0.00483	0.01021	0.01354

10	0.00023	0.00089	0.00145	0.00561	0.00605	0.01318
11	0.00018	0.00031	0.00255	0.00735	0.01056	0.01370
12	0.00049	0.00112	0.01190	0.01595	0.01399	0.02208

Table 2-4 Summary of first order rate constant for all cheeses

2.4.4.1 DATA INTERPRETATION

2.4.4.1.1 Compositional effects on rate

The reaction rates observed for the different composition cheeses at each of the different temperatures are very different. The effect of temperature is so large it dwarfs any other effects that may be present in the complete rate-constant data set. In order to investigate the effects of composition it is possible to plot the individual rates against each of the compositional inputs for any one temperature. Below are three plots corresponding to each of the three important compositional inputs identified; salt in Figure 2.6, moisture in Figure 2.7, and rennet in Figure 2.8. Each from the -2°C data set.

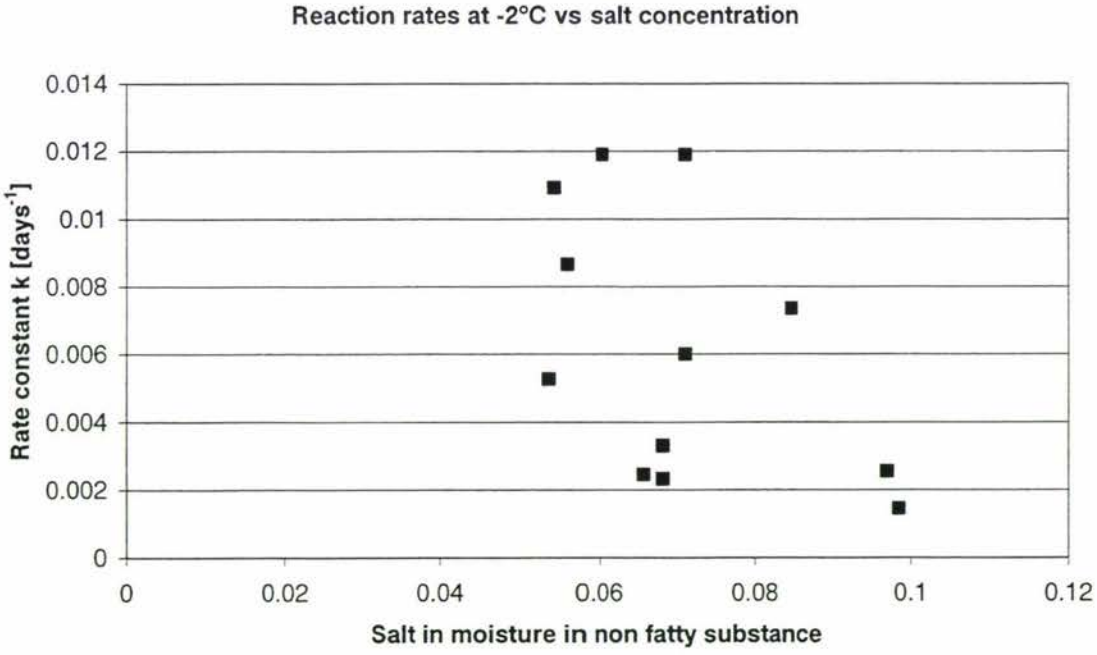

Figure 2.6 First order reaction rates at -2°C vs salt

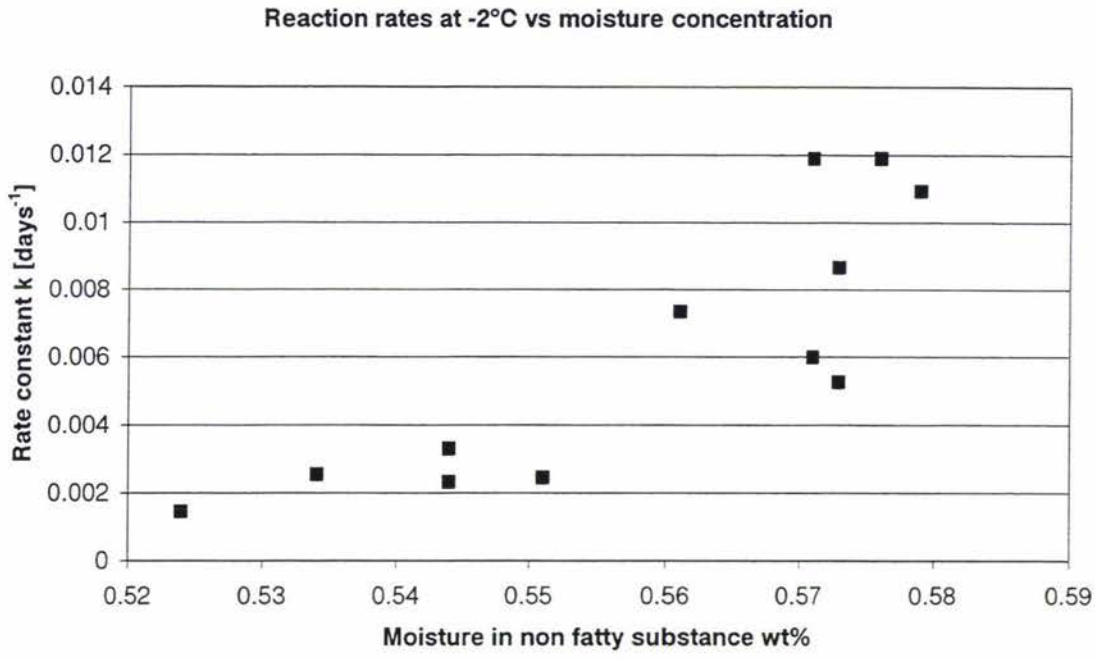

Figure 2.7 First order reaction rates at -2°C vs moisture

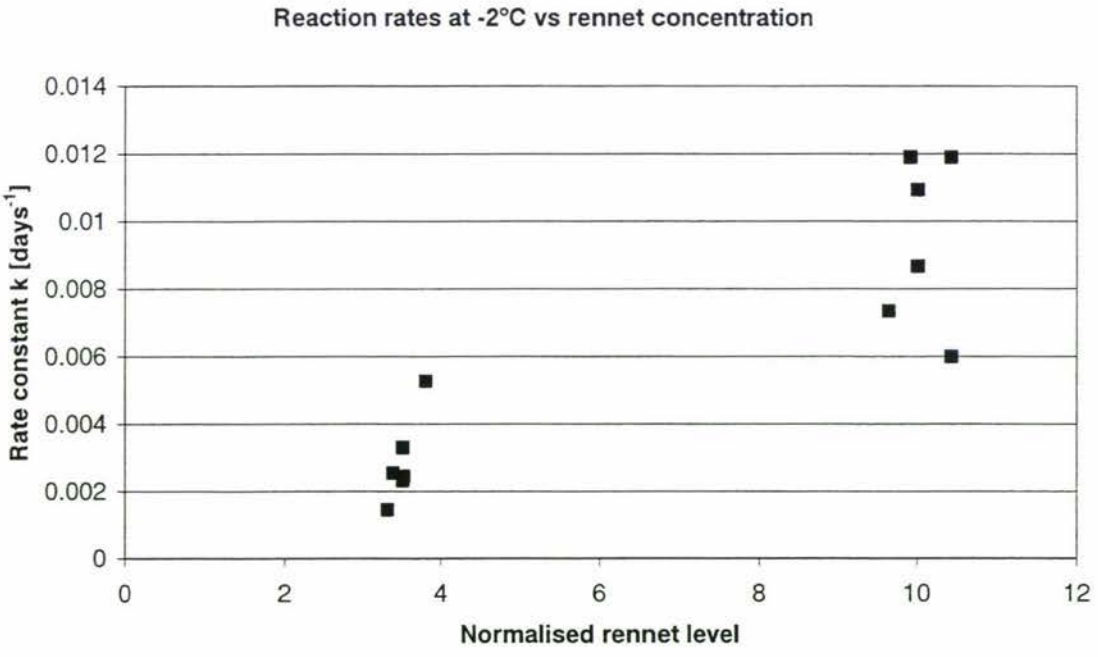

Figure 2.8 First order reaction rates at -2°C vs rennet

It can be seen from these graphs that there is a definite relationship between the level of rennet in the cheese and the reaction rate of primary proteolysis. Although only two levels of rennet were used, it appears as though there is an approximately linear

relationship between the rennet level and the rate constant. It would be expected that for an enzyme catalysed reaction, the reaction rate constant would be proportional to the enzyme concentration.

It can be seen from these graphs that the trends, which would be expected for moisture and salt, are difficult to observe in the experimental range investigated here. This may be because there is no clear relationship between the reaction rate constant and salt or moisture, or it could be because the effects are small in the range investigated here and are simply not large enough to observe in the experimental resolution of this investigation. For this reason the rate constant data was analysed statistically using the multiple regression analysis tool from the Minitab statistical package.

In order to investigate the effects of composition it is possible to regress the individual rates against each of the compositional inputs for any one temperature. This has been carried out for each of the temperatures used and is tabulated below. The significant factors are those with low p-values. The statistical outputs pertaining to the –2°C data graphed above are italicised below.

Estimated Regression Coefficients for -18 [°C]

Term	Coef	StDev	T	P
Constant	0.001796	0.007350	0.244	0.813
MNFS	-0.002695	0.012502	-0.216	0.835
rennet	0.000028	0.000044	0.630	0.546
salt/moi	-0.001852	0.009931	-0.186	0.857

S = 0.0002173 R-Sq = 11.8% R-Sq(adj) = 0.0%

Estimated Regression Coefficients for -10 [°C]

Term	Coef	StDev	T	P
Constant	0.01655	0.011629	1.424	0.192
MNFS	-0.02806	0.019782	-1.418	0.194
rennet	0.00012	0.000070	1.690	0.129
salt/moi	-0.01711	0.015713	-1.089	0.308

S = 0.0003438 R-Sq = 26.6% R-Sq(adj) = 0.0%

Estimated Regression Coefficients for -2 [°C]

Term	*Coef*	*StDev*	*T*	*P*
Constant	***-0.04431***	*0.062829*	*-0.705*	*0.501*
MNFS	***0.08273***	*0.106879*	*0.774*	*0.461*
rennet	***0.00065***	*0.000379*	*1.725*	*0.123*
salt/moi	***-0.00221***	*0.084895*	*-0.026*	*0.980*

S = 0.001858 R-Sq = 83.7% R-Sq(adj) = 77.5%

Estimated Regression Coefficients for 2 [°C]

Term	Coef	StDev	T	P
Constant	-0.1013	0.058873	-1.721	0.124
MNFS	0.1712	0.100149	1.710	0.126
rennet	0.0012	0.000355	3.360	0.010
salt/moi	0.1256	0.079550	1.579	0.153

S = 0.001741 R-Sq = 94.2% R-Sq(adj) = 92.1%

Estimated Regression Coefficients for 10 [°C]

Term	Coef	StDev	T	P
Constant	0.0962	0.151045	0.637	0.542
MNFS	-0.1466	0.256942	-0.571	0.584
rennet	0.0014	0.000911	1.551	0.160
salt/moi	-0.1378	0.204092	-0.675	0.519

S = 0.004466 R-Sq = 46.6% R-Sq(adj) = 26.5%

Estimated Regression Coefficients for 15 [°C]

Term	Coef	StDev	T	P
Constant	0.004761	0.222587	0.021	0.983
MNFS	0.003640	0.378643	0.010	0.993
rennet	0.001603	0.001342	1.194	0.267
salt/moi	0.028448	0.300760	0.095	0.927

S = 0.006581 R-Sq = 48.3% R-Sq(adj) = 29.0%

In general it can be seen from the above statistical data that the dependency of the rate constants on cheese composition were only significant at temperatures above –10°C. This is because the rate of reaction in these frozen systems is essentially zero. In such cases it is not surprising that the effect of composition is not noticeable. It was also evident that rennet was the most significant factor to have an observed effect within the range of compositions tested. These results do not disagree with the expected trends discussed earlier in this work section 2.2 that suggests that moisture and salt do effect proteolysis, but suggest that in the range investigated in this work the trends were difficult to observe.

2.4.4.1.2 Temperature

The largest observable trend was the dependence of reaction rate on temperature. It can also be seen from the analysis at individual temperatures above that the experimental uncertainty is quite large at the lower temperatures (-18,-10°C) and it is not possible to state that the reaction rates observed here are significant. The reaction rates occurring at higher temperatures however, are significant. This allows the application of Arrhenius law to the reaction rate constants observed and so mathematically describe the variation of the rate constant with temperature (Levenspiel, 1999). The Arrhenius law is given in Equation 2-5:

$$k = k_o e^{\left(\frac{-E}{RT}\right)}$$

Equation 2-5

where:

k	= Rate constant	[$days^{-1}$]
k_o	= Pre exponential term	[$days^{-1}$]
R	= Ideal gas constant	[$J.mol^{-1}.K^{-1}$]
E	= Activation energy	[$J.mol^{-1}$]
T	= Temperature	[K]

Linearising gives:

$$\ln(k) = \frac{-E}{R}\frac{1}{T} + \ln(k_o)$$

Equation 2-6

Continuing with the two example cheeses from above one can plot ln(k) vs reciprocal temperature [K^{-1}]. The slope is then –E/R and the intercept $\ln(k_o)$. These have been plotted below in Figure 2.9.

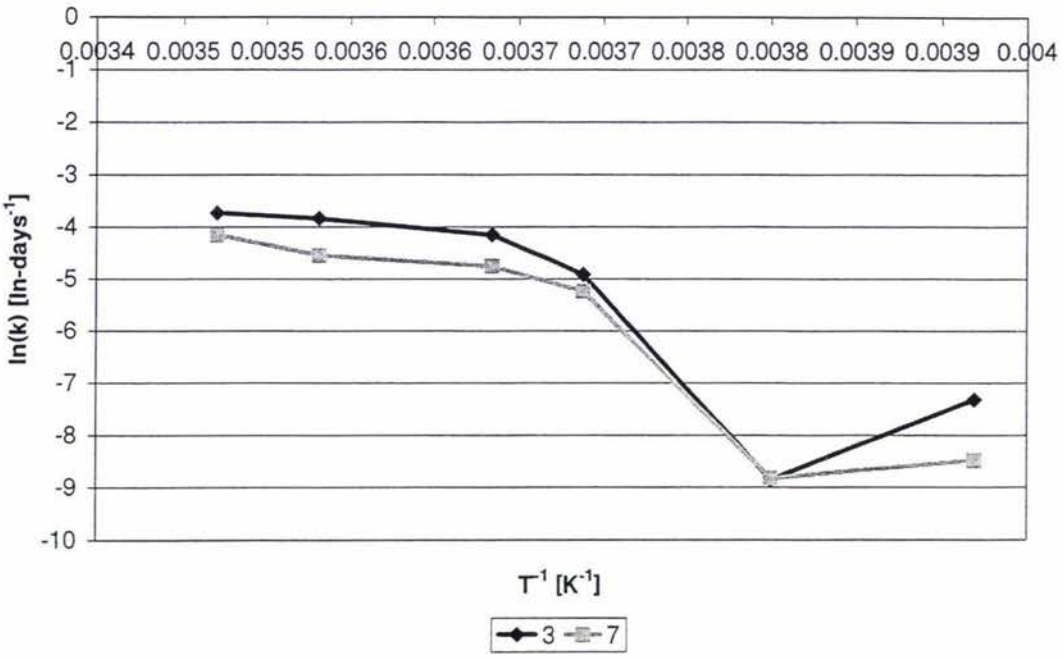

Figure 2.9 Arrhenius plots for vat 3 and vat 7

The two right hand points on the graph from each cheese represent the rate constants at the two below freezing temperatures. The rates at these temperatures can be assumed to be negligible and therefore those points can be dropped.this results in a straight line as expected. The Arrhenius data for every cheese at temperatures above freezing have been plotted below in Figure 2.10.

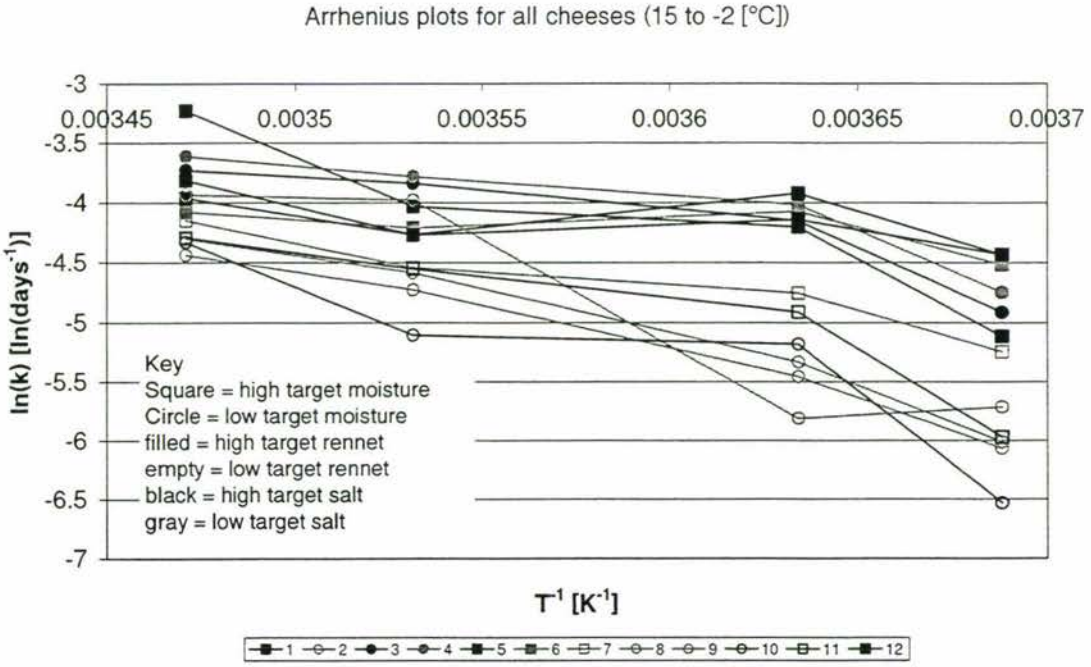

Figure 2.10 Arrhenius plot for all cheese vats (-2°C to 15°C)

Inspection of Figure 2.10 shows that these data follow Arrhenius law as indicated by a linear relationship above freezing. The high rennet cheeses (indicated by the filled symbols) are clearly separated from the low rennet cheeses (indicated by the hollow symbols). The high rennet cheeses exhibited higher reaction at each temperature as discussed above. There is, however, no discernible trend for moisture and salt evident on the plot. This is in agreement with the discussion above for cheeses stored at –2°C.

It is also clear from the graph that there is no reason to believe that there is a significant relationship between the slopes of these plots and the composition. If it is assumed that the slopes are equal then this implies that the activation energy is not a function of composition. It then follows that the Arrhenius pre-exponential term is all that is required to explain the variation in reaction rate due to composition. The data can now be analysed in terms of all factors to produce one overall model, which describes the reaction rate (and therefore the level of primary proteolysis with respect to time), in terms of all the investigated parameters; temperature, rennet, moisture, and salt.

2.4.5 MODELING THE RATE OF PROTEOLYSIS OF α_{s1}CASEIN.

In order to make predictions, which can be used to estimate the level of proteolysis in cheese at some given MNFS content, normalised rennet level, and time temperature scenario, a unified predictor equation is required. It was proposed that using the data above for MNFS content, normalised rennet level, and temperature data one single equation to predict a rate constant could be formulated.

It is assumed that the degradation of α_{s1}-casein, as an enzyme catalysed process, can be approximated by Michelis-Mentin enzyme kinetics. ie.

$$\frac{\partial[C]}{\partial[t]} = \frac{k_3[E_0][C]}{k_m + [C]}$$

Equation 2-7

In Equation 2-7[C] represents the concentration of α_{s1}casein in the cheese and [Eo] would represent the background level of available proteolytic activity. Since rennet contains enzymes responsible for the breakdown of α_{s1}-casein it would be expected that the addition of rennet would be proportionally additive to the $[E_0]$ term ie

$$\frac{\partial[C]}{\partial[t]} = \frac{k_3(k_r[R]+[E_0])[C]}{k_m+[C]}$$

Equation 2-8

Salt inhibits the breakdown of casein and since salt does not resemble protein it is reasonable to consider it as a non-competitive inhibitor. The rate equation can now be adjusted to include salt/moisture concentration.

$$\frac{\partial[C]}{\partial[t]} = \frac{k_3(k_r[R]+[E_0])[C]}{(1+k_s[s])(k_m+[C])}$$

Equation 2-9

If it were assumed that an increase in moisture content directly increases the availability of the proteolytic enzymes then the moisture content would be expected to be directly proportional to the rate of casein degradation. A term for moisture content is then simple to include.

$$\frac{\partial[C]}{\partial[t]} = \frac{k_w[m]k_3(k_r[R]+[E_0])[C]}{(1+k_s[s])(k_m+[C])}$$

Equation 2-10

Including the effect of temperature on the rate constant k_3 by applying Arrhenius law gives Equation 2-11 below:

$$\frac{\partial[C]}{\partial[t]} = \frac{k_w[m](k_r[R]+[E_0])k_{3o}e^{\left(\frac{-E}{RT}\right)}[C]}{(1+k_s[s])(k_m+[C])}$$

Equation 2-11

If [C] is smaller than k_m by a factor of 0.5 then the overall reaction rate can be approximated as a first order reaction with an over all reaction constant which is a function of moisture content, salt content, rennet addition, and temperature. It has also been observed in the analysis of data above that first order kinetics are a good description for individual reaction rates.

It has also been observed above that the rate constant is directly proportional to rennet concentration and that the rate of proteolysis at very low levels of rennet would be very low. This implies that the [Eo] term in Equation 2-11 is negligibly small and can be approximated to zero.

Since the effect of salt on the reaction rate was not found to be significant in the range of salt compositions investigated here, the salt inhibition term was removed from Equation 2-11 provided predictions are only made for cheeses made within the range of salt levels investigated here. These simplifications result in the rate relationship Equation 2-12 below.

$$\frac{\partial[C]}{\partial[t]} = k_w[m]k_r[R]k_{3o}e^{\left(\frac{-E}{RT}\right)}[C]$$

Equation 2-12

Or in terms of the extent of the proteolysis reaction

$$\frac{\partial Xc}{\partial[t]} = k_w[m]k_r[R]k_{3o}e^{\left(\frac{-E}{RT}\right)}(1-Xc)$$

Equation 2-13

By combining constants and allowing the reaction rate to be a non-linear function of composition results in the Equation 2-14 below:

$$k=k_c[MNFS]^{kw}[\text{rennet (normalised)}]^{kr}\exp(-E/(RT))$$

Equation 2-14

2.4.6 EMPIRICAL REGRESSION OF RATE RELATION

The coefficients and indices in Equation 2-14 can be found by taking the log of the equation to make the equation linear. The linearised equation (Equation 2-12)is given below:

$$\ln(k)=\ln(k_c)+k_w\ln([MNFS])+k_r\ln([\text{rennet(normalised)}]) - E/(R.T)$$

Equation 2-15

The coefficients in Equation 2-15 can be found by conducting multi-linear regression for ln(k) vs ln(MNFS), ln(rennet(normalised)), ln(salt/MNFS), and 1/T. resulting statistical output of this regression is given below:

```
ln K = 16.4 - 5540 1/T + 3.93 lnmoisture + 0.627 lnrennet

Predictor       Coef        StDev          T        P
Constant      16.441        2.727       6.03    0.000
1/T[K-1]     -5540.1        587.6      -9.43    0.000
lnmoistu       3.929        2.581       1.52    0.135
lnrennet      0.6274       0.1556       4.03    0.000

S = 0.3464      R-Sq = 79.0%      R-Sq(adj) = 77.6%

Analysis of Variance

Source        DF          SS          MS          F        P
Regression     3     19.8761      6.6254      55.23    0.000
Error         44      5.2786      0.1200
Total         47     25.1547

Source        DF       Seq SS
1/T[K-1]       1      10.6654
lnmoistu       1       7.2614
lnrennet       1       1.9493

Unusual Observations
Obs  1/T[K-1]        ln K         Fit  StDev Fit   Residual     St Resid
 10   0.00369     -6.5346     -5.7775     0.1331    -0.7571       -2.37R
 32   0.00353     -3.9776     -4.7280     0.0763     0.7504        2.22R

R denotes an observation with a large standardized residual
```

The resulting geometric relationship is then:

$$k=\exp(16)[MNFS]^{3.9}[\text{rennet (normalised)}]^{0.63}\exp(-46000/(R.T))$$

Equation 2-16

The model proposed here is suitable for use in calculating the rate constant provided that the cheese composition lies within the bounds of the composition used in this investigation. (51.1% to 57.9% MNFS, 5.4% to 9.8% salt in MNFS. The level of rennet used in this investigation ranged from 4.6ml/100l to 12ml/100l but this value was normalised against MNFS content and fat to using Equation 2-2 to give a range of : 3.3-10.4 [ml/100l milk.wt%MNFS]).

2.4.7 COMPARISON OF MODEL TO RAW DATA

In order to test the validity of this model it is required that it be tested against real cheese samples. For the purposes of testing the model produced above (Equation 2-13 and Equation 2-16) can be solved for any given time provided constant

temperature, moisture, salt, and rennet levels are maintained. The solved rate equation is given below:

$$X_c = e^{-e^{1.6}[\mathrm{MNFS}]^{3.9}[\mathrm{rennet(normalised)}]^{0.63}e^{\left(\frac{-46000}{RT}\right)}t}$$

Equation 2-17

The cheeses (vat 3 and vat 7) used as examples throughout this discussion have been used here to illustrate whether or not the model produced from these data is self-consistent. The raw data from vat 3 and vat 7 (Figure 2.2 and Figure 2.3) have been plotted along side the protein level predicted by the above model (Equation 2-17) in Figure 2.11 and Figure 2.12 below

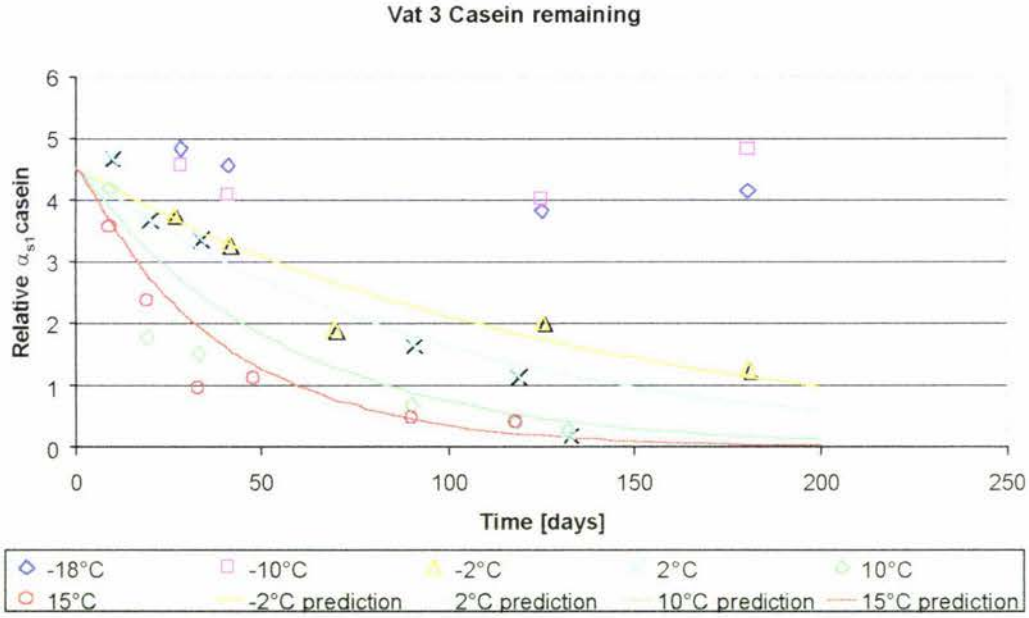

Figure 2.11 Vat 3 prediction of remaining intact α_{s1} casein

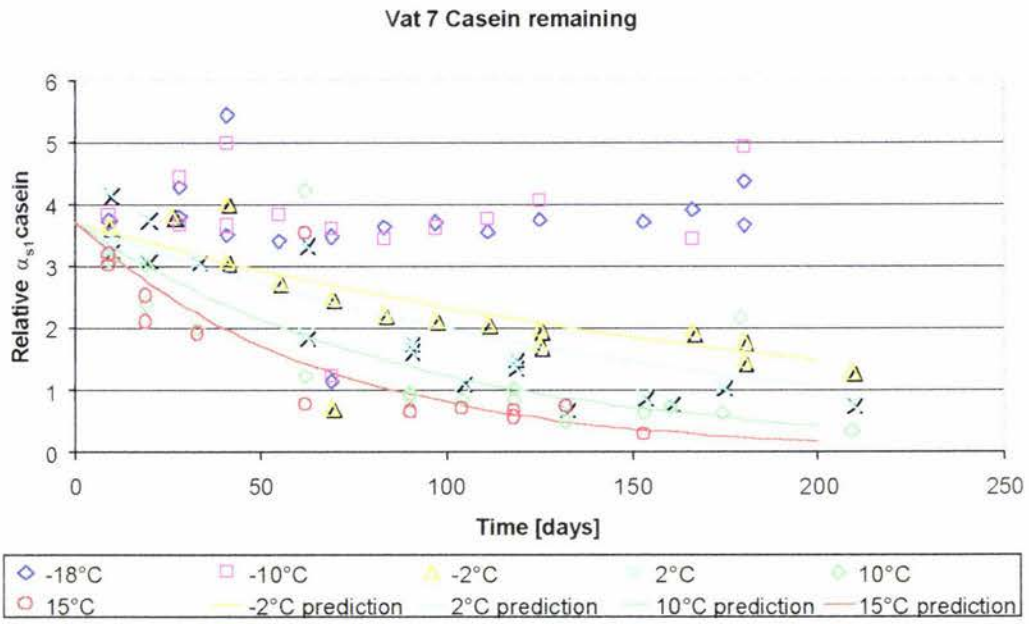

Figure 2.12 Vat 7 prediction of remaining intact α_{s1} casein

From these plots it can be seen that there is some uncertainty involved in the estimation of the level of proteolysis in cheese. The model does however give a good indication of the level of primary proteolysis occurring and the model follows the trends observed. It would be reasonable therefore to use this model for predictive purposes provided that the cheeses used are within the compositional range investigated in this work and that the results gained be viewed in light of the uncertainty observed.

2.5 PROTEOLYSIS CONCLUSIONS

Important factors determining the rate of proteolysis in cheddar cheese were identified as temperature, rennet, moisture, and salt. An experiment was designed to investigate the influence of these factors on the rate of disappearance of α_{s1} casein. A number of cheeses were produced with different levels of those factors listed above. Each cheese produced was divided among six temperature levels. The level of α_{s1} casein was measured in each cheese at each temperature over time using a reverse phase HPLC. Trends observed in the resulting data included a positive influence of temperature on the rate of disappearance of α_{s1} casein and a positive influence of rennet on the rate of disappearance of α_{s1} casein. First order kinetics were applied and the rate constant for each cheese-temperature combination was calculated. From these it was

found that the temperature relationship observed followed Arrhenius law. The rennet and moisture levels had an approximately proportional effect on the rate of primary proteolysis. The higher the moisture content the greater the rate of disappearance of α_{s1}casein. The higher the level of addition of rennet the greater the rate of disappearance of α_{s1}casein. No effect of salt was observed within the range investigated (3.6 to 6.5 salt in moisture wt%). An overall kinetic model was developed to describe the rate of proteolysis with respect to temperature, moisture, and rennet.

CHAPTER 3

THERMOPHYSICAL PROPERTIES OF CHEESE

3.1 INTRODUCTION

The mathematical modelling of the chilling or freezing of a block or pallet of cheese requires knowledge of the thermal properties of cheese. The properties of interest are specific heat capacity, thermal conductivity and density. This chapter will deal with each in turn describing how the values can be obtained from literature, theory or experimental determination.

During chilling at low temperatures (below –5°C)(Polley *et al.*, 1980) cheese undergoes freezing. The freezing of the water and fats in cheese each requires the removal of latent heat. The initial freezing point is also effected by solute concentration. Moreover as water freezes out, other soluble components are freeze concentrated resulting in freezing point depression. The thermal properties will therefore be needed for different cheese compositions and over the entire range of freezing.

Discrete constant values can be found in the literature for the determination of most thermophysical properties above and below freezing (Polley *et al.*, 1980). Alternatively some simple empirical formulas can be found when more accuracy is required (Willix &Amos, 1995; Thomareis & Hardy, 1985). Some authors (Willix &Amos, 1995; Thomareis & Hardy, 1985) have simply assumed a discrete phase change temperature and called different model functions on either side of that point. This method has some advantages in that it is simple and easy to apply. Unfortunately the temperature range at which freezing occurs, errors can be large (Willix &Amos, 1995, Saad & Scott, 1996). The range at which this occurs will have a corresponding range of thermal property values. Alternatively a material can be modelled as a simple binary system (Saad & Scott, 1996). Here the thermal properties during the freezing process are analytically evaluated. In highly concentrated systems and/or systems with a significant fat content, the simple system assumption that this is based on, is invalid.

Saad & Scott (1996) found that for some materials this method did not agree well with observed data due to the complex nature of the system, (i.e. the non-idealiality of macro molecular structures). For a simple homogeneous sucrose system the predictive measures of thermal conductivity and heat capacity give results that agree well with observed estimated values. However for protein suspensions the predictive methods did not agree within experimental error (Saad & Scott, 1996).

Miles *et al.*, (1983) extensively reviewed predictive methods for calculating thermal properties of foods and suggested a series of equations from which they could be calculated. They also state that the equations were not rigorously tested due to lack of data. Testing the equations was conditional on knowledge of the state and nature of the foodstuff that was unavailable to the author at the time. Paradoxically they also suggest that more empirical data is required to test and improve accuracy of the predictions.

3.2 THERMAL PROPERTY DATA IN LITERATURE

Because the apparent heat capacity and thermal conductivity are dependent on the ice fraction at temperatures below the initial freezing point methods to measure or predict the measurement or prediction of ice fraction was investigated first.

3.2.1 ICE FRACTION

The ice fraction of a material is an important factor to estimate the thermal properties discussed above. This is because the thermal properties of liquid water are significantly different from those of ice and therefore the thermal properties of any material with a significant moisture content will change significantly as the water freezes. An obvious consequence of this is that, if the ice fraction can be adequately described over the whole temperature range of interest, then the other thermal properties can be predicted.

Ice fraction can be defined as the proportion of freezable water that is frozen, or:

$$x_{ice}' = \frac{X_{ice}}{x_w'}$$

Equation 3-1 ice fraction definition

where:

x_{ice}'	= Ice fraction	[kg ice/kg freezable water]
X_{ice}	= Total mass fraction of ice	[kg ice/kg total mass]
x_w'	= Mass fraction of freezable water	[kg freezable water/kg water]

In order to predict the other thermal properties required, a relationship is needed that expresses the ice fraction as a function of temperature, salt content, and moisture content. Rahman (1995) has extensively reviewed this field and suggest that empirical equations are the simplest option. The form of the empirical equations given follows:

$$(1 - x_{ice})x_w = \hat{a} + \hat{b}\left[\frac{1}{\theta}\right] + \hat{c}\left[\frac{1}{\theta}\right]^2 + \hat{d}\left[\frac{1}{\theta}\right]^3$$

Equation 3-2

Where:

x_w	= Water mass fraction of total	[kg water /kg total mass]
x_{ice}	= Ice fraction of water	[kg ice /kg total water]
$\hat{a}$	= Empirical constant	[kg/kg]
$\hat{b}$	= Empirical constant	[kg.°C/kg]
$\hat{c}$	= Empirical constant	[kg.°C^2/kg]
$\hat{d}$	= Empirical constant	[kg.°C^3/kg]
θ	= Temperature	[°C]

The ice fraction can be determined graphically from phase diagrams using the Lever rule. As a phase diagram is not available for a cheese system in literature, the diagram would have to be determined experimentally.

Finally equations based on the Clausius-Clapeyron and Roults Laws can be used (Rahman, 1995). These equations only apply to simple systems and are based entirely on a measure of initial freezing point which can range from –5 to –15 °C (Kosikowski & Mistry, 1997).

3.2.1.1 Summary of Predictive Equations

Sakai and Hosokawa (1984) extensively reviewed predictive equations for determination of ice fraction. Calculations were compared with actual data for dilute solutions using phase equilibrium diagrams. The equations investigated included:

1) Simple method (Schwartzberg, 1976):

$$x_{ice} = \left(1 - \frac{T_f}{T}\right) x_w$$

Equation 3-3

2) Bartlett's method:

$$x_{ice} = \left(1 - \left[\frac{\exp\{k_1(T_{fo} - T_f) + k_2(T_{fo} - T_f)^2\} - 1}{\exp\{k_1(T_{fo} - T) + k_2(T_{fo} - T)^2\} - 1}\right]\right) x_w$$

Equation 3-4

3) Heldman's method:

$$x_{ice} = \left(1 - \left[\frac{\{1 - \exp(AB)\}\{\exp(AC)\}}{\{1 - \exp(AC)\}\{\exp(AB)\}}\right]\right) x_w$$

$$where:$$

$$A = (H_{mo} M_a / R), B = (1/T_{fo}) - (1/T_f), C = (1/T_{fo}) - (1/T)$$

Equation 3-5

4) Reidel's method:

$$x_{ice} = \left[\frac{H_{fp} - H_{fb}}{H_{mo}} - \frac{H_p - H_b}{H_m}\right]$$

Equation 3-6

5) Enthalpy balance:

$$x_{ice}(1) = \left[\frac{1}{x_w H_m}\right][H_t - (1 - x_w)H_s - x_w x_{ice}(2)H_{ws} + x_w x_{ice}(2)H_m - x_w(1 - x_{ice}(2))H_w 1]$$

Equation 3-7

For the enthalpy method $x_{ice(1)}$ is the ice fraction which is being calculated $x_{ice(2)}$ is some known value for x_{ice} at some temperature other than that being investigated.

Sakai and Hosokawa (1984) found that the most accurate method was method 5 (the enthalpy balance). The enthalpy balance method requires knowledge of the ice fraction at some point below freezing. It may be used to estimate the ice fraction at a

point close in temperature to the known value. The model assumes a straight-line relationship between temperature and sensible heat change due to changing ice fraction. If a large step is taken then curvature is ignored.

In the past, approaches for determining thermal data were based on ice content data that was predicted from equations rather that measured, due to the difficulty of direct measurement. Sakai and Hosokawa (1984) compared a number of different predictive equations against experimental data reference points. They found that an enthalpy balance was the most accurate method for determining ice fraction after the use of phase diagrams. However detailed enthalpy data are required for all the component parts and the analysis of overall enthalpy data becomes more complex as the number of components increases.

3.2.2 INITIAL FREEZING POINT

Estimation of the freezing point is important in terms of heat transfer modelling as it determines where the energy of latent heat begins to limit temperature change within the solid undergoing freezing/thawing. Since the temperature-time relation has a hold up at the freezing point, this implies any prediction of temperature in a freezing solid will be in error by the same amount as the error in freezing point data. The freezing point needs to measured experimentally as the onset of freezing (completion of thawing) and depends on salt and moisture content as well as cheese style (Kosikowski & Mistry, 1997).

The freezing point can readily be determined from Differential Scanning Calorimetry data (DSC) results. It has been shown that the freezing point of cheese is also effected by the amount of proteolysis that has occured (Kosikowski & Mistry, 1997, Ramanauskas & Alencikiene, 1999). This may be due to the colligative effects of the amino acids released during the process of proteolysis.

3.2.3 HEAT CAPACITY

The heat capacity is defined as the amount in heat required to achieve a change in the temperature of a material. The heat capacity of substances undergoing freezing is complicated by the latent heat effect. Latent heat is the energy required, be added or removed, to cause a phase change in the material of interest. The heat capacity observed

during freezing includes both sensible heat and latent heat effects. The heat capacity observed during this period is often termed the apparent heat capacity.

In the case of cheese, substances undergoing phase change in the region 12°C to -20°C are water and fat. The water constitutes ≅ 30% of the mass of cheese. If the moisture present freezes in the temperature range of interest this corresponds to an apparent latent heat of 0.30×333 ≅ 100 kJ/kg cheese. Fat constitutes ≅ 35% of the mass of cheddar cheese (see appendix section 7.1) the fat has a sensible heat capacity of ≅ 2kJ/kg above and below freezing and has a melting range between –30 and 35°C . In the range of interest (-30 to 12°C) the total enthalpy change is ≅ 100kJ/kg of which 84kJ/kg can be attributed to sensible heat capacity (at 2kJ/kg). This leaves 16 kJ/kg of latent heat per kg of milk fat. This corresponds to an apparent latent heat of 0.35×16 = 5.6 kJ/kg of cheese. This is small in comparison to the latent heat of freezing water.

3.2.3.1 PREDICTION

Literature values for the specific heat capacity of cheese range from 1.3 – 2.1 $kJ.kg^{-1}.K^{-1}$ for the frozen and unfrozen cheese respectively (Polley *et al.*, 1980, Rahman,1995).

In addition to this significant difference between frozen and unfrozen cheese heat capacity it can be expected that the apparent heat capacity will also be effected to a large degree by latent heat. An alternative to the use of literature constants is the application of empirical formulae. Thomareis and Hardy (1985), for example, give an empirical formula for the specific heat of processed cheese in the temperature range of 40-100°C for a range of industrial compositions. Their results have been tabulated by Rahman (1995) and the heat capacity ranges from 1.3 – 2.1 $kJ.kg^{-1}.K^{-1}$. Unfortunately the data does not include freezing. Lindsay and Lovatt (1994) fitted parameters for cheese between –40°C and 40°C to an integrated form of Schwartzberg's (1976) approximate equation of enthalpy (below freezing) and a simple component summation of enthalpies (above freezing). They found that for cheese with a given composition (35%moisture, 26.4%protein, 30.5%fat, 3.8ash, 1.8%salt). The enthalpy (and therefore effective heat capacity) could be estimated by:

$$H = A + c_f\theta + \frac{B}{\theta}$$

Equation 3-8

for temperatures below the freezing point of cheese and:

$$H = H_0 + c_u\theta$$

Equation 3-9

for temperatures above the freezing point of cheese

Where for both equations:

H	= enthalpy		[kJ/kg]
θ	= temperature		[°C]
A	= empirical constant	= 48.5	[kJ/kg]
c_f	= heat capacity of frozen substance	= 1.65	[kJ/kg K]
B	= empirical constant	= -643	[kJ K/kg]
c_u	= heat capacity of unfrozen substance	= 3.41	[kJ/kg K]
H_0	= enthalpy at datum temperature	= 167	[kJ/kg]

Initial freezing point as measured by Linsay and Lovatt (1994) = -5.93 °C

These results were found to compare well with experimental data, having correlation coefficients (r^2) close to 1.000 ± 0.001. They were also in close agreement with other literature values for other substances tested. Although the results are only strictly valid for cheese of the same composition the authors proposed that comparison could be made for different water contents by adjusting coefficients with enthalpy data for water and ice. The adjustment for fat was carried out by adjusting the relative molecular ratio in Schwartzberg's (1976) approximate equation. This was found to be invalid for large differences between fat content used and in the literature. Overall they found that experimental predictions agreed to within 5% of other literature.

As a general basis for determining the specific heat capacity of biological materials a weighted sum can be used if the specific heats of the component parts are known. This is given below:

$$c = \sum_{i=1}^{n} (x_i c_i)$$

Equation 3-10

Alternatively empirical equations using the most important components can be applied to any individual foodstuff, (Miles *et al.*, 1983). Usually these are simple linear functions of moisture content, dry matter specific heat, and in the case of freezing or frozen systems, a term for ice fraction is also included. The equations assume that the material of interest is made up only of those parts and there is no interaction between parts.

3.2.3.2 Experimental Estimation

3.2.3.2.1 Adiabatic calorimeter

This was the method used by Pham (1994) to calculate enthalpy of various food products over a temperature range. It is series of nested vessels. The material of interest is placed into the centre most vessel surrounded by a calorimetric fluid into which an immersion heater applies a constant rate of heat input. The temperature of the calorimetric fluid, is then measured using thermocouples. The system is isolated from ambient conditions using a vacuum flask jacketed by alcohol that is kept at the temperature of the calorimetric fluid. Although it is a simple apparatus the development of a system able to provide accurate data would be time consuming and would not be suitable for this work

3.2.3.2.2 The method of mixtures

The method of mixtures involves the addition of water at some temperature to a sample at some other temperature and measuring the temperature change [Ohlsson, 1983]. Peralta-Rodriguez *et al.,* (1995) propose a simple variation on this method. Here a Dewar flask was used to hold the calorimetric fluid. The flask was placed in a thermos flask that was surrounded by expanded polystyrene. A sample was placed in a retortable pouch. Finally the Dewar flask was flooded with water at a known temperature and the temperature of the sample was recorded until steady state was reached. Any heat loss to ambient can be measured. This method gives the enthalpy difference between the start and final temperatures and the average specific heat between these temperatures also. The method has the advantage that it is easy to apply and is simple to assemble. However, the system relies on having a calorimetric fluid available at the temperature range of interest and to get useful results for apparent heat capacity many experimental runs would need to be performed.

3.2.3.2.3 Differential scanning calorimeter (D.S.C.)

In this method a sample is maintained at the same temperature as a reference material throughout a period of controlled temperature change. The rate of heat input that is required to maintain the same temperature in each is recorded. Thermal events such as freezing and thawing and in fact any deviation from constant specific heat is recorded as a deviation from the DSC output baseline (Brown, 1988). This method has been used for the determination of specific heat and enthalpy of fats (Ohlsson, 1983). The method is directly applicable to the determination of the thermal properties of cheese. In addition the equipment was available for use in this work.

3.2.3.2.4 Microcalorimeter

Ohlsson (1983) suggested this method as an alternative to DSC Thermopiles are placed around the sample and an around an empty reference cell. Specific heat is determined by the difference between the heat flows into the sample and reference cell. This method is therefore a special case of the D.S.C. where the reference material is absent.

3.2.4 THERMAL CONDUCTIVITY

Literature constants can be found for the thermal conductivity of cheese above and below the freezing point (Polley *et al* 1980, Rahman 1995) but these do not apply during the freezing range itself and do not take into account compositional differences between cheeses.

In food products the thermal conductivity is simply related to its composition, ice fraction, and temperature (Pham & Willix, 1989). During the freezing process the ice fraction changes from zero to one and this can radically alter the materials thermal conductivity. The greater the fraction of freezable water, the greater the increase in thermal conductivity due to ice formation.

3.2.4.1 PREDICTION

One method to obtain data is to apply an empirical model. Rahman (1995) lists various authors who show that the most important determinant of conductivity in food stuffs is moisture content. Rahman (1995) and Miles (1983) give a range of empirical formulae for thermal conductivity based on the moisture content, fat content, and non fatty substance of foods. However the formulae given do not take into account the ice fraction during freezing which has a significant effect on the conductivity. For this, more complex multiphase models are required.

Multiphase models for calculating the conductivity of the bulk material are based on the conductivity's of each phase. For multiphase materials the conductivity also depends on the structure and direction of heat flow. Koppelman (1966) proposed a two-phase model for calculating the thermal conductivity. The model essential works as a weighted sum of the conductivity's of each of two phases where one phase is assumed as continuous and the second as a phase dispersed within the first. Heldman & Gorby (1975) modified this to include multiple phases. In general the thermal conductivity of multi-phase systems are calculated as a series of two phase system calculations nested within one another. Koppelmans equation is:

$$\lambda = \lambda_c \left(\frac{1 - V_{d(\theta)}^{2/3} \left(1 - \lambda_d / \lambda_c\right)}{1 - V_{d(\theta)}^{2/3} \left(1 - \lambda_d / \lambda_c\right)\left(1 - V_{d(\theta)}^{1/3}\right)} \right)$$

Equation 3-11

where:

λ	= Thermal conductivity of material of interest	[$W.m^{-1}.C^{-1}$]
λ_c	= Thermal conductivity of continuous component	[$W.m^{-1}.C^{-1}$]
λ_d	= Thermal conductivity of discontinuous component	[$W.m^{-1}.C^{-1}$]
$V_{c(\theta)}$	= Volume fraction of continuous component as a function of temp	[-]
$V_{d(\theta)}$	= Volume fraction of discontinuous component as a function of temp	[-]

Another approach is to apply the effective medium theory. This theory assumes that the system is a simple homogenous mixture of parts where each component part has a known conductivity. This structure is consistent to that of cheese and therefore it is the method used in this work to calculate the thermal conductivity of cheese. The whole systems conductivity can then be calculated by;

$$\sum_{i=1}^{n} V_i \left(\frac{\lambda - \lambda_i}{\lambda_i - n \cdot \lambda} \right) = 0$$

Equation 3-12

where:

V_i	= Volume fraction of component i	[$m^3.m^{-3}$]
λ_i	= Thermal conductivity of component i	[$W.m^{-1}.C^{-1}$]
λ	= Thermal conductivity of material of interest	[$W.m^{-1}.C^{-1}$]
n	= Number of components	[-]

Again, for multiple systems, a two phase pair is calculated first and then repeated for each subsequent phase calculated in combination with the preceding component pair. When Equation 3-12 is expanded for a two component pair this gives:

$$2\lambda^2 + \lambda(3V_1\lambda_2 - 3V_1\lambda_1 + \lambda_1) - \lambda_1\lambda_2 = 0$$

Equation 3-13

Which is a quadratic equation and can be solved for λ.

$$\lambda = \frac{-(3V_1\lambda_2 - 3V_1\lambda_1 + \lambda_1) \pm \sqrt{(3V_1\lambda_2 - 3V_1\lambda_1 + \lambda_1)^2 - 8\lambda_1\lambda_2}}{4}$$

Equation 3-14

When the material of interest has a three-dimensional structure, such as layers or fibres, the conductivity will depend on the direction of heat flow. For layered materials such as these found in stacks of cheese cartons heat transfer is in a direction perpendicular to the carton side and the thermal conductivity can be calculated using the "components in series" model (Miles *et al.*, 1983, Rahman 1995):

$$\frac{1}{\lambda} = \sum_{i=1}^{n} \frac{V_i}{\lambda_i}$$

Equation 3-15

For heat flow parallel to the carton side the equation can be calculated using "components in parallel".

$$\lambda = \sum_{i=1}^{n} V_i \lambda_i$$

Equation 3-16

Where for both models:

V_i	= Volume fraction of component i	[-]
λ_i	= Thermal conductivity of component i	[W/m.°C]
λ	= Thermal conductivity of material of interest	[W/m.°C]
n	= Number of components	[-]

3.2.4.2 Experimental Estimation

Thermal conductivity can be experimentally determined by steady state or transient methods (Ohlsson, 1983, Rahman, 1995). In its simplest form, the steady state method applies the one dimensional Fourier heat transfer equation, which is used to describe the heat flow after application of a temperature gradient. Specific methods include the guarded hot plate method, comparison to a reference material, and the equation of continuity.

An alternative is to use transient methods. These methods involve the application of a known heat flow and measuring the temperature at various points throughout the material as a function of time.

Listed below are some steady state and transient methods available to measure conductivity.

3.2.4.2.1 Guarded hot plate method

Here a heat source is surrounded with a sample that in turn is surrounded with a heat sink in a layered slab configuration. The ends and sides are insulated in order to reduce edge effects. The conduction can be calculated from the simple one-dimensional slab heat transfer equation.

Alternatively the samples can be set up in a cylindrical configuration and the conductivity calculated during steady state heat transfer using the uni-directional radial heat transfer equation (Rahman, 1995).

$$Q = A_{ou}\lambda\left[\frac{\theta_{ou} - \theta_{in}}{r_{ou}\ln {r_{in}}/{r_{ou}}}\right]$$

Equation 3-17

Where:

Q	= Heat flow rate	[J/s]
A_{ou}	= Outside area of heat transfer	[m^2]
r_{ou}	= Outside radius of sample	[m]
r_{in}	= Inside radius of sample	[m]
θ_{ou}	= Outside temperature	[°C]
θ_{in}	= Inside temperature	[°C]

3.2.4.2.2 Differential scanning calorimetry

The DSC can be used to measure the thermal conductivity (Brown, 1988). Here an attachment is required and the thermal conductivity is measured by measuring the temperature above and below the sample when the device reaches steady state with a constant heat input. The method can then be repeated at a range of temperatures. Using this method an accuracy of ±3% may be achieved (Brown, 1988).

3.2.4.2.3 Line source method

Rahman (1995) suggests that the line source method is the most widely used method for foodstuffs due to its convenience, cost, and speed of measurement. This method involves the insertion of a thin probe heat source. The temperature of the surrounding sample is then a function of conductivity and can be calculated from the equation below.

$$\theta = B + \left[\frac{q}{4\pi\lambda}\right] \ln t$$

Equation 3-18

Where:

θ	= Temperature of a point close to the source	[°C]
B	= Experimental constant	[°C]
q	= Heat source per unit length	[$W.m^{-1}$]
λ	= Sample thermal conductivity	[$W.°C^{-1}.m^{-1}$]
t	= Time of experiment	[s]

This method is prone to error due to edge effects and therefore requires a sufficiently large sample size. As long as the sample is large enough such that boundaries do not under go temperature change, the method is good.

3.2.5 DENSITY

Since enthalpy and heat capacity values are given on a per-mass basis their application to describe heat transfer through space requires them to be transformed into their volumetric equivalent using density.

If mass and volume are conserved then, for any material with component parts, the bulk density can be calculated from the weighted sum of those parts (Rahman, 1995, Miles *et al.*, 1983). i.e.

$$\frac{1}{\varrho_T} = \sum_{i=1}^{n} \frac{x_i}{\varrho_i}$$

Equation 3-19

Where:

ϱ_T	= Bulk density	[kg.m^{-3}]
ϱ_i	= density of component i	[kg.m^{-3}]
x_i	= mass fraction of component i	[-]

Rahman (1995) give a table of common food components from which the density can be calculated.

Mayes and Radford (1983) give tables from which the density of cheddar cheese can be calculated based on moisture fat and salt content. They found that density was significantly correlated with salt content, moisture content, temperature, and pressing method. This indicates that the conservation of volume does not necessarily hold and that empirical or experimental data is required. Unfortunately the tables given by Mayes and Radford (1983) do not give values for density at temperatures lower than freezing. The range of values observed for a number of cheddar cheeses from 8-20°C was 1073-1096 [kg/m^3]. This corresponds to a change in density of $\cong$ 2%

One of the important components in determining density during freezing is the ice fraction. When water freezes the density changes from 1000 [kg/m³] to 920 [kg/m³]. For a 30% moisture cheese which freezes to $x_{ice} = 50\%$, this will cause a change of $\cong$ 1.2%. This is almost equal to all other effects combined. It would be expected that as cheese freezes the density would decrease following this trend.

Rahman (1995) suggests as an alternative that an empirical model can be fitted to experimental density data in the form of a simple polynomial including linear and square terms for moisture content and temperature.

3.2.5.1 Experimental Estimation

Density can be measured by weighing a sample in air then suspended in liquid. Density is then given by the formula (Mayes & Radford, 1983):

$$\varrho = \frac{W}{W_l}\Delta + \sigma\left(1 - \frac{W}{W_l}\right)$$

Equation 3-20

Where:

ϱ	= Materials density	[kg/m³]
Δ	= density of the liquid	[kg/m³]
W	= Weight of material in air	[-]
W_l	= Weight of material in liquid	[-]
σ	= Density of air	[kg/m³]

A more simple method can be used if the sample is significantly more dense than air. In this case the sample can be weighed in air and then have the volume measured by immersion in fluid.

3.2.5.2 Density conclusions

The density of cheese is a function of composition, temperature, and ice fraction. The ice fraction is the most important factor as it individually contributes the most to the observed changes in density. It is suggested that a weighted-sum of densities could be used over the temperature range of interest to account for density effects of freezing water. How ever the maximum error which could be expected, if a constant density of

1000 [kg/m^3] is assumed, is < 4% . If this error is within the experimental error observed it can be assumed constant and this will greatly simplify the issue.

3.3 LITERATURE CONCLUSIONS

Experimental data gathering is expensive and time consuming (Cleland, 1985). For food undergoing phase change data needs to be gathered over the whole range of temperature and at sufficient points during the phase change to ensure that the large changes in thermal properties that are observed are recorded accurately. Only if it is found that literature values and equations are inadequate should the time and expense be set aside to gather thermal data.

It has been shown that the major determinant of the thermal properties of food substance undergoing a freezing/thawing phase change is the ice fraction. If the ice fraction is known well, it can be used to estimate all other thermal properties. It was found that the heat capacity during freezing is wholly influenced by ice content due to the latent heat of freezing and that the measurement of one, implies information of the other. The thermal conductivity ranges from 0.3 to 0.4 W/m.K and this is entirely attributable to the changing ice fraction. This change due to composition is less than 5%.

The ice fraction itself can be predicted from theory. This requires accurate knowledge of the freezing point however. A shift in the actual freezing point will correspond to a shift in all the thermal data predicted and hence a shift in any time temperature predictions. It was found that experimental estimation of ice fraction was difficult. This can be seen by the lack of data present in the literature for cheese. The best method found to determine ice fraction was the enthalpy method. It is therefore proposed that this method be used for determination of ice fraction in cheese from specific heat data measured using a differential scanning calorimeter.

3.4 EXPERIMENTAL DETERMINATION OF ICE FRACTION FROM SPECIFIC HEAT DATA

3.4.1 METHOD DEVELOPMENT

In an attempt to improve existing knowledge of the thermal properties of cheese at and around its freezing point, the DSC technique was used to determine the specific heat, freezing point, and ice content of cheddar cheese. In order to explain the method proposed here for the calculation of ice fraction it is useful to define the terms used to characterise the functions of water and ice present in the cheese.

x_w	= moisture content	[kg water / kg cheese]
x_i	= mass fraction of component I	[kg component i /kg cheese]
X_{ice}	= total ice mass fraction	[kg ice / kg cheese]
x_{ice}	= ice fraction	[kg ice / kg water]
x_{ice}'	= freezable ice fraction	[kg ice / kg freezable water]
x_w'	= freezable moisture mass fraction	[kg freezable water / kg cheese]

3.4.1.1 THE ENTHALPY BALANCE METHOD APPLIED TO HEAT CAPACITY DATA

For frozen foods, the effect of freezing on heat capacity can be described by two terms (Miles *et al.*, 1983). One term represents the effect of a change in ice content and the other represents the properties that are constant with respect to ice formation. The heat capacity of a material during freezing can therefore be written as Equation 3-21:

$$c = \frac{\partial h}{\partial T} = \left(\frac{\partial h}{\partial T}\right)_{x_{ice}} + \left(\frac{\partial h}{\partial x_{ice}}\right)_T \left(\frac{\partial x_{ice}}{\partial T}\right)$$

Equation 3-21

Or

$$c = \frac{\partial h}{\partial T} = \left(\frac{\partial h}{\partial T}\right)_{x_{ice}} + L\left(\frac{\partial x_{ice}}{\partial T}\right)$$

Equation 3-22

Where L is defined as the heat required to affect a change in ice content. The first term in Equation 3-22 can be described by a weighted-sum of the sensible heats of component parts. Unfortunately during the freezing process two of the most important

components of food products change dramatically. This is due to the difference in thermal properties between water and ice. As ice freezes out, the thermal properties of the bulk material alter concurrently. As the equation stands, this effect is included in the second term. To simplify, the equation can be rewritten in three terms. One that describes the sensible heat effect assuming zero ice content (trivial above freezing, and analogous to a super-cooled material below freezing), another that describes the effect of changing ice content on the weighted sum of the sensible heats, and finally a third that describes only the latent heat of fusion of water. Equation 3-22 can therefore be rewritten as Equation 3-23:

$$c = \frac{\partial h}{\partial T} = \left(\frac{\partial h}{\partial T}\right)_{supercooled} + x_w\left(\frac{\partial x_{ice}(h_{ice} - h_w)}{\partial T}\right) + x_w\left(\frac{\partial x_{ice}}{\partial T}\right)L$$

Equation 3-23

Where; L now represents only the latent heat of fusion. The equation above can be summarised as the sum of three terms (T_1, T_2, and T_3) or:

$$c = T_1 + T_2 + T_3$$

Equation 3-24

Where; T_1 describes the temperature dependence of specific heat. The remaining two terms modify this sensible heat to account for freezing. T_2 describes the change in sensible heat due to changing ice content. T_3 is simply the latent heat effect.

Upon integration of term 3 up to any temperature (T) below the initial freezing point, gives the ice content at that temperature ie.

$$x_w \int_{-\infty}^{T}\left(\frac{\partial x_{ice}}{\partial T}\right)L \cdot dT = L \cdot x_w \cdot x_{ice(T)}$$

Equation 3-25

One can now analyse the apparent specific heat of a material against temperature and calculate ice content data from this and then predict the thermal properties. Equation 3-24 can be rearranged to:

$$T_3 = c - T_1 - T_2$$

Equation 3-26

If a graph of apparent specific heat vs temperature is available, the ice content at any temperature below freezing point can be calculated by integrating the specific heat graph with an estimate of T_1 and T_2 removed. Since T_2 is small in comparison to T_3 ignoring T_2 or applying a straight-line relation for it can be used to make a first estimate of x_{ice} as a function of temperature. If an estimate of ice content is known with respect to temperature then T_2 can be rearranged to give:

$$T_2 = x_w \cdot x_{ice(T)} \cdot \left(\frac{\partial (h_{ice} - h_w)}{\partial T} \right)$$

Equation 3-27

Or

$$T_2 = x_w \cdot x_{ice(T)} \cdot (c_{ice(T)} - c_{w(T)})$$

Equation 3-28

Having determined a first estimate of ice content vs. temperature, improved estimates can be made by applying Equation 3-26 directly and then iterating the procedure until convergence is observed.

The proposed method can be considered as a modified case of the enthalpy balance method. It uses a very low temperature as an index that is assumed to have 100% of the freezable water in a frozen state. If the food material in question is never expected to go below this temperature then this method will produce a good estimate of the water which freezes at temperatures above this index. The ice fraction can be calculated at *any* large temperature difference from the index temperature due to the iterative correction factor that is used. The proposed method results in a complete relationship for ice fraction as a function of temperature, based on the apparent heat capacity of the sample.

3.4.1.2 Model Data Testing

Having modified the enthalpy method so as to estimate ice fraction from specific heat vs. temperature data, the method was tested using model data. Miles *et al*, (1983) suggest Equation 3-29 as an approximation of the specific heat of a material under going freezing.

$$c = c_s(1-x_w) + c_w x_w \frac{T_f}{T} + c_{ice}\left(1-\frac{T_f}{T}\right)x_w - Lx_w\frac{T_f}{T^2}$$

Equation 3-29

Where:

c_s	= Specific heat of proteins	≅ 1900	[J/kgK]
c_w	= Specific heat of unfrozen water	≅ 4180	[J/kgK]
c_{ice}	= Specific heat of frozen water	≅ 2000	[J/kgK]
L	= Latent heat of ice	≅ 333600	[J/kgK]
T_f	= Freezing point	≅ –5	[°C]
T	= Temperature		[°C]

This equation is a sum of the specific heats of the component parts and implies the relationship for ice content below holds:

$$x_{ice} = \left(1-\frac{T_f}{T}\right)x_w$$

Equation 3-3

Equation 3-3 is based on the premise that the concentration of the solution is directly proportional to the freezing point depression relation (Sakai and Hosokawa, 1984) and strictly only applies to dilute aqueous solutions. As pure water freezes out, the remaining solution becomes more concentrated and reduces the freezing point Equation 3-3. For the purpose of model testing this simple approach will suffice. In addition, the heat capacities of all component parts were assumed to be constant. This was carried out for simplicity but is not required for analysis of real systems. The process does however require that the heat capacities vary linearly with temperature both above, and below freezing.

The output from Equation 3-29 is given below in Figure 3.1.

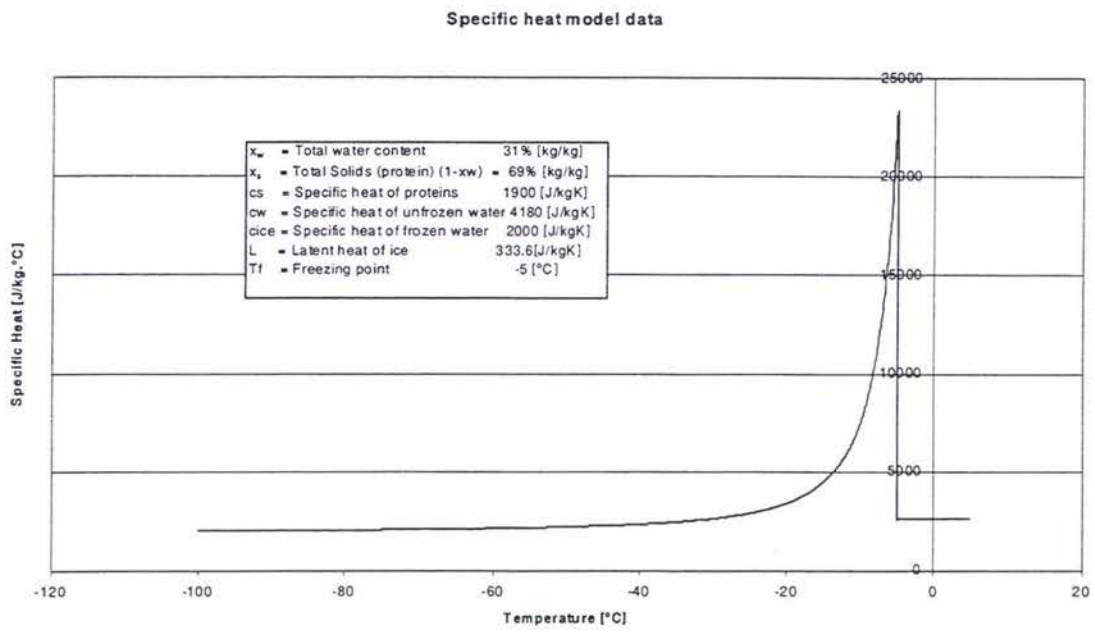

Figure 3.1 Specific heat model data from Equation 3-29

Once the model data is generated the analysis can begin. Due to the simplicity of the data the straight-line portion above freezing it can be regressed easily and subtracted from the curve. The area under the curve between two temperatures now represents only the latent heat for melting the ice that changes phase across that temperature range. The area under the curve can now be incrementally determined by numerical integration and divided by the total area under the curve. The result is an estimate of $(1\text{-}x_{ice}')$. The value of X_{ice} at any temperature can be calculated by multiplying the estimate of x_{ice}' by the fraction of freezable water x_w'. The fraction of freezable water (x_w') is the total area under the curve divided by the latent heat of melting/freezing for pure water L(333.6 kJ/kg.K). The ice content (x_{ice}) can then be calculated from Equation 3-30

$$x_{ice}=X_{ice} \times x_w.$$

Equation 3-30

The x_{ice} data calculated here is then used to estimate T_2 which is subtracted from the graph to make a second estimate of x_{ice} iterating the procedure above. The first, second, and third estimate of x_{ice} are plotted along side the original model data for comparison in Figure 3.2.

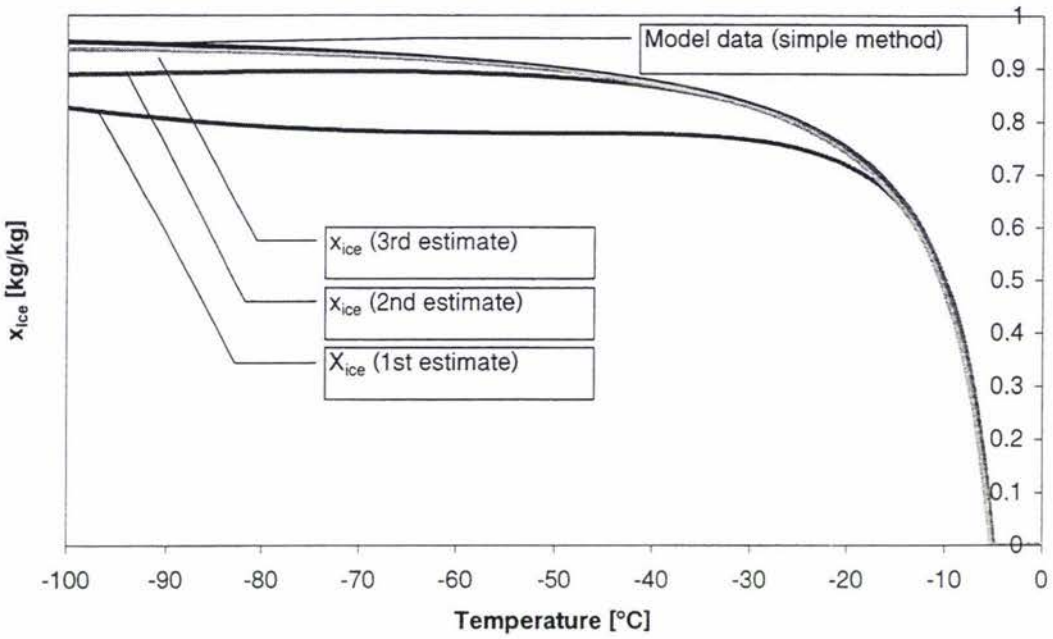

Figure 3.2 Ice fraction from model data

It can be seen from this that the method is mathematically correct. The method converges quickly to the actual ice fraction used in the model data.

3.4.2 REAL SYSTEM VALIDATION

3.4.2.1 MATERIALS AND METHODS:

In an attempt to produce cheese with different compositions for proteolysis studies outlined in chapter 2, twelve cheeses were made. The resulting compositions ranged from 31-34% moisture and 3.6-6.5% salt in moisture content. Three cheeses were chosen to represent the maximum and minimum of each factor. A fourth cheese of low moisture content was also made available. The full composition of this is listed as vat 15 in appendix section 7.1. The cheeses were matured at 2°C for 6 months. From each cheese, two 5mg samples were taken and sealed in 20 μl aluminium volatile DSC pans. Firstly one cheese sample was tested at different scanning rates in order to see the effect of scanning rate on the resulting data. The scanning rate is the rate of temperature increase that the sample is subjected to. For example, a scanning rate of 5°C/min means the sample temperature was increased by 5°C every minute. The resulting thermogram DSC outputs have been plotted in Figure 3.3 below.

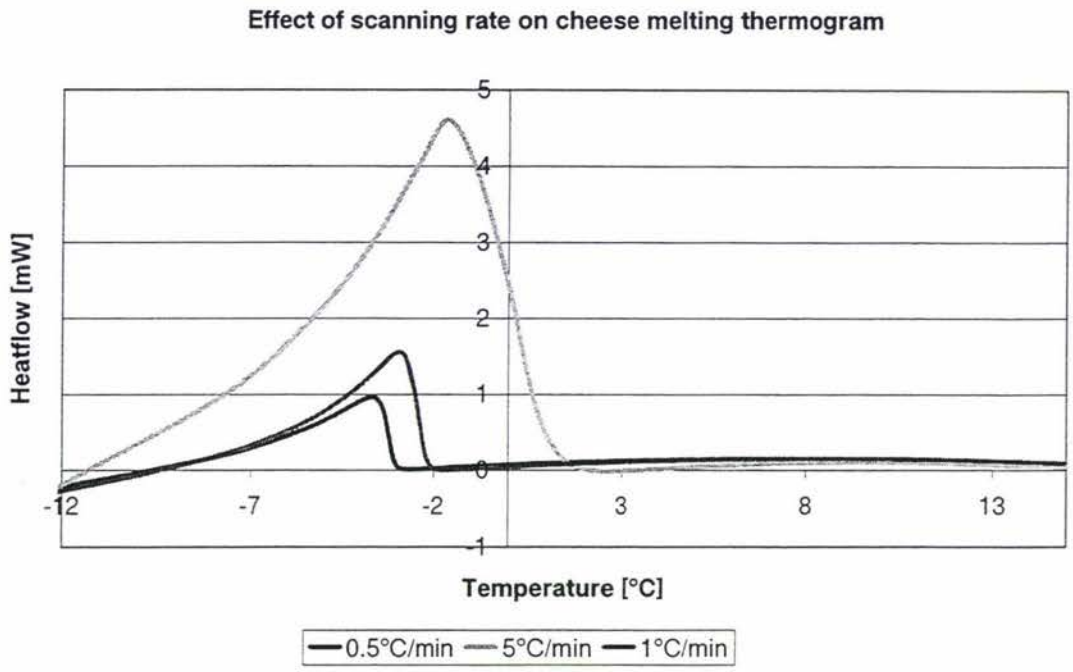

Figure 3.3 Effect of scanning rate on cheese melting thermogram

It can be seen from Figure 3.3 that scanning rate has a large effect on the measurement of the initial freezing point. The DSC is a physical device that gathers specific heat data by subjecting a sample to a constant rate of temperature change and measuring the energy input required for this. If the experiment is run with too high a scanning rate the end of melting as indicated on the specific heat data becomes shifted to the right. It can be seen therefore that it is important to run the experiment at a low scanning rate. It can also be seen from Figure 3.3 that the error in freezing point expected by reducing the scanning rate from 1°C/min to 0.5°C/min is less than 1°C. Since reducing the scanning rate to 0.5°C/min results in the experiment taking twice as long as at 1°C/min it was concluded that a scanning rate of 1°C/min was the most appropriate for this work.

Each of the four samples were cooled from room temperature to –30°C at a rate of 5°C/min, held for 5 minutes then heated at1°C/min to 15°C using a Perken-Elmer DSC 7. The DSC output for the different cheeses are given below.

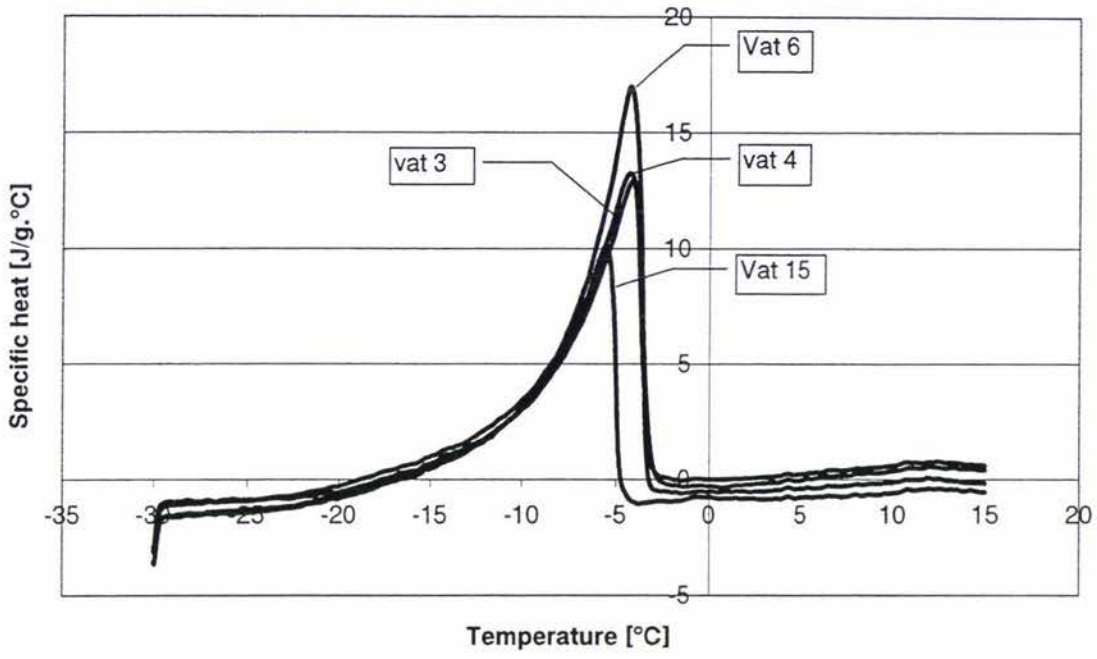

Figure 3.4 Heat capacity - real cheese data

It can be seen from Figure 3.4 that the low moisture cheese (vat 15) has a lower initial freezing point than other cheeses. This was expected as the lower moisture content implies a higher solute concentration and freezing point depression. The apparent area under the curve for the lower moisture cheese is also smaller as would be expected as there is less latent heat required to melt the lower mass of water present in the cheese. It was found that the latent heat of fat is a small effect in comparison to the latent heat effect of water. So for the analysis of cheese here it was assumed that all latent heat observed belongs to the melting of water. It can be observed that the heat capacity, after melting of ice is complete, is linear and there is no evidence of the fat melting. The assumption that the latent heat effect of melting fat is small is reasonable. This suggests that this assumption results in any contribution of the latent heat of fat being included as latent heat of ice in the ice fraction calculation. It would not effect the heat transfer calculations which follow as the error incurred on the ice fraction data will be small. The analysis method described above has been applied to each of these cheeses and the heat capacity and ice fraction has been determined and plotted in appendix section 7.5. The estimation of ice fraction for vat 3 is summerised in Figure 3.5 below.

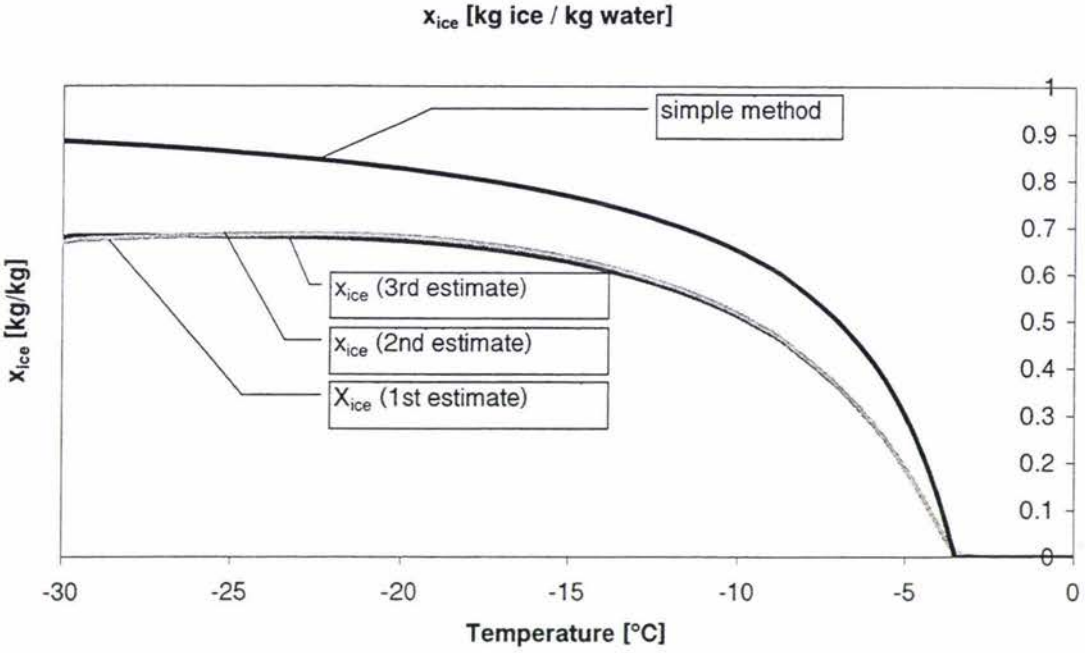

Figure 3.5 Ice fraction for vat 3

At this stage the method produces similar shaped results as those predicted using the simple method (Equation 3-3) with the exception of low temperature results. This is due to the fact that the simple method only applies to simple solutions. In the case of cheese there is a high content of fat, salt, and protein. The high solids content of cheese leads to a high proportion of bound water which does not freeze. This leads to a lower over all ice content in cheese at any given temperature, especially at lower temperatures. The large discrepancy between the model and the experimental data is due therefore to the fact that not all moisture in cheese is available for freezing.

3.5 SUMMARY OF THERMAL PROPERTIES

The thermal properties used in the rest of this work were obtained as described below.

3.5.1 HEAT CAPACITY

A method was found to determine the heat capacity of cheese over the freezing range using a DSC. The heat capacities for four cheeses of varied composition have been plotted in the appendix section 7.6. (The full data set is extensive and is available on the CD accompanying this work).

3.5.1.1 ICE FRACTION

A method was developed to determine the ice fraction of cheese over the temperature range of interest from the DSC heat capacity data. The resulting ice fraction data has been plotted in appendix section 7.5. The remaining thermal properties can be estimated from this ice fraction data. (The full data set is extensive and is available on the CD accompanying this work).

3.5.1.2 THERMAL CONDUCTIVITY

It was found that the effective medium theory (Equation 3-12) was an appropriate method to calculate the thermal conductivity of cheese undergoing freezing, providing adequate data on the ice content at any given temperature is available. Further more it was found that the heat transfer in series model was appropriate for determining the heat transfer in bulk stacked blocks of cheese.

3.5.1.3 DENSITY

It was found that the density of cheese under going freezing could be approximated to be 1000 kg/m^3 with an expected loss of accuracy in heat transfer results of less than 4%.

CHAPTER 4

HEAT TRANSFER

4.1 FREEZING AND THAWING EFFECTS

4.1.1 FREEZING

During the chilling process there is a point at which cheese begins to freeze. The initial freezing point of cheese is around –5°C. At first crystals of pure water form. This removal of water in the form of ice leaves behind solutes, causing the solute concentration in the unfrozen water to increase. The increase in concentration further depresses the freezing point due to the solutes colligative behaviour. (Fennema, 1975). The freezing out of water and the freeze concentration which follows, carries on until cooling stops or the eutectic point is reached. At or below the eutectic point, the rest of the material freezes as a whole.

In mobile freezing systems (such as fruit juice), the concentration polarisation caused by freezing at the freezing front can dissipate into the surrounding fluid. The amount of solute that is caught up in the ice matrix depends on freezing rate and solute mobility (Miyawaki et al., 1998). In the case of cheese and other gel substances, the gel matrix hinders the diffusion of solutes from the freezing front. For this reason it is not expected that solute diffusion away from the freezing front will be significant within the cheese system studied here.

4.1.2 THAWING

Unfortunately the thawing process cannot be considered the time-reversed process of freezing. This is due to thermophysical properties not being symmetrical over the temperature range of freezing. If there is a large difference in thermal conductivity between the frozen and unfrozen components in the solid, then this will have profound effects on the way the solid thaws in comparison to the way it freezes. For example, a solid with a high moisture content would have a larger value for thermal conductivity in the frozen state compared with the unfrozen state. This causes the heat applied during a freezing or thawing process to diffuse at different a speed through different parts of the solid. Faster heat diffusion occurs through parts with a higher ice content in comparison

to parts with a lower ice content. For example, during freezing the outside freezes first and has a higher thermal conductivity. This results in a freezing front which can remove the latent heat of freezing faster than during melting where the heat travels through the unfrozen (lower conductivity cheese) region first before it reaches the thawing front.

It is important to note here that this means that a non-homogeneous product will result from a large volume freeze thaw process. This is because the phase change front will move at different speeds into and out of a large block of cheese even in a symmetrical freeze thaw process. This effect is simply a result of changing parameters due to phase change, therefore the model used to investigate the freeze thaw process will illustrate these effects as long as the phase change dependant effects on parameters are included. The dis-symmetry only needs to be recognised as important in the final predictions and not in the formulation of models to estimate those predictions.

4.2 HEAT TRANSFER MODELS

In order to predict the extent of proteolysis as a function of position in a block or pallet of cheese a model describing how the temperature and ice content of the system changes with time and position is required. This section outlines the development and solution of the heat transfer model that was developed for this purpose.

4.2.1 HEAT TRANSFER EQUATIONS

The governing equation for one dimensional conduction heat transfer is Fouriers law, Equation 4-1:

$$\frac{\partial C\theta}{\partial t} = -\lambda(\theta)\frac{\partial^2 \theta}{\partial x^2} \qquad t > 0$$

Equation 4-1

Where:

C	= volumetric heat capacity	$[J.K^{-1}.m^{-3}]$
θ	= temperature	[K or °C]
t	= time	[s]
λ	= thermal conductivity	$[W.m^{-1}.K^{-1}]$
x	= spatial distance	[m]
A	= area normal to direction of heat transfer	$[m^2]$

Applying this to describe heat transfer through three dimensional Cartesian co-ordinates requires two more spatial co-ordinates (y,z) giving:

$$C\frac{\partial\theta}{\partial t}=\frac{\partial}{\partial x}\left(\lambda\frac{\partial\theta}{\partial x}\right)+\frac{\partial}{\partial y}\left(\lambda\frac{\partial\theta}{\partial y}\right)+\frac{\partial}{\partial z}\left(\lambda\frac{\partial\theta}{\partial z}\right) \quad t>0$$

Equation 4-2

In terms of the freezing process, the variables C and λ are heavily dependent on temperature and state (frozen/un-frozen). As such, they will also depend on position. In addition to this the frozen/unfrozen state of the solid is not a discrete function but a continuum due to the freeze concentration of solutes and subsequent freezing point reduction.

The heat transfer model requires boundary and initial conditions. That is conditions which describe the temperature at the surface of the object and the temperature throughout the object at time zero.

4.2.1.1 Boundary conditions

Boundary conditions can be categorised into four types (Cleland, 1985).

- Surface temperature = ambient temperature [°C] (1^{st} kind)
- Constant heat flux [$J.s^{-1}$] (2^{nd} kind)
- Convective and radiative heat transfer (3^{rd} kind)
- Surface remains at some arbitrary temperature. (4^{th} kind)

Cleland (1985) suggests that the third kind of boundary condition is the most realistic, the first and fourth kinds are in fact special cases of the third and that the second kind of boundary condition occurs infrequently.

4.2.1.2 Initial conditions

When cheese is packed into pallets, the blocks are still cooling from the cook process and so the temperature may or may not be uniform depending on the process used to pre-cool the cheese blocks. In general blocks are cooled to a core temperature of 15°C. The surface temperature after packing can range from the ambient temperature of the pack room to the coolant temperature used in the blast cooler.

4.2.2 MODEL SOLUTION TECHNIQUE

4.2.2.1 ANALYTICAL SOLUTIONS

Analytical solutions exist only for simplified systems with no phase change and relatively constant thermal properties. In these cases, analytical solutions are available for the first and third boundary conditions for simple shapes (Adams & Rogers, 1973). The variable nature of the thermal properties especially around and during the freezing process mean that these solutions will not apply to real situations.

The analytical solutions published in the literature, which explicitly deal with the freezing problem, are poor representations of real world three-dimensional situations. In general, the analytical solutions which exist for freezing systems make the assumption that freezing occurs at a finite temperature and that thermal properties are constant on either side of a discrete phase-change boundary. Such solutions include the Neumann's solution and Plank's equation (Abdalla & Singh, 1985). These solutions are also applicable only to the one dimensional infinitely thick slab in the case of Planks equation and its derivatives, or to the semi-infinitely thick slab in the case of the Neumann model. For these reasons numerical solutions to the heat transfer freezing problem are the most appropriate

4.2.2.2 NUMERICAL SOLUTIONS

Due to the nature of the freezing problem, the simplest method to solve the Fourier equations for real world scenarios, is by using numerical methods. This is due in part to the fact that the only limit to the complexity that can be included in the model is computation time. The best methods available for solution of freezing models are finite element methods and finite difference methods (Cleland, 1985). Which of these methods is used depends on the real situation that they are modelling. Finite difference methods are limited to regular shapes, while finite element methods, which can handle complex geometry's, are intrinsically more complex to formulate and take longer to solve (or compute). The ultimate purpose of this work is to model cuboid blocks of cheese and pallets of many of these blocks. These shapes are of simple regular geometry and as such the use of a finite differences solution scheme is the best approch for this work. (Cleland, 1985).

It should also be noted that these methods should be checked and compared with experimental data to authenticate their validity (Cleland, 1985).

4.2.3 LITERATURE CONCLUSIONS

The formulation of a model to describe the chilling or freezing of a pallet of cheese is relatively simple to achieve. The complications of the phase changes occurring during the chilling and freezing process can be dealt with by modelling the cheese with temperature dependant thermal properties. These properties take into account the latent heat and effects of changing ice content of thermal conductivity. The solution of such a model is not possible by analytical means, due to the complexity brought about by variable thermal properties. As a result a numerical solution is required.

In the past numerical methods have been used to some success to model processes undergoing phase change. It was also found that finite difference solutions can be used for simple shape and finite element solutions are more appropriate for complex geometry's but are intrinsically harder to formulate and longer to solve. It was therefore proposed that for the simple shapes involved in cheese chilling, that finite difference methods should be used to solve the model. The heat transfer model would then be coupled with the results from the proteolysis study to achieve the objective of a working model that could be used to predict the ageing of cheese under a variety of conditions.

4.3 MODEL DEVELOPEMENT

4.3.1 MODEL PURPOSE

Commercial cheddar cheese is produced at around 30°C in blocks about 20 kg in size. The cheeses are blast cooled to 15°C at the surface then packed for maturation. One common method of maturation involves packing 6 layers of 9 blocks into a bulk bin which is boxed in corrugated cardboard and chilled to some temperature (5-10°C) or sometimes frozen (<-5°C). The model to be formulated was required to be able to accurately predict the chilling and freezing behaviour in a cheese pallet stored in an industrial store. This included the prediction of the temperature at any point in the pallet, as a function of time. Due to the variable ambient conditions in a commercial store the inclusion of time variable ambient temperatures was also required. The

resulting temperature predictions were also required to be in a form that allowed the solution of the proteolysis kinetic equations as a function of position in the pallet.

4.3.1.1 CONCEPTUAL MODEL FORMULATION

The system being modelled was a single stack of cheese being chilled or frozen in a cool store. On each pallet nine 20kg blocks are placed in a square. Each block was fresh from the rapid chill process at around 12°C and had been individually vacuum sealed in plastic. In each pallet there were 6 layers of blocks. Each stack of 59 blocks was boxed in one large cardboard box and placed on a wooden pallet. The stack is schematically represented in Figure 4.1 below:

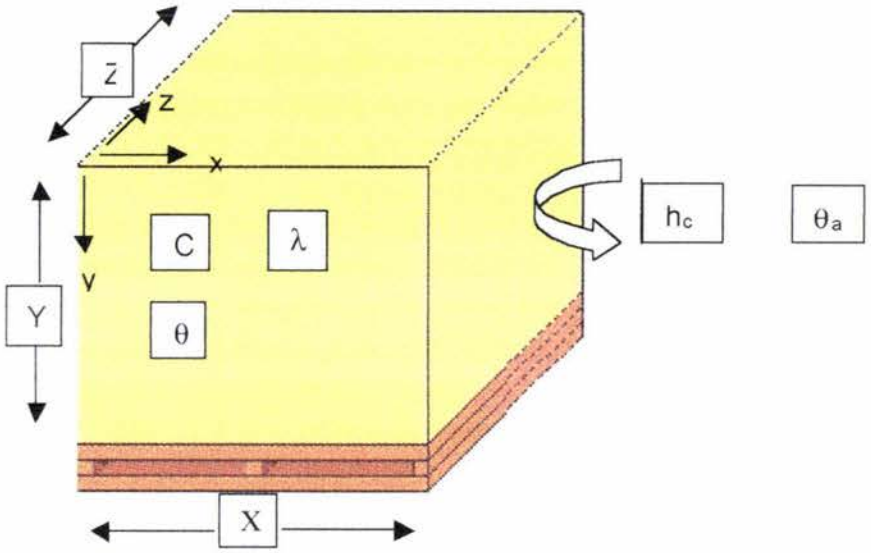

Figure 4.1 Cheese pallet

Where:

t	= time	(independent variable)	[s]
θ	= temperature	(time variable system input)	[°C]
θ_a	= ambient temperature	(time variable system input)	[°C]
h_c	= surface heat transfer coefficient	(system input)	[W/m^2.°C]
x,y,z	= dimensions in space	(dependent variable)	[m]
X,Y,Z	= the size of those dimensions for one pallet of cheese (S.I)		[m]
$\lambda_{(\theta)}$	= thermal conductivity of cheese	(consequential value)	[w.m^{-1}.°C^{-1}]
$C_{(\theta)}$	= volumetric heat capacity	(consequential value)	[J.m^{-3}.°C^{-1}]

($_{(\theta)}$indicates that these variables vary with temperature)

The purpose of the model was to accurately predict the temperature time profile in a real pallet of cheese that may or may not become frozen. The pallet was surrounded by 0.01 m thick cardboard with a constant thickness and thermal conductivity. Heat

removal from the surface was by convection to the surrounding ambient chiller air. The heat capacity and ice-content followed the relation measured in this work section 3.4.1. The cardboard box was included in an effective external heat transfer coefficient.

4.3.2 ASSUMPTIONS

1) Constant density: Mayes and Radford (1983) found less than 0.5% difference in density over a range of cheddar cheese compositions. They found the change in density due to temperature over the range 8-20°C to be a decrease of 1-2 % from 1090-1100 kg/m^3. As the cheese freezes it is expected that the density will decrease also. If 50% of all moisture present in a 30% moisture cheese freezes, then since the density of ice is 920kg/m^3 Rahman (1995), the density of cheese can be expected to change by 12kg/m^3. This results in approximately 1% error. The increase in volume caused by freezing would cause the model to over estimate the thermal conductivity and under estimate volumetric heat capacity also by $\leq$ 1% It follows from these estimates that the assumption of constant density is reasonable for the purposes required in this work.

2) Super cooling will not be significant. The rate of cooling in an industrial freezing process is slow. In the cheese system it is also likely that nucleation sites for ice crystal formation will not be limiting. As a result, it was not expected that super cooling would be significant.

3) No internal heat generation. Internal heat generation could be caused by microbial growth/respiration or chemical oxidative reactions. It would be expected that these reactions would proceed with a rate in proportion to the temperature and would therefore result in observations of slower than predicted cooling and higher than predicted heating. Since the cheeses are sealed in plastic, oxidative reactions would be expected to be small. Heat generation by microflora could be investigated if these situations were observed.

4) Latent heat can be included in an effective heat capacity as has been calculated earlier in this work. The error associated with this assumption is equivalent to the experimental error found in the data. The largest uncertainty is due to the estimation of freezing point using the DSC,

which had an associated error of approximately ± 1°C. due to selection of the appropriate scanning rate.

5) Uniform initial conditions: On observation of temperature data from industry the cheese pallet has uniform initial conditions within ±0.5°C

6) Symmetric cuboid geometry: The size of the pallet was measured four times in each axis with an error of <±10mm. This corresponds to a maximum difference of less than1%. Therefore modelling the system using regular geometry is reasonable

7) Variable time-temperature ambient conditions. Observations of industrial stores showed that the temperature commonly varies by up to 4°C. This indicated that it was necessary to have variable conditions.

8) Homogenous mass within the cardboard box and can be assumed as one entire effective medium for conductivity. This approach has been taken in the past and found to work well {Jamieson, Cleland, et al. 1993 #720}.

9) Thermal conductivity is composition dependant. The data collected on the DSC showed that the initial freezing point changes with composition. As a result it follows that thermal conductivity will also be a function of composition. This suggests that care must be taken to use the ice fraction data collected for the cheese that closely matches the cheese composition of interest.

10) Significant air fraction within box in cheese pallet. It was found that air makes up to 6% of the volume within a pallet of cheese. Since the air lie between blocks of cheese and therefore normal to the direction of heat flow it is sensible to use the series model (Equation 3-15) to include air {Jamieson, Cleland, et al. 1993 #720}. For example, for a pallet of cheese with air $\lambda = 0.024$ $W.m^{-1}.°C^{-1}$ and cheese $\lambda = 0.3$ $W.m^{-1}.°C^{-1}$. This results in a pallet of $\lambda = 0.18$ $W.m^{-1}.°C^{-1}$. The air is therefore significant and is required to be included.

11) No effect of plastic shrink-wrap around cheese blocks: Since the plastic cover is thin (≅ 1mm) and the conductivity 0.29 is close to that of cheese. The error caused by making this assumption can be expected to be small.

12) Uniform heat transfer across surface of pallet. In some coolstores air velocity could vary with position. During the experiment the temperature at the surface was measured to be uniform within <0.5 °C. This observation supports this assumption.

4.3.3 EQUATION FORMULATION

A heat balance can be applied to any internal differential three-dimensional space to give:

$$C_{(\theta)}\frac{\partial\theta}{\partial t}=\frac{\partial}{\partial x}\left(\lambda_{(\theta)}\frac{\partial\theta}{\partial x}\right)+\frac{\partial}{\partial y}\left(\lambda_{(\theta)}\frac{\partial\theta}{\partial y}\right)+\frac{\partial}{\partial z}\left(\lambda_{(\theta)}\frac{\partial\theta}{\partial z}\right)\text{for t}>0\text{and }0>x,y,z>X,Y,Z$$

Equation 4-3

Boundary conditions are:

$$\lambda_{(\theta)}\cdot\left(\frac{\partial\theta}{\partial x}\right)=h_c\cdot(\theta_a-\theta)\qquad\text{for t}>0\text{ and }x=0$$

$$\lambda_{(\theta)}\cdot\left(\frac{\partial\theta}{\partial y}\right)=h_c\cdot(\theta_a-\theta)\qquad\text{for t}>0\text{ and }y=0$$

$$\lambda_{(\theta)}\cdot\left(\frac{\partial\theta}{\partial z}\right)=h_c\cdot(\theta_a-\theta)\qquad\text{for t}>0\text{ and }z=0$$

symetry boundary conditions at the pallet centre

$$\lambda_{(\theta)}\cdot\left(\frac{\partial\theta}{\partial x}\right)=0\qquad\text{for t}>0\text{ and }x=X/2$$

$$\lambda_{(\theta)}\cdot\left(\frac{\partial\theta}{\partial y}\right)=0\qquad\text{for t}>0\text{ and }y=Y/2$$

$$\lambda_{(\theta)}\cdot\left(\frac{\partial\theta}{\partial z}\right)=0\qquad\text{for t}>0\text{ and }z=Z/2$$

Equation 4-4

For uniform initial conditions:

Chilling experiment:

$\theta=\theta_{inc}$ for t = 0, 0<x<X, 0<y<Y, 0<z<Z

Equation 4-5

4.4 MODEL SOLUTION

The computer program RADS (Cleland and Cleland 1991) was used in this work to solve the formulated model. This applies the finite difference method and requires user input for the dimensions, thermal properties, and cooling regime. The use of a pre-tested numerical solution package offered the advantages of an implicit finite difference solver that had been extensively used in the past for solving heat transfer models for freezing systems. The package required input of the thermal properties in the form of text files. The input data as required by RADS are discussed below.

4.5 SYSTEM INPUT PARAMETERS

4.5.1 SIZE

The model formulated can handle any size. Typically the dimensions of a pallet of cheese are:

X = 1.1 m

Y = 1.0 m

Z = 0.9 m

In addition to the object dimensions, RADS also requires that a space step be defined in order to divide the three dimensional volume into equal sized nodes for the purpose of numerical integration. The smaller the space step the less numerical error will be incurred but the greater the computation time required. RADS has a maximum of 10 nodes in each direction over half a dimension width. In general 10 nodes are sufficient to obtain accurate predictions from finite difference solutions.

4.5.1.1.1 Ambient Conditions

The numerical solution has the ability to apply varying ambient conditions. However, this is limited to 50 time-temperature positions and one constant heat transfer coefficient. These conditions are supplied in the form of a text file.

4.5.2 HEAT TRANSFER COEFFICIENT

The surface of the pallet of cheese is covered in a cardboard box of 10mm thick. The thermal conductivity of cardboard is 0.061 $W.m^{-1}.°C^{-1}$ (Jamieson, *et al.*, 1993)

10mm cardboard at $\lambda = 0.061$ W/m.K. The air flow through the store is sufficiently high such that it is expected that the thermal resistance will be dominated by the cardboard. For this reason the thermal conductivity is taken as hc = 6.1 $W.m^{-2}.K^{-1}$

4.5.3 Initial Conditions

For a three dimensional situation RADS requires uniform initial temperature. The program will handle any given temperature. The temperature of a pallet prior to chilling is typically 12-15°C

4.5.4 Time frame

In order to solve the model RADS requires the input of a time data file. This file includes a period over which to carry out the simulation, a time step interval to apply to the numerical solution, and an output time interval to exhibit the resulting data. It is suggested by Cleland (1984) that the time step used follows the relation below:

$$\Delta t < \frac{C\Delta x^2}{2\lambda}$$

Equation 4-6

In this case this approximates to $\Delta t<2000000\times0.05\times0.05/2/0.3 = 8300$ seconds or just over 2 hours. The time step used in the program may be as low as 1 second (although this would be prohibitively time consuming).

4.5.5 Thermal conductivity Data

A conductivity vs temperature data file is required by the RADS program. The conductivity of materials being frozen changes concurrently with changing ice fraction. To calculate the conductivity in bulk cheese the effective medium theory was used:

$$\sum_{i=1}^{n} V_i \left(\frac{\lambda - \lambda_i}{\lambda_i - n \cdot \lambda} \right) = 0$$

Equation 3-12

In order to apply this to cheese with different ice contents, the conductivity of component parts is required. The cheese can be considered to be a mixture of ice, water, and remaining solids. Since the conductivity of water and ice are known, the conductivity of the remaining solids component can be back calculated from the rearrangement of the effective medium theory using a literature value of the thermal

conductivity for an unfrozen cheese (0.3 $W.m^{-1}.°C^{-1}$ Rahman, 1995)with a known moisture content using Equation 4-7.

$$\lambda_1 = \frac{2\lambda_2\lambda - 3x_1\lambda_2\lambda - 2\lambda^2}{\lambda - 3x_1\lambda - \lambda_2}$$

Equation 4-7

4.5.5.1 CHEESE CONDUCTIVITY

With all the component parts known the conductivity of bulk cheese can be built up by the successive calculation of combined conductivity of component pairs using the equation below.

$$2\lambda^2 + \lambda(3V_1\lambda_2 - 3V_1\lambda_1 + \lambda_1) - \lambda_1\lambda_2 = 0$$

Equation 3-13

Using ice fraction data obtained by DSC the water-ice mixture thermal conductivity can be calculated first, this allows the calculation of the cheese thermal conductivity by combining the ice-water mixture and solids thermal conductivity. This results in a cheese conductivity relation vs. temperature below freezing.

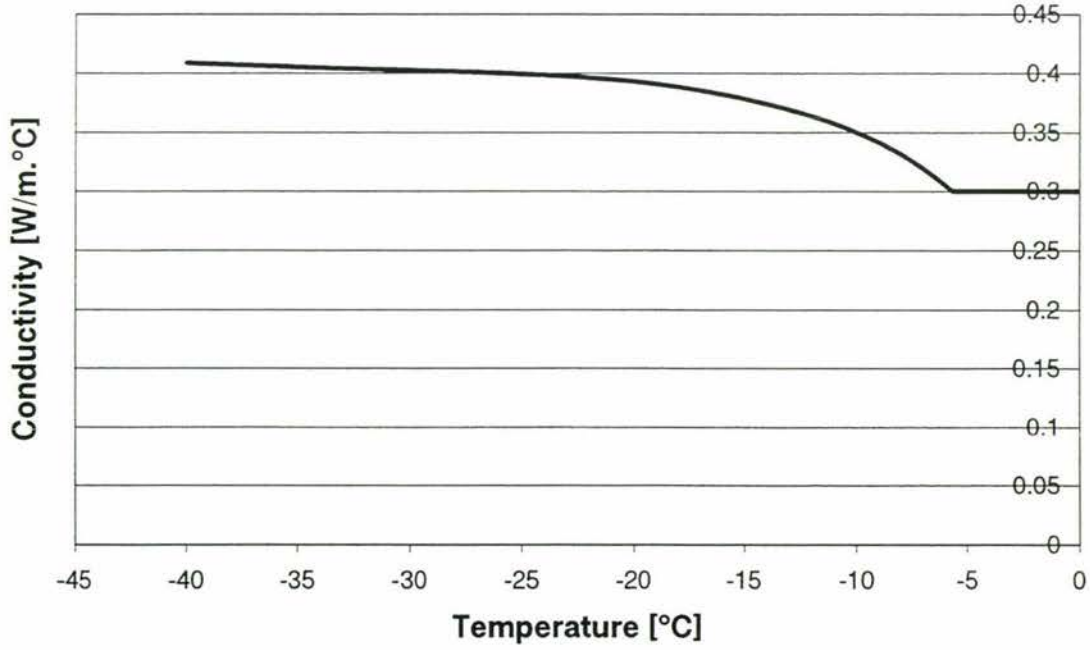

Figure 4.2 Thermal conductivity used in heat transfer model

4.5.5.2 BULK BIN CONDUCTIVITY

To account for the void fraction in bulk storage bin the series model was used as the air gaps lie at right angles to heat flow (Jameison, *et al.*, 1993).

4.5.6 VOLUMETRIC HEAT CAPACITY

The heat capacity measured earlier in this work was multiplied by the density to give volumetric heat capacity vs. temperature. An example of heat capacity is given below for a typical cheddar cheese. When multiplied by a constant density the scale will change but the trend remains the same.

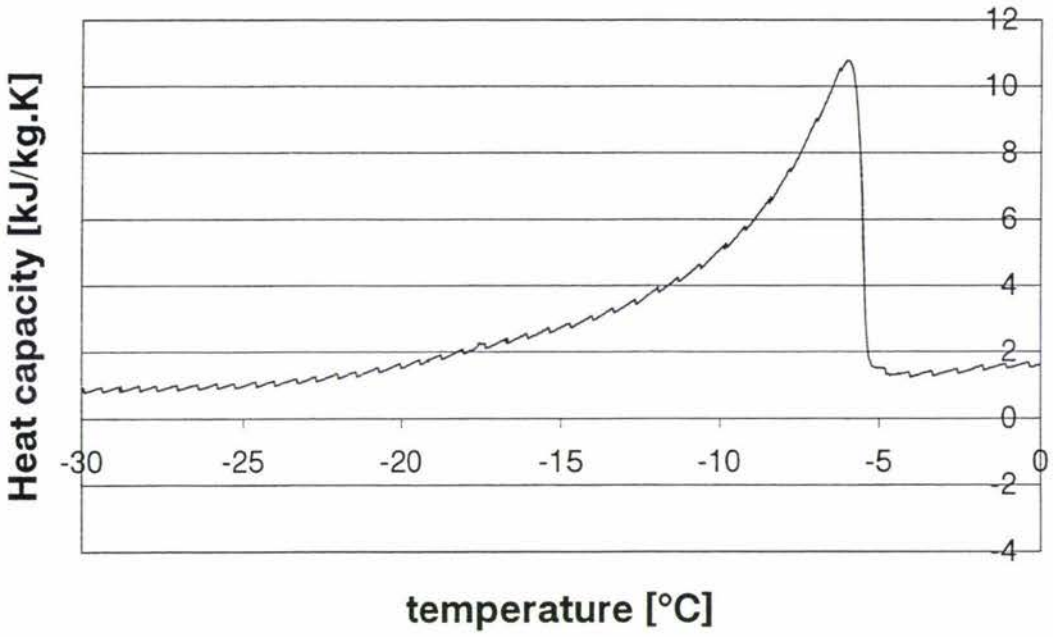

Figure 4.3 Heat capacity used in heat transfer model

4.6 NUMERICAL ERROR CHECKING

A study to determine if there was significant errors caused by using a time step or space step that was too large was carried out. The maximum time step used for stability purposes is given by:

$$\Delta t_{max} = \frac{C\Delta x^2}{2\lambda}$$

Equation 4-6

In general the space divisions used should be as small as possible until the point at which rounding error becomes significant. Cleland (1985) suggests using symmetry conditions to reduce the simulation by half over each dimension. This results in $1/8^{th}$ the volume required for simultion. With a maximum of ten space divisions in each dimension for simulation of heat transfer available in RADS. This gives the space divisions outlined below:

$\Delta x=X/20$, $\Delta y=Y/20$, $\Delta z=Z/20$.

This gives a resulting output of $11\times11\times11=1331$ nodes over the $1/8^{th}$ volume. Different simulations were then carried out. The bulk freezing simulation was repeated at 500 second time steps and 250 second time steps for which the results showed deviation of less then 0.05°C over the entire period of the simulation for all thermocouple positions. This indicated that numerical errors were not significant and that the model could then be compared with experimental data

4.7 MODEL VALIDATION

4.7.1 NUMERICAL SOLUTION DATA VISUALISATION

The numerical solution produces the time temperature profile for each of the 1331 nodes simulated in the problem. Outputting this data at 500 second intervals over 21 days produces. 13975500 data points for one simulation. In order to visualise this information, the data was read into a four dimensional array in Matlab, which could be easily manipulated. The Matlab script file used for this is given in Appendix section 7.3.1.

In order to compare the real data gathered experimentally to the model, a non-invasive method of thermocouple positioning was chosen to coincide with simulation nodes, which would experience the extremes of temperature that would be expected. Those positions were those nodes from the pallet center horizontally out to a surface corner. The actual positions of thermocouples are illustrated below in Figure 4.4. To compare the model data with experimental data the four dimensional array was de-compiled into the equivalent thermocouple readouts at those positions. The relevant MATLAB script used to achieve this is given in Appendix section 7.3.2.

4.7.1.1.1 Experimental data collection

Collection of commercial chilling and freezing data was carried out at Kiwi Dairies, Hawera, New Zealand during November-December of the 1999 season. The pallet was packed as follows; Each 20 kg block was wrapped in an airtight plastic bag. Nine blocks were placed in a square configuration at each level and 6 levels were packed into each pallet. The final dimensions of the cheese were: 1150 x 1060 x 930mm high. The box was made of corrugated cardboard 10mm thick.

Thermocouples were placed between the two central layers of cheese (vertical centre) at 70mm intervals from the corner to the centre. Two thermocouples were placed at the center. Figure 4.4 illustrates the packing and thermocouple arrangement.

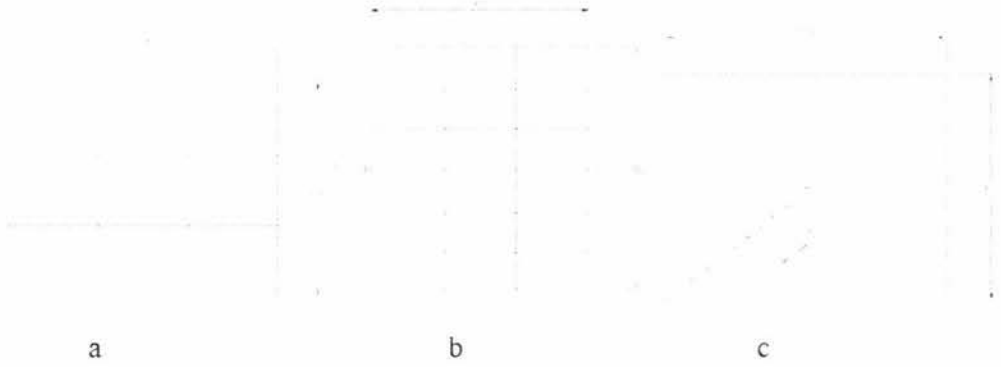

a b c

Figure 4.4: a: Cheese pallet (plan), b: Cheese pallet (side elevation), c: Thermocouple positions (plan)

On the outside of the box four thermocouples were taped in place using aluminium tape halfway into the centre from each corner. Temperatures were logged every five minutes for a period of three weeks in a chiller operated at 2°C. The results are plotted below in Figure 4.5

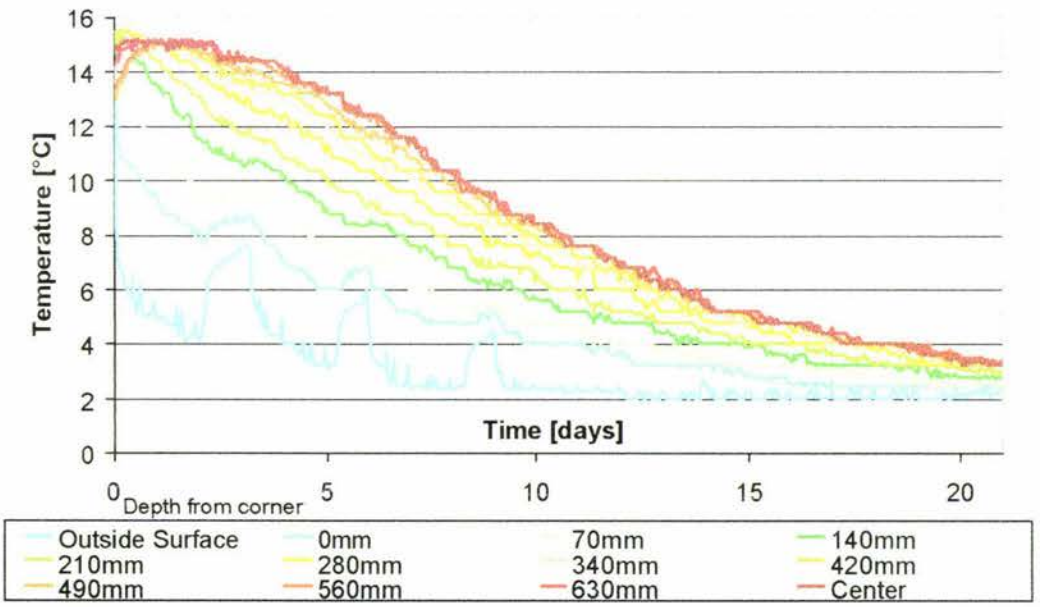

Figure 4.5 Temperature-Time profile for a pallet undergoing chilling

After chilling the pallet to a uniform temperature (2.5°C) the pallet was placed in a freezing room at –12°C for 20 days and the data logged as outlined above for the chilling trial. These freezing data have been plotted below Figure 4.6.

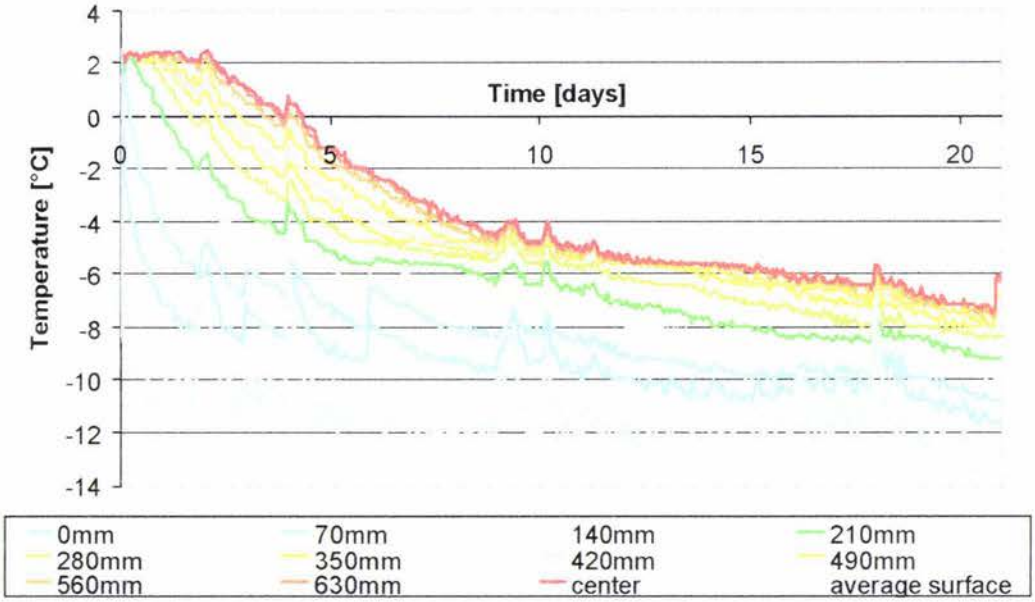

Figure 4.6 temperature -time profile for a pallet undergoing freezing

One dimensional freezing data was also collected, to investigate the validity of the freezing data using a single 25mm thick slab. Thermocouples were placed through the cheese into the centre at regular intervals and the temperature logged. The cheese began with an initial temperature of 1°C and was placed in a plate freezer operated at ≡-27°C. A 2.5mm thick section of card was placed between the cheese and the freezing plates. The card resulted in a heat transfer coefficient of 24.4 $W.m^{-2}.°C^{-1}$. The slab was ≡ 10×10 cm. The edges were packed with expanded polystyrene. This ensured that data from the slab would approximate the 1 dimensional model. The results of the 1D trial are plotted below Figure 4.7.

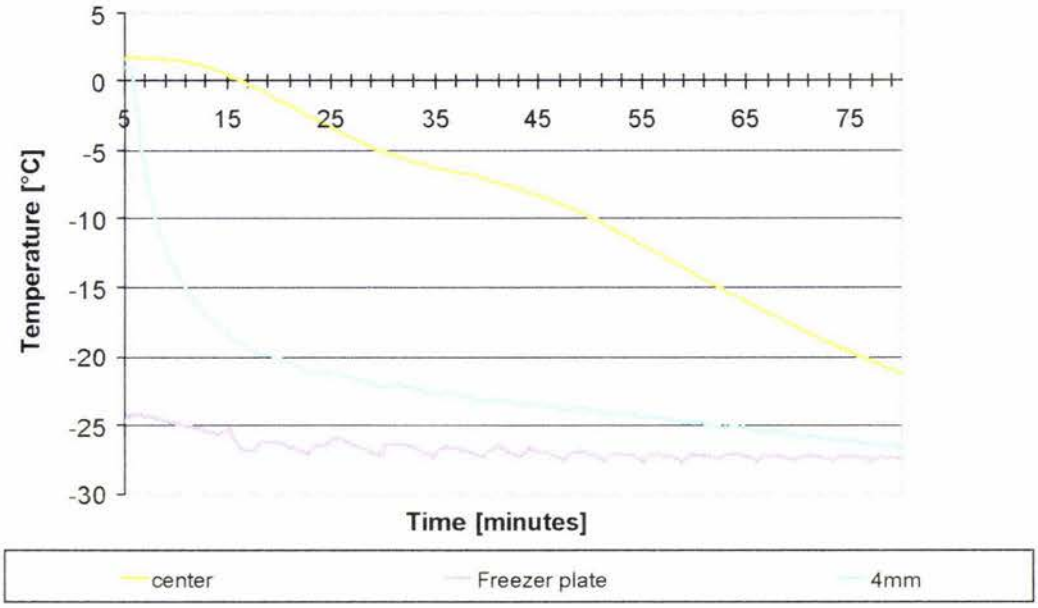

Figure 4.7 Center/surface temperature for a slab undergoing freezing

4.7.2 MODEL PERFORMANCE

The model was used to predict temperature using a smoothed measured surface temperature for the driving force and the thermal properties stated above. The predictions obtained for the chilling in a commercial storeroom, freezing in a lab scale plate freezer and commercial freezing of a pallet have been graphed below in Figure 4.8, Figure 4.9, and Figure 4.10 respectively. Only the centre and outside surface data have been graphed for illustrative purposes. The system-input data measured for these simulations are summarised below.

4.7.2.1 RADS INPUT DATA VALUES

To test the model the program developed by Cleland and Cleland (1991) was used. The system inputs required were entered into a preparation file following the example in Appendix section 7.4 The data values used are outlined below.

4.7.2.1.1 Size

X = 1150 ± 10 mm

Y = 1060 ± 10 mm

Z = 931 ± 10 mm

Each dimension was measured four times and averaged in each direction using tape measure

4.7.2.1.2 Ambient Conditions

For the industrial trials the temperature on surface of cardboard box was measured and averaged over 10 hour periods to give 50 time temperature point over the period of the simulation. The maximum deviation from the model surface temperature used was less than 2°C and the average deviation was less than 1°C. The actual temperatures used in the simulation have been plotted alongside measured data below (Figure 4.8, Figure 4.9, and Figure 4.10).

Since the surface data was measured the heat transfer coefficient needs to be calculated for heat transfer only across the cardboard box. In this case the cardboard was measured to be 10 ± 1 mm thick at λ = 0.061 W/m.K (Jamieson, *et al.*, 1991) gives:

hc = 6.1 ± 0.6 W/m.K

For the slab freezing experiment 3±1mm of cardboard was used between the cheese and the freezing plates resulting in

hc = 20 ± 7 W/m.K

4.7.2.1.3 Initial Conditions

Uniform initial temperatures were used for each simulation These are given for each in the table below:

	Pallet Chilling	Pallet freezing	Slab freezing
θi [°C]	12 ± 0.5	2.5 ± 0.5	4 ± 1

Table 4-1 Heat transfer initial temperatures

4.7.2.1.4 Time frame

The time frames and time steps are summarised in Table 4-2 below

	Pallet Chilling	Pallet freezing	Slab freezing
Simulation time	500 [hours]	500 [hours]	5360 [seconds]
Time step	250 [seconds]	250 [seconds]	2 [seconds]

Table 4-2 Heat transfer simulation times

4.7.3 PREDICTIONS

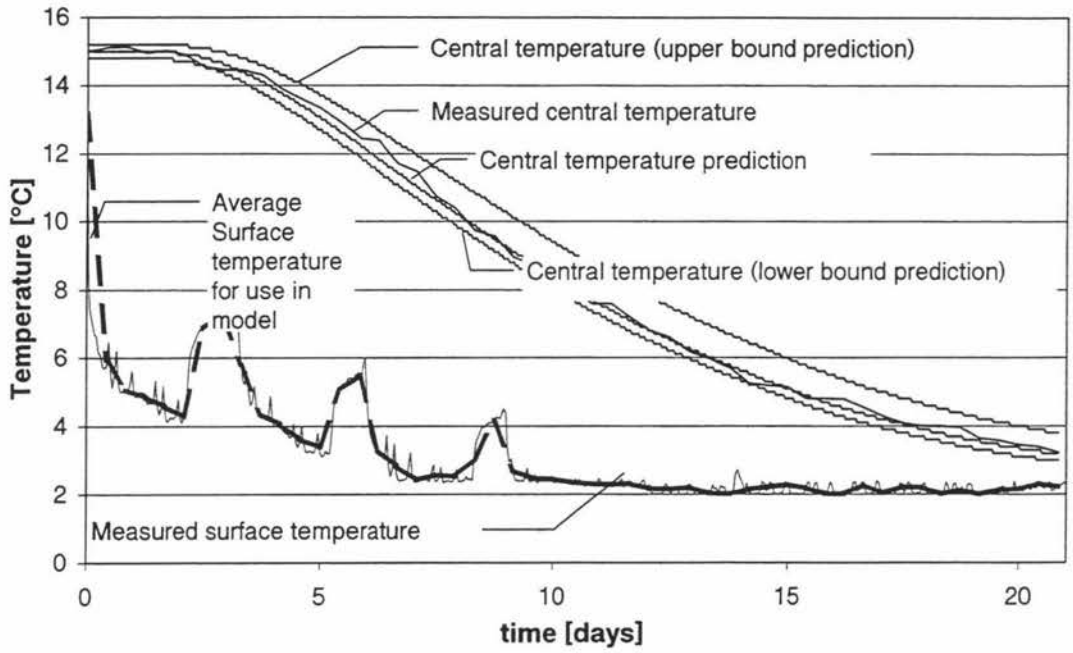

Figure 4.8 Model performance for experimental chilling data

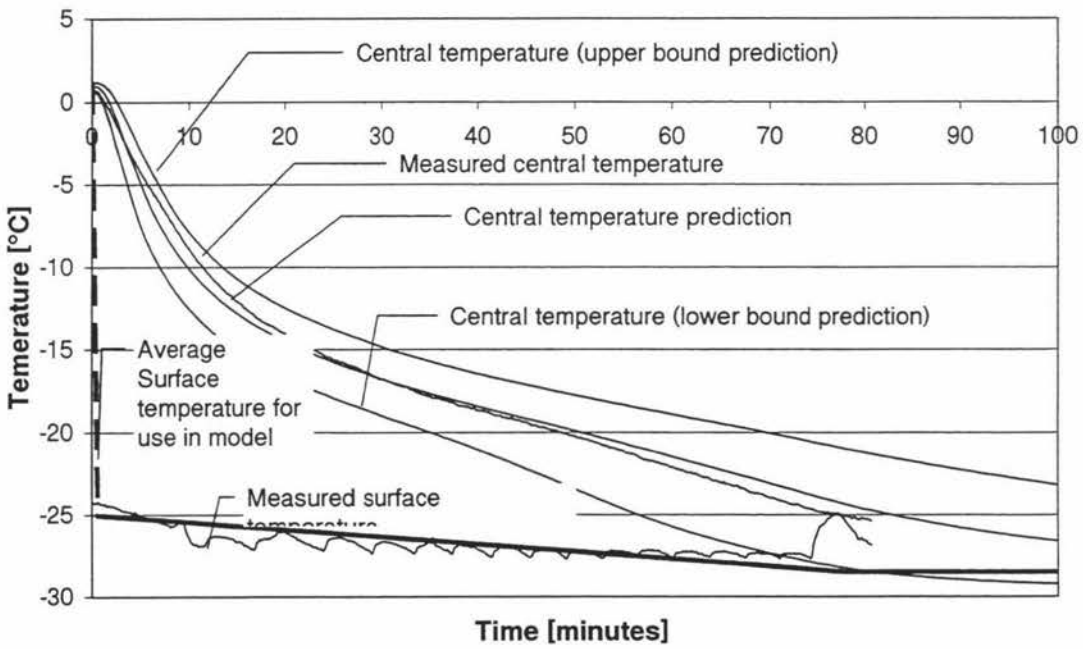

Figure 4.9 Model performance for experimental 1D freezing data

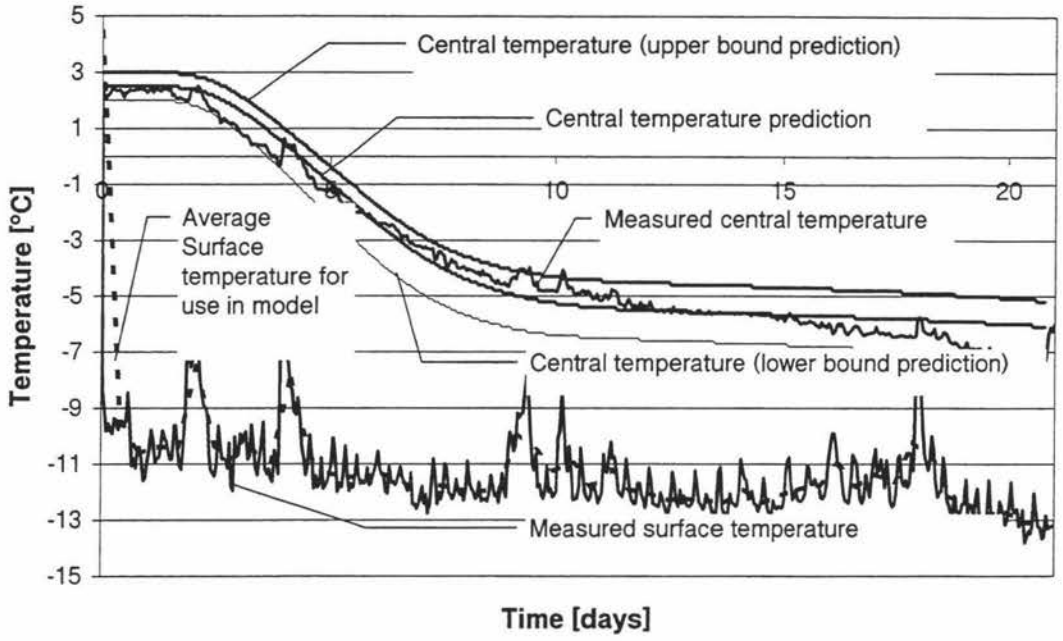

Figure 4.10 Model performance for experimental freezing data

4.7.3.1 SENSITIVITY ANALYSIS

For each of the system inputs used in the simulation, it was determined which of its experimental bounds (high or low error margins) would increase or decrease the temperature measured at any point in the cheese pallet. Two more simulations were completed in which the appropriate combination of those high or low error bounds were used. This provided a maximum and a minimum bound on the temperature prediction that could be made considering the uncertainty in the system input data.

The model centre temperature fits well for the measured chilling data indicating that the model gives excellent predictions above freezing. The larger error bounds observed in the freezing data are due to the error in heat capacity data measured using a differential scanning calorimeter. The deviation from the measured data is also likely to be due to this as the lack of fit occurs to the greatest extent around the freezing point, which is where the largest deviation in heat capacity data was observed. Further calorimetric data is required to reduce the error here. It is important to note however that the largest source of error in the estimation of the temperature at any point in the cheese is due directly to the estimate of freezing point. The freezing point is the temperature at which the temperature profile across the pallet constricts as latent heat is removed. Any error in the freezing point causes a vertical shift of the model response on the graph to

the same degree as the error. This is therefore an indication that accurate information is required on the freezing point for any cheese investigated. It can be seen from the predictions compared to the experimental data, that the model performs very well.

4.7.4 Conclusions

The formulated model successfully describes the observed temperature in the centre of a pallet of cheese under going chilling. The model was also used to predict temperature time profiles in freezing cheese. The error bounds on the predictions could be improved further through more accurate specific heat data, however the accuracy of predictions was sufficiently good for the purposes of estimating the degree of proteolysis required in this work. The next chapter outlines how the results of predictions of the heat transfer model described here can be combined with the proteolysis kinetics described in chapter 2.

CHAPTER 5

PRODUCT VARIABILITY IN A PALLET OF CHEESE DUE TO HEAT TRANSFER

5.1 INTRODUCTION

During the chilling process, a pallet of cheese undergoes a non-homogeneous temperature-time profile through the pallet. This may or may not result in non-homogeneous cheese. Previously in this work (chapter 2) the relationship between proteolysis of α_{s-1}casein and temperature was investigated and Arrhenius constants for the proteolysis reaction were determined for a number of cheeses. In chapter 4 a model was developed to describe the time temperature relationship within a pallet of cheese in a commercial chiller. As the cheese pallet cools, a temperature gradient is observed from the warm centre of the pallet to the cooler surface. Since the proteolysis reaction proceeds faster at a higher temperature, the level of proteolysis observed across a fully chilled or frozen cheese would be expected to exhibit some non-homogeneity. In order to quantitatively investigate that level of non-homogeneity, a model was required to combine the rate of proteolysis data with the chilling/freezing data.

The specific objectives of this chapter were to;

1) Formulate a mathematical model that determines the extent of the proteolysis reaction for a piece of cheese undergoing some given temperature-time profile.
2) Incorporate the time temperature data produced by the model developed in chapter 4.
3) Use the model to predict the level of proteolysis for any position in a real pallet of cheese undergoing a freeze/thaw process.

5.2 MODEL FORMULATION

The time temperature relationship in a commercial pallet of cheese has already been successfully modelled in chapter 4. The model needs only to be able to model some small piece of cheese undergoing an arbitrary time-temperature profile. Once completed the model can then be applied to the temperature time history predicted from the model derived in chapter 4.

5.2.1 VARIABLES

t	= time	(Independent variable)	[hr]
X_c	= extent of α_{s1}casein depletion	(Dependant variable)	[-]
k	= proteolysis rate constant	(Consequential variable)	[hr^{-1}]
k_o	= Arrhenius rate constant	(Consequential variable)	[hr^{-1}]
E	= activation energy of reaction	(System input)	[J/mol]
R	= gas constant (8.314)	(System input)	[J/mol]
θ	= temperature	(Time variable system input)	[°C]

5.2.2 ASSUMPTIONS

Those assumptions required for the model in chapter 4 (although not stated explicitly) are also assumed here. In addition the assumptions listed below were made also;

1) The proteolysis reaction follows first order kinetics
2) The first order kinetics follow Arrhenius law
3) The Arrhenius pre-exponential function follows the geometric empirical model developed in this work in chapter 2

5.2.3 EQUATION FORMULATION

An unsteady state mass balance can be applied to the cheese using first order rate kinetics

Mathematically, in terms of the extent of reaction this can be expressed as:

$$\frac{dX_c}{dt} = k(1 - X_c) \text{ for } t>0$$

Equation 5-1

With the initial conditions:

$X_c=0$ at $t=0$

The algebraic equation describing the rate constant k [hr^{-1}] is the relationship described in chapter 2 Equation 2-14:

Rate constant relation:

$$k = k_c[MNSF]^{kw}[\text{rennet(normalised)}]^{kr} e^{\left(\frac{-E}{R(\theta+273.15)}\right)} \ [hr^{-1}]$$

Equation 2-14

Where the indices found for cheddar cheese in chapter 2 are given below:

$$k=e^{16}\,[MNFS]^{3.9}\,[\text{rennet (normalised)}]^{0.63}(1/24[\text{day/hr}])\exp(-64000/(R.T))$$

Equation 2-16

As the reaction rates observed at or below –10°C in chapter 2 were negligible the reaction rate k was assumed to be 0 at temperatures below –10°C and follow the relation described above only for temperatures greater than –10°C.

5.3 MODEL SOLUTION

The model was solved numerically using the program MATLAB 5.2 The function ODE45 was employed to numerically solve the rate equation. This was carried out for each of the 1331 positions in the pallet of cheese as defined in the heat transfer model formulated in chapter 4. At any time during the numerical solution for the proteolysis reaction in the pallet the temperature at every position was calculated by interpolating the time-temperature data from the four-dimensional data array produced from the heat transfer solution. The solution produced by the ODE45 function is another four-dimensional array containing the extent of reaction at 1331 different positions in three dimensions changing with time. The programs used here are given in the appendix section 0.

5.3.1 MODEL CHECKING

Mathematical correctness of the reaction model was tested by assuming a constant temperature for the entire time period and comparing the numerical solution results the analytical solution for a first order reaction. The analytical solution for a single reaction at a constant temperature is given below:

$$X_c = 1 - e^{-kt} \qquad \text{for } t>0$$

Equation 5-2

The maximum difference between the analytical solution and the numerical solution for the value of X_c (percentage) was 5.7e-009 so the numerical solution can be seen to be mathematically correct. Since the numerical solution was found to be so close to the analytical solution (error <0.000006%) over 2000 hours the model can be said to be mathematically correct and have negligible numerical error.

5.4 MODEL APPLICATION

The model formulated above was used to investigate the proteolysis in a pallet of cheese undergoing a given temperature regime, in order to quantify the variability of the level of α_{s1}casein remaining throughout the pallet. Three possible industrial applications have been investigated; Investigating the level of proteolysis in a pallet of fresh cheese being chilled to 2°C, investigation of the level of proteolysis of α_{s1}casein in a pallet being frozen to –15°C and then thawed to 12°C, and investigation of the level of proteolysis of α_{s1}casein being frozen to –15°C and thawed to 2°C.

5.4.1 PROTEOLYSIS IN A PALLET OF CHEESE BEING CHILLED

One industrial application of this model is the process of chilling fresh cheese. Typically a pallet of cheese is packed at 12°C and may be chilled to 2°C. A simulation was carried out where the mathematical model developed in chapter 4 was used to simulate a fresh pallet of cheese chilled to 2°C. The system inputs used were the same as used in chapter 4 with the exception of the ambient conditions and experimental run time.

Initial Conditions:

Uniform initial temperature

= 12 °C

Ambient conditions:

-15°C for 0>t>1000 [hrs]

12°C for 1000>t>2000 [hrs]

Time frame:

Time period = 2000 hours

Time step = 250 seconds

The centre temperature as calculated by the heat transfer model is plotted in Figure 5.1 below:

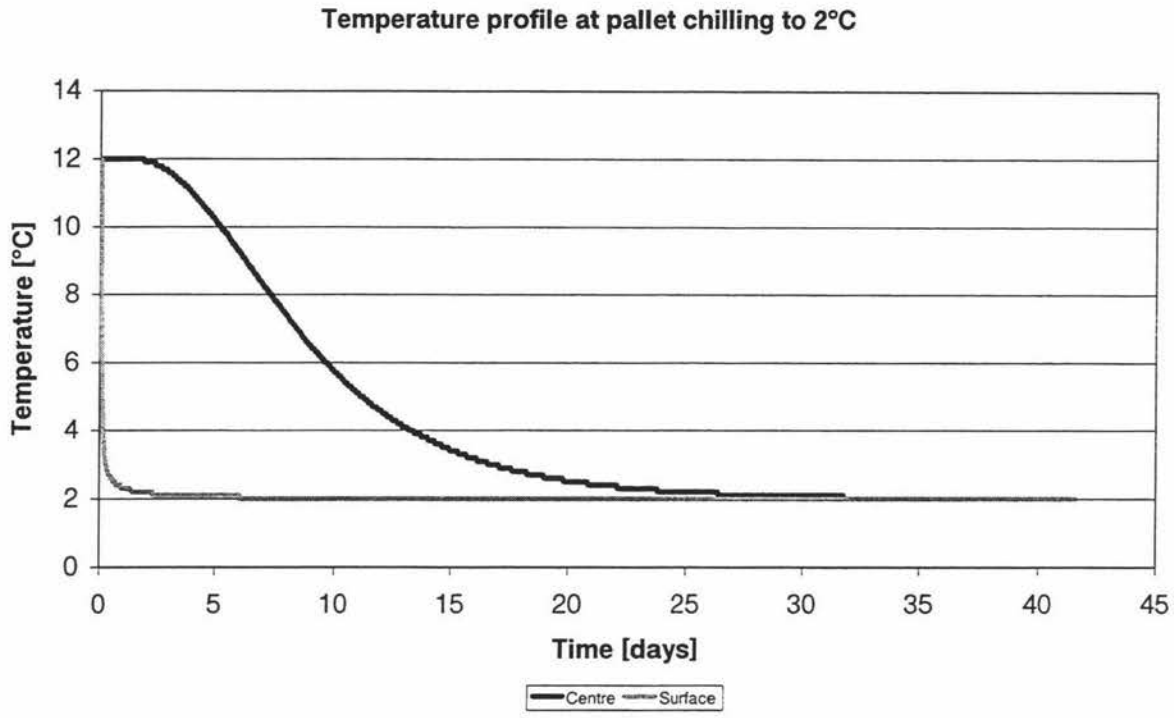

Figure 5.1 Time-temperature profile for a pallet of cheese chilled to 2°C

Here the surface temperature reaches 2°C instantly and the centre temperature reaches 2°C after ≅ 30 days. It is this variation in temperature across the pallet which could cause variation in the level of proteolysis observed throughout the pallet. To determine what the variation in cheese functionality would be, the kinetic model developed above was used to determine the extent of the proteolysis of α_{s1}casein reaction. In order to observe the largest effect the cheese simulated in the proteolysis model was input with a high moisture content and high level of rennet.

	Levels
MNFS	57.90%
Rennet (normalised)	10.4

The extent of proteolysis of α_{s1}casein has been plotted for in Figure 5.2 for the outside surface corner, the centre and the mass average.

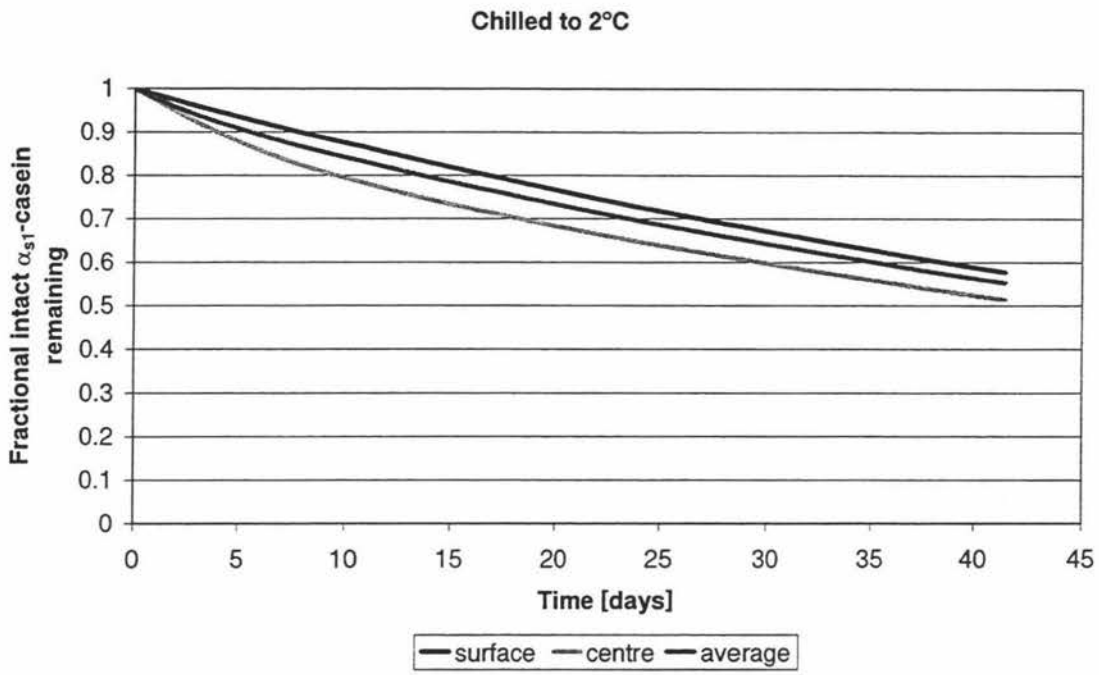

Figure 5.2 Level of proteolysis in a pallet undergoing chilling

It can be seen from this plot that the centre of the cheese pallet changes noticeably faster than the outside surface corner for about the first 15 days. After this initial period the centre temperature has dropped to ≅3°C at this point there is little difference in temperature across the pallet (≤ 1°C). This means that the rate of proteolysis across the pallet begins to even out, as illustrated by the lines in Figure 5.2 becoming parallel. As the level of α_{s1}casein is depleted, the lines in Figure 5.2 begin to converge again. The variation across the pallet is best illustrated by calculating the standard deviation in the extent of reaction across the 1331 positional nodes used in the simulation and plotting this against time. This has been carried out for this chilling simulation and is plotted in Figure 5.3 below:

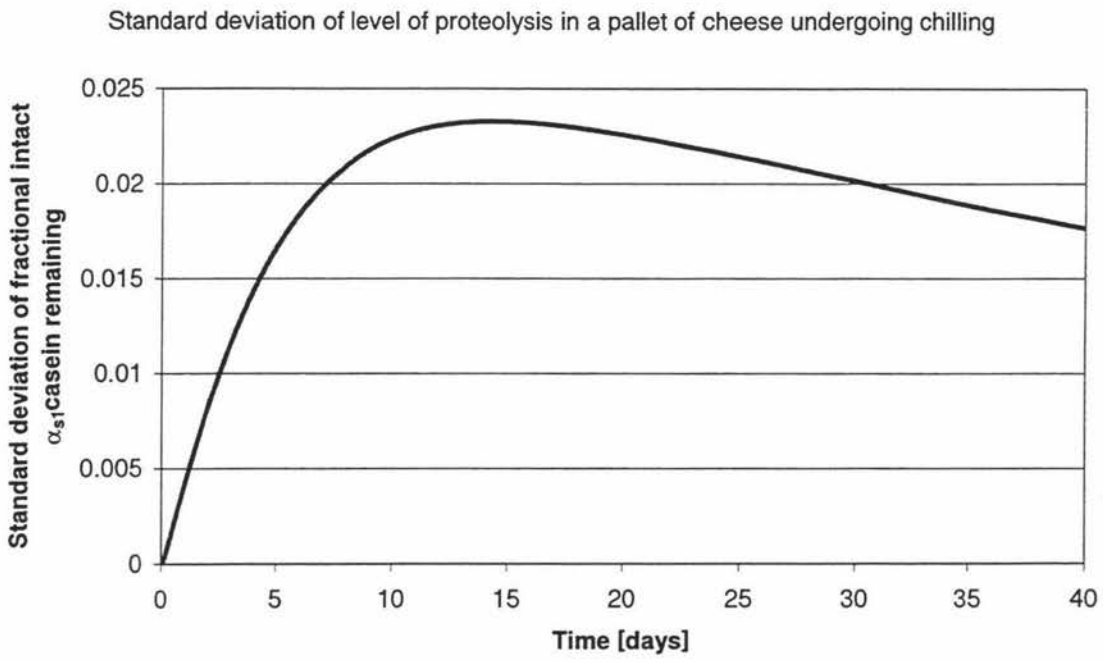

Figure 5.3 Variation in proteolysis in a pallet of cheese undergoing chilling

Here the trends discussed above can plainly be seen in Figure 5.3. As the pallet is chilled, the outside cools quickly and this reduces the rate of the proteolysis reaction. At the centre the α_{s1}casein continues to be broken down at a faster rate due to the high temperature observed. As the temperature variation across the pallet reduces (ie as the centre temperature approaches the ambient temperature), the rate of reaction experienced across the whole pallet approaches the same value and the variation in the level of proteolysis across the pallet reaches a peak at about 15 days. Finally, as the level of intact α_{s1}casein is reduced, the reaction rate at the centre became lower than the surface and the levels of remaining intact α_{s1}casein begin to converge. This is illustrated by the variation across the pallet reducing over time after 15 days.

5.4.2 PROTEOLYSIS IN A PALLET OF CHEESE UNDERGOING A FREEZE THAW CYCLE

Using the model formulated in chapter 4 a simulation of a pallet of cheese undergoing a freeze thaw cycle was carried out. Again the system inputs used were the same as used in chapter 4 with the exception of the ambient conditions and experimental run time. These are given below:

Initial Conditions:

Uniform initial temperature

= 12 °C

Ambient conditions:

-15°C for 0>t>1000 [hrs]

12°C for 1000>t>2000 [hrs]

Time frame:

Time period = 2000 hours

Time step = 250 seconds

The resulting temperature output has been plotted (Figure 5.4)for the centre of the pallet below:

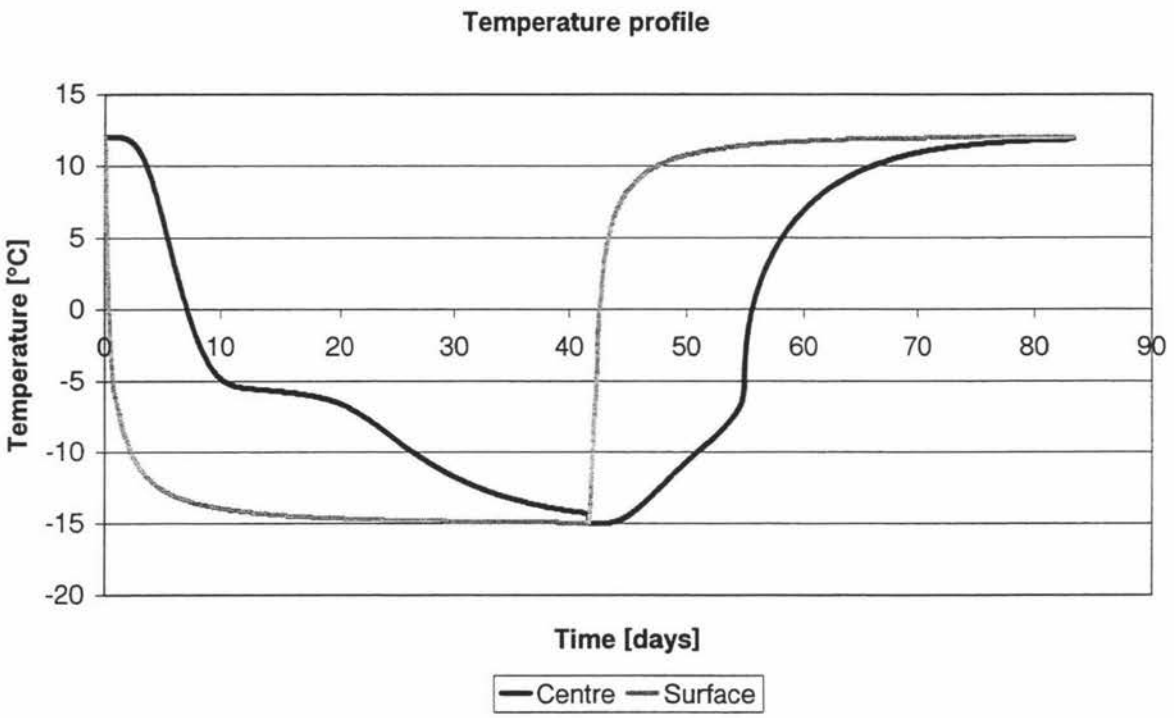

Figure 5.4 Time-temperature profile for freeze thaw cycle 12 to -15 to 12°C

The ambient conditions begin at –15°C. The period up to day 10 is the centre cooling to its freezing point. The period from days 10-20 is the centre freezing. The period from day 20 to day 40 is the centre of the pallet cooling to ambient (–15°C). After 2000 hours the ambient conditions are set to 12°C to simulate thawing. From day 41 to day 55 the centre is thawing. After day 55 the centre is completely thawed and is warming to ambient (12°C). When the

temperature is high the reaction rate will be high and the level of intact α_{s1}casein will degrade quickly. When the temperature is low, the level of α_{s1}casein will degrade at a slower rate. When the temperature drops below –10°C the reaction rate will be negligible and so the level of intact α_{s1}casein will remain constant with time.

The complete four-dimensional data set was then used as a system input for the reaction model. The integration of the rate data using this temperature data set was carried out twice. Firstly with a set of MNFS and rennet at the low extreme of investigated values from chapter two so as to give a k value at the low end of the reaction rates as observed in chapter two, and secondly with high values of MNFS and rennet as with section 5.4.1 above in order to observe a large variation in the level of proteolysis. i.e.

	low k_o	high k_o
MNFS	51.10%	57.90%
Rennet	3.3	10.4

Table 5-1 Cheese compositions used for freeze/thaw simulations

The MATLAB program integrates the rate equation and returns a four dimensional array of the extent of the proteolysis reaction (X_c) at 11×11×11 positions in the pallet with time. The fraction of remaining α_{s1}casein is then 1-X_c. This has been plotted below in Figure 5.5 and Figure 5.7. In each case the outside surface corner, the center and the mass average fraction of α_{s1}casein remaining is plotted.

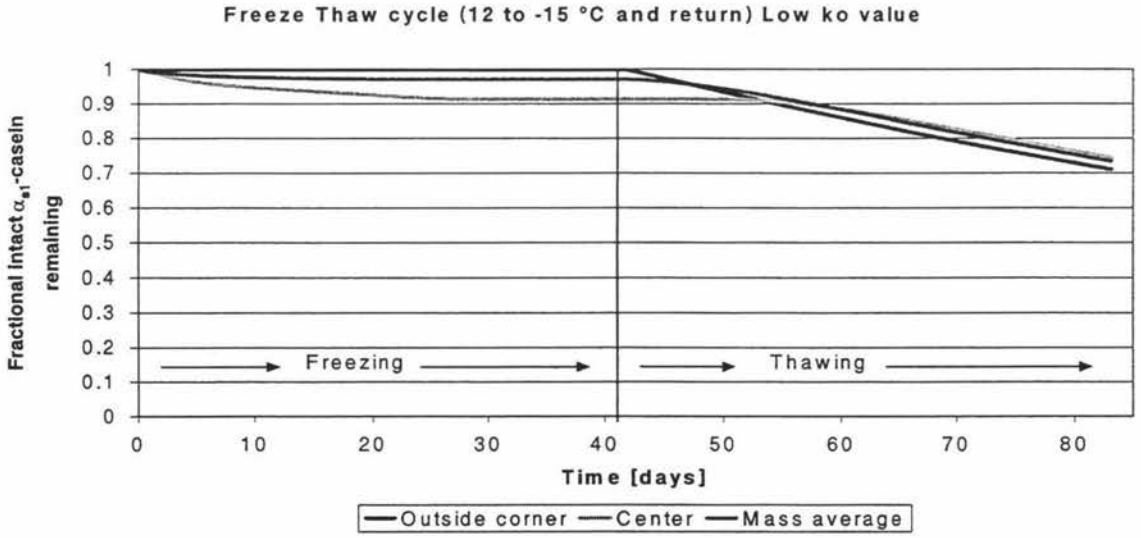

Figure 5.5 Casein remaining for a low k_o cheese in a freeze thaw cycle

An interesting point to note here is that although there is a variation of the level of proteolysis across the pallet of ≅10% once the block is fully frozen, the maximum variation observed once the whole pallet is thawed is only ≅5%. However it is important to note here that while the cheese is thawed at 12°C, the proteolysis is proceeding quickly due to this high temperature and therefore the level of intact casein present once the pallet is fully thawed to 12°C is only 75%(mass average). This differs from the fully frozen cheese, which has a mass average level of intact α_{s1}casein of 97%. Also the variation observed during thawing has a minimum between 50-60 days, which is well before the thawing process is completed. This is illustrated by the standard deviation of the fraction of intact casein remaining, which is plotted against time below in Figure 5.6.

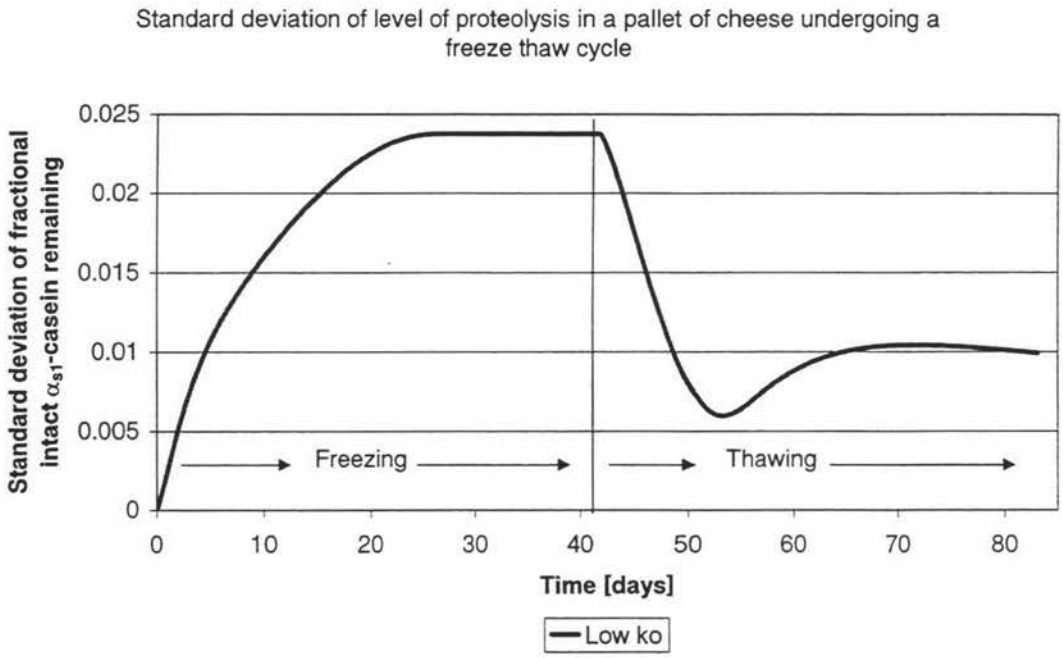

Figure 5.6 Variation of proteolysis in low k_o cheese undergoing a freeze thaw cycle

From this plot it can be seen that the highest observed variation in proteolysis across the pallet is after the cheese is fully frozen (<-10°C). At this point the standard deviation is 0.024. This means that 95% of the cheese has a range where the percentage of intact α_{s1}casein remaining is within ± 1.9617×0.024 = ± 4.7% of the mean level of proteolysis.

The point of lowest variation in the level of proteolysis occurs before the pallet is fully thawed. This local minimum is due to the high temperature of thawing. Since the outside cheese is subjected to such a warm temperature during thawing, the rate at which the protein is degraded is accelerated with respect to the center of the pallet. The level of remaining intact α_{s1}casein reduces to a point equal to the center then overshoots it. This in turn continues to reduce the average variation across the pallet at the expense of reducing the overall level of α_{s1}casein remaining intact. So this would appear to be a good thing in terms of producing a uniform pallet of cheese but it has the negative impact of reducing the level of α_{s1}casein in the pallet.

The same simulation was carried out for a cheese with high levels of rennet and moisture as outlined above. The fraction of remaining α_{s1}casein for this high k_o cheese is plotted below in Figure 5.7 for the outside surface corner, the center and the mass average position in the pallet.

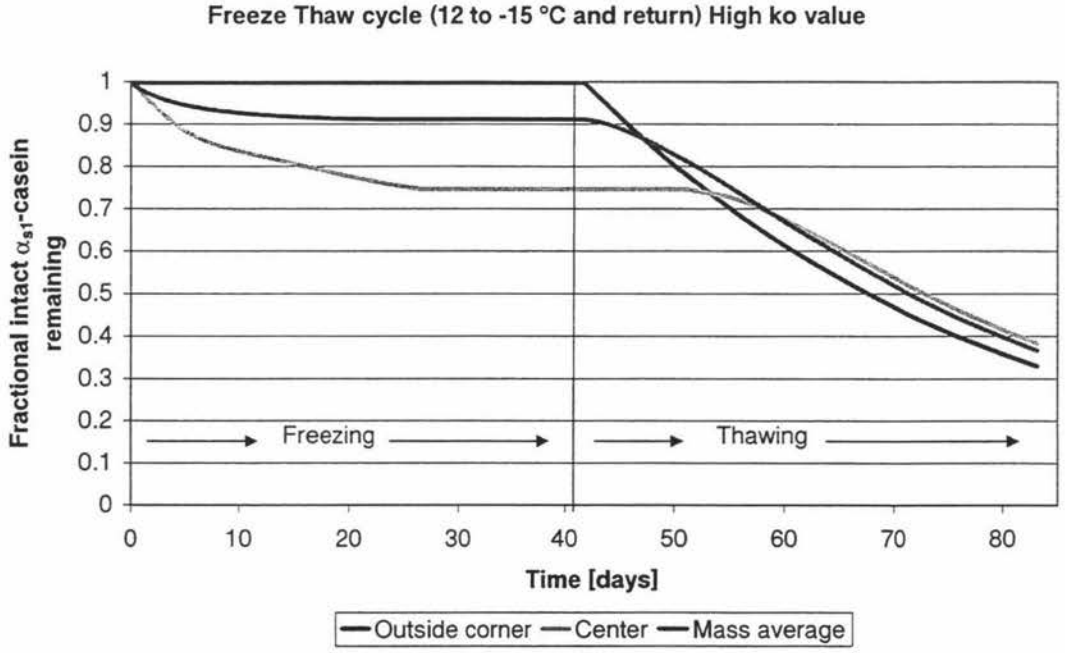

Figure 5.7 Casein remaining for a high k_o cheese in a freeze thaw cycle

Here the trend is the same as the low k_o cheese with the exception that the observed difference between the level of proteolysis in the outside corner cheese and centre when the cheese is fully frozen is much greater. Also the observed fractional level of α_{s1}casein is much

lower at the completion of thawing (the mass average level of fraction intact α_{s1}casein remaining ≅37%). This is due to the combined effect of a high ko cheese and the high temperature used for thawing.

The standard deviation for the high k_o cheese is plotted along side that of the low k_o cheese below in Figure 5.8:

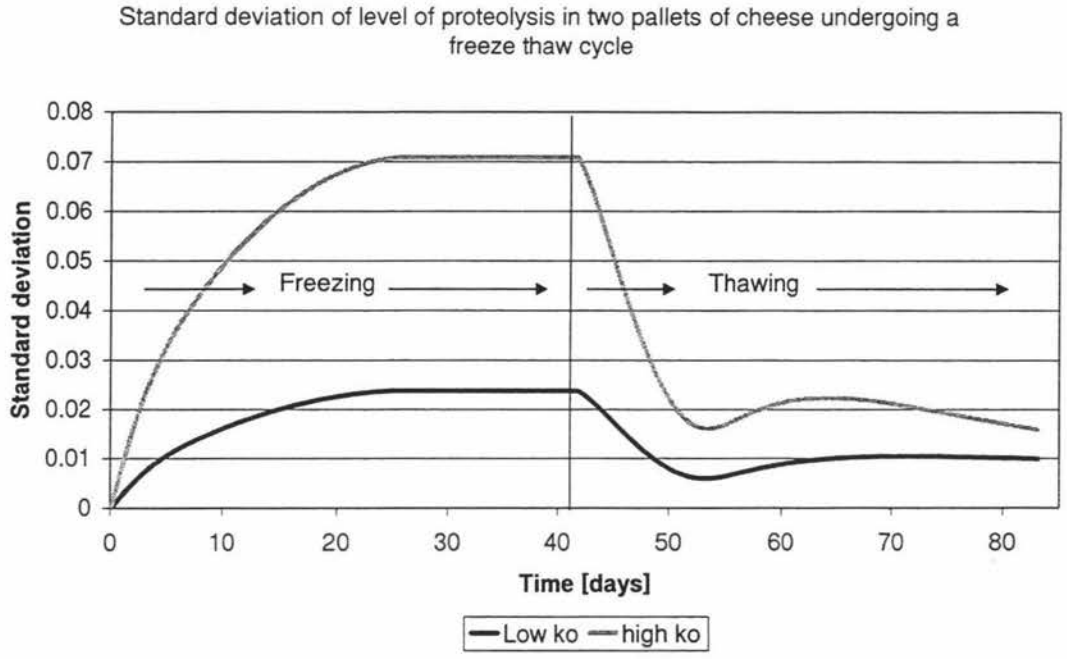

Figure 5.8 Variation of proteolysis in two cheeses undergoing a freeze thaw cycle

The variance in the cheese during freezing is much greater for the cheese with higher MNFS and rennet levels, as would be expected. Once thawing begins, the variance of the level of proteolysis is greatly reduced until a local minimum of variance is reached at the same point in time as the low rennet / low moisture cheese.

In order to avoid the large degree of proteolysis observed when thawing at 12°C the cheese once frozen, could be thawed at 2°C. This temperature regime has been simulated and the pallet centre temperature is plotted below.

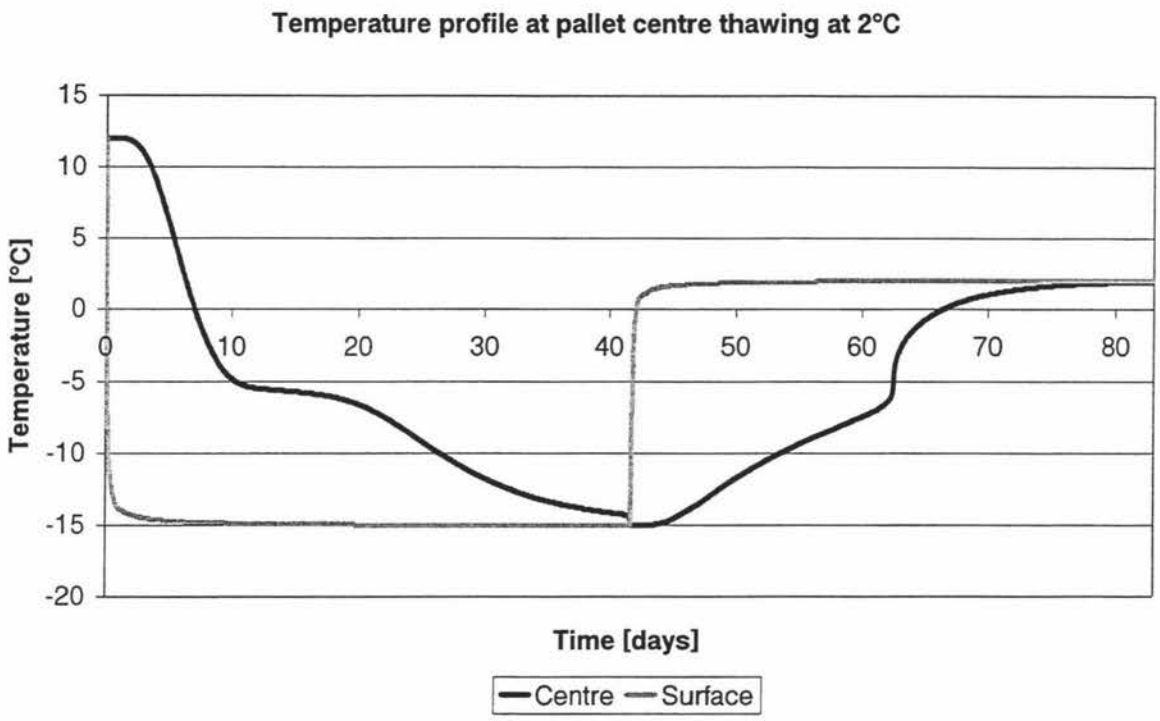

Figure 5.9 Time-temperature profile for freeze thaw cycle 12 to -15 to 2°C

Again the same process of freezing and thawing can be observed as with the time-temperature when a thawing ambient temperature of 12°C is used. The exception is that the centre temperature asymptotes to 2°C. This means that the bulk of the cheese remains at a cooler temperature during the thawing process. The resulting levels of proteolysis for the surface, the centre and the mass average are plotted below.

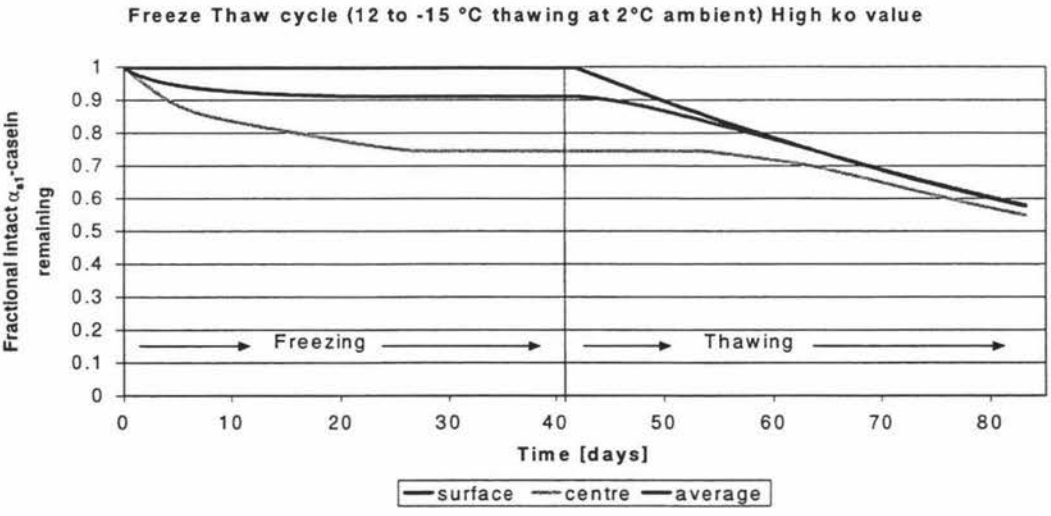

Figure 5.10 Casein remaining for a high k_o cheese thawed at 2°C

The final level of remaining intact α_{s1}casein is greater than 50% throughout the cheese. This is much greater than the 37% observed for the mass average of the same cheese when thawed at 12°C. In order to compare the variance the calculated standard deviations throughout each pallet for each of the three situations outlined above vs time have been plotted below in Figure 5.11:

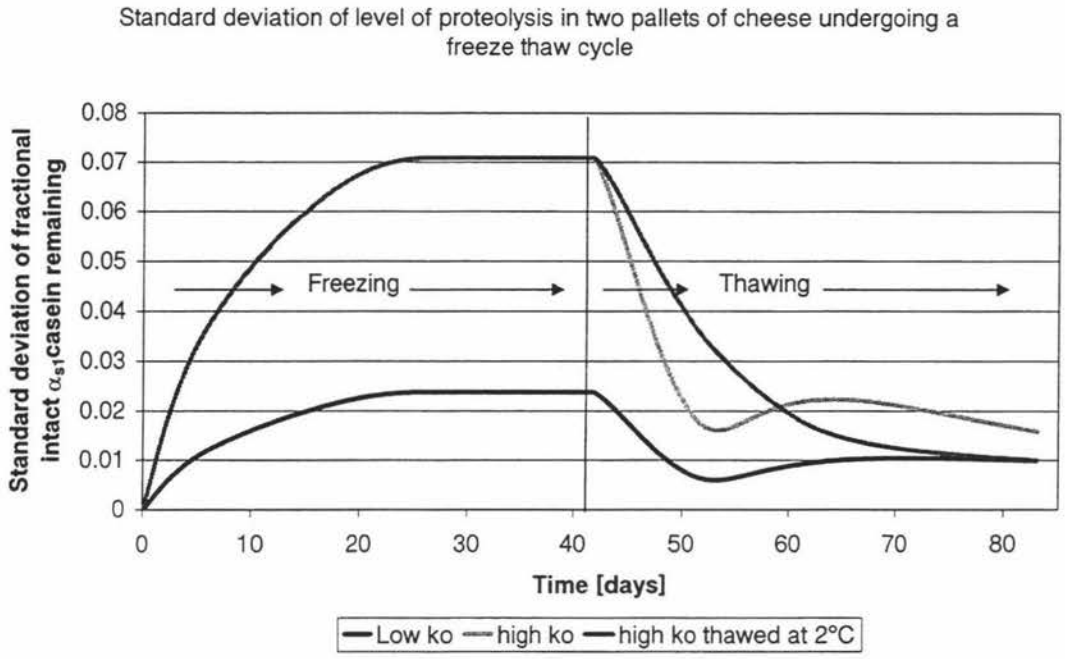

Figure 5.11 Variation in the level of proteolysis for different thawing regimes

5.5 CONCLUSIONS

The heat transfer model formulated in chapter 4 was applied to produce data describing the time-temperature profile throughout a pallet of cheese for a variety of industrial storage conditions possible. The kinetic model developed in chapter 2 was then used to predict the extent of proteolysis in each case.

It was found that significant heterogeneity was observed across the pallet during chilling and freezing (± 4.7to 14% depending on composition and ambient conditions). During chilling the heterogeneity reached a maximum as the temperature became uniform after 15 days. During freezing the same trend was observed, however during thawing the temperature gradient experienced across the pallet was inverted and to some extent the

heterogeneity was reduced. These effects were less evident for cheese with low residual rennet and low moisture content compared with high rennet and low moisture cheeses.

CHAPTER 6

CONCLUSIONS

The rate of proteolysis in cheese was measured by following the disappearance of α_{s1}casein over time for a range of cheddar compositions and at a range of temperatures. It was found that the rates approximately followed first order kinetics and the effect of temperature could be explained using the Arrhenius law. An overall kinetic model was developed to describe the rate of primary proteolysis with respect to temperature, residual rennet, and moisture content. The effect of salt was not found to be significant in the range investigated (3.6 to 6.5 salt in moisture wt%). Cheeses with a lower level of rennet and moisture result in lower level of proteolysis for all time-temperature scenarios. Low temperatures during storage and thawing also result in a lower level of proteolysis.

A differential scanning calorimeter was used to measure the apparent heat capacity for cheddar cheese undergoing freezing. A method was developed to determine the ice content from this heat capacity data. The full range of thermal properties required to model the chilling and freezing of cheese could then be estimated.

A three dimensional heat transfer model was formulated to describe the heat transfer in industrial chilling and freezing operations. The model was found to accurately predict the time-temperature profile of experimental data collected for both freezing and chilling.

The heat transfer model was combined with the kinetic description of α_{s1}casein proteolysis to allow the estimation of heterogeneity of cheese functionality as a function of position in a pallet. A number of maturation scenarios were investigated including chilling, and freeze-thaw cycles. It was found that significant heterogeneity was observed across the pallet during chilling and freezing ($\pm$ 4.7 to 14% depending on composition and ambient conditions). During thawing, the temperature gradient experience across the pallet is inverted and to some extent the heterogeneity is reduced. These effects are less evident for cheese with low residual rennet and low moisture content.

It is recommended that additional work be carried out to improve the quality of the proteolysis data collected in this work. Such improvements could include expansion of the range of compositions and cheese styles investigated in this work. The model could be used to analyse a greater range of industrial situations. To more easily do this, it is suggested that the kinetic model be incorporated directly into the heat transfer model to produce a combined easy-to-use predictive tool. This could be used in industry to assist in the management of cheese product functionality.

APPENDIX

7.1 CHEESE COMPOSITIONS

Cheese vat	Moisture	rennet	salt/moisture	Fat	MNFS	FDM(fat in dry matter)	pH	TN(Total Nitrogen)	NPN(Non protein Nitrogen)	NCN(Non casein nitrogen)	[rennet] (available rennet)	salt/moisture/ non fat	moisture non fat
1	39%	12	4.90%	31.00%	57.10%	54.70%	4.9	3.72	0.206	0.362	10.43709	0.071014	57.10%
2	36%	4.6	4.50%	34.00%	54.40%	53.00%	5.41	3.85	0.186	0.314	3.513617	0.068182	54.40%
3	37%	12	5.60%	34.00%	56.10%	54.00%	5.5	3.78	0.173	0.374	9.652174	0.084848	56.10%
4	38%	12	3.70%	34.00%	57.30%	54.70%	5.28	3.73	0.204	0.426	10.01325	0.056061	57.30%
5	39%	12	4.90%	31.00%	57.10%	54.70%	5.24	3.72	0.206	0.362	10.43709	0.071014	57.10%
6	39%	12	3.70%	32.00%	57.90%	52.80%	5.09	3.69	0.201	0.395	10.01695	0.054412	57.90%
7	38%	4.6	3.60%	33.00%	57.30%	53.60%	5.09	3.76	0.199	0.307	3.806897	0.053731	57.30%
8	36%	4.6	4.50%	34.00%	54.40%	53.00%	5.41	3.85	0.186	0.314	3.513617	0.068182	54.40%
9	37%	4.6	4.40%	33.00%	55.10%	52.10%	5.39	3.85	0.193	0.306	3.524426	0.065672	55.10%
10	35%	4.6	6.50%	34.00%	52.40%	52.00%	5.53	3.92	0.178	0.315	3.315833	0.098485	52.40%
11	36%	4.6	6.50%	33.00%	53.40%	51.40%	5.51	3.89	0.141	0.371	3.388477	0.097015	53.40%
12	39%	12	4.10%	32.00%	57.60%	52.60%	5.22	3.65	0.167	0.335	9.924051	0.060294	57.60%
15	32%	8	5.16%	37.00%	50.79%	54.41%	5.2	3.78	0.185	0.351	5.615267	0.081904	50.79%

7.2 CASEIN VS TIME COMPLETE DATA SET

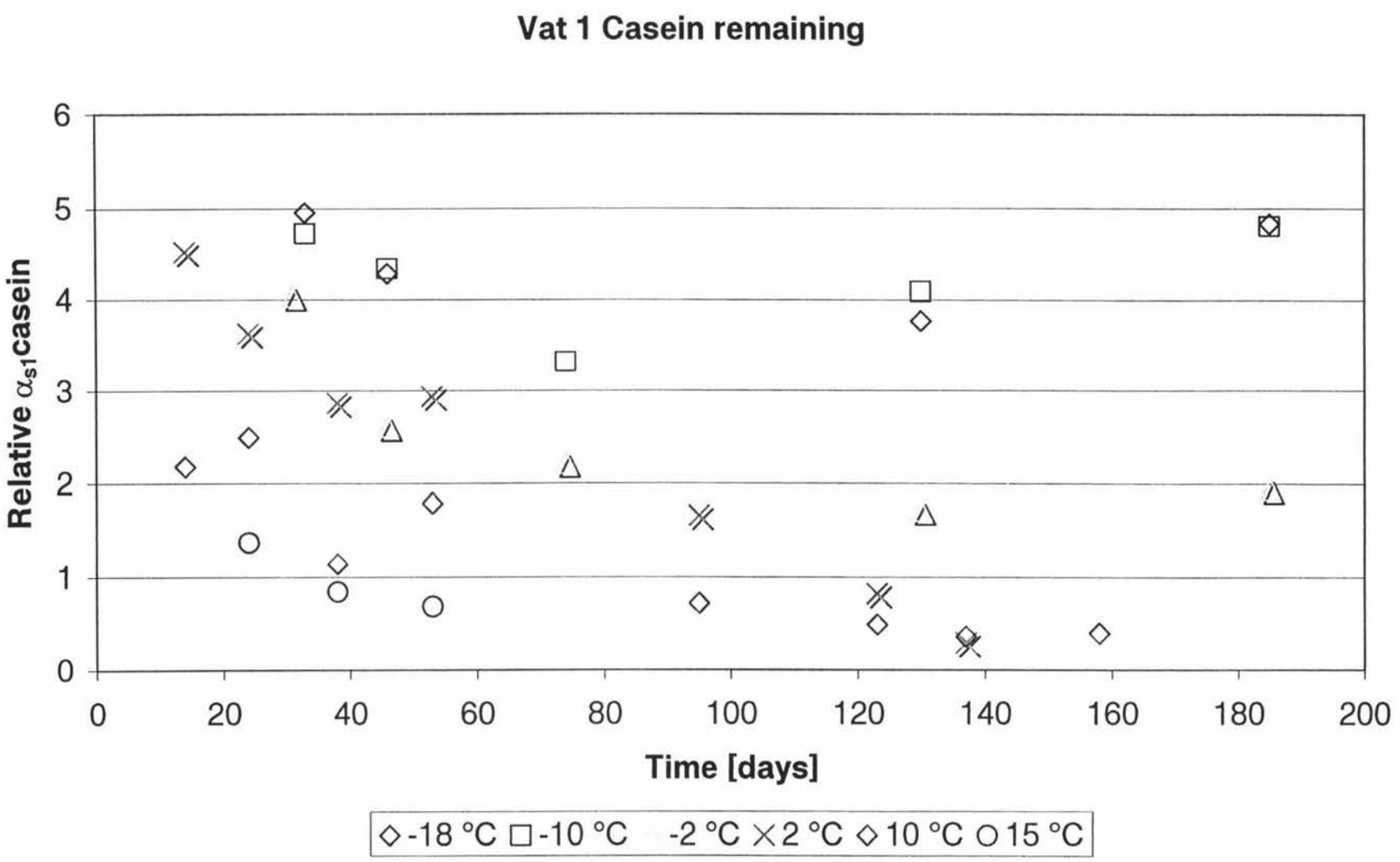
Vat 1 Casein remaining
Relative α_{s1}casein
0
1
2
3
4
5
6
0
20
40
60
80
100
120
140
160
180
200
Time [days]
◇ -18 °C □ -10 °C -2 °C × 2 °C ◇ 10 °C ○ 15 °C

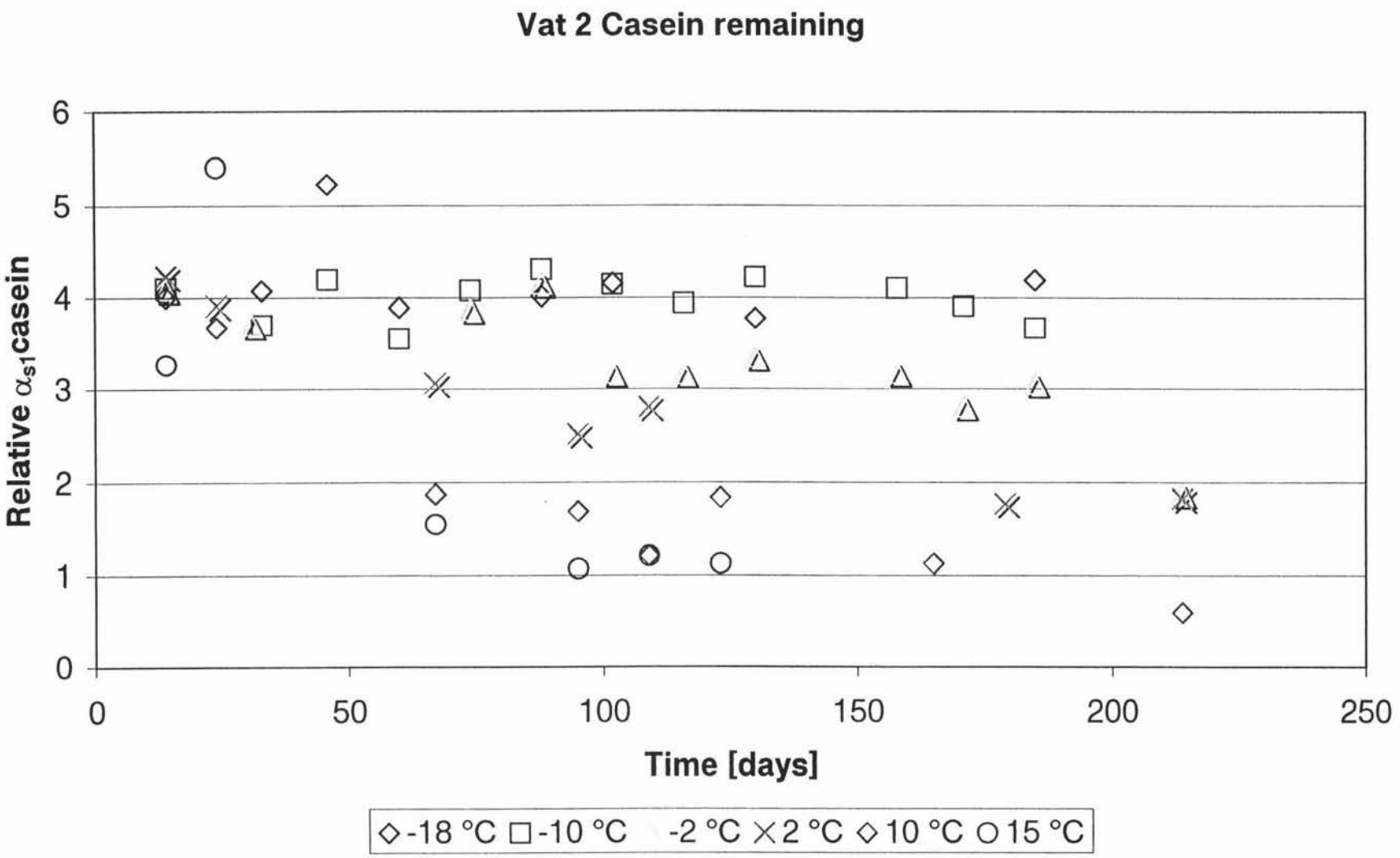
Vat 2 Casein remaining
Relative α_{s1}casein
0
1
2
3
4
5
6
0
50
100
150
200
250
Time [days]
-18 °C
-10 °C
-2 °C
2 °C
10 °C
15 °C

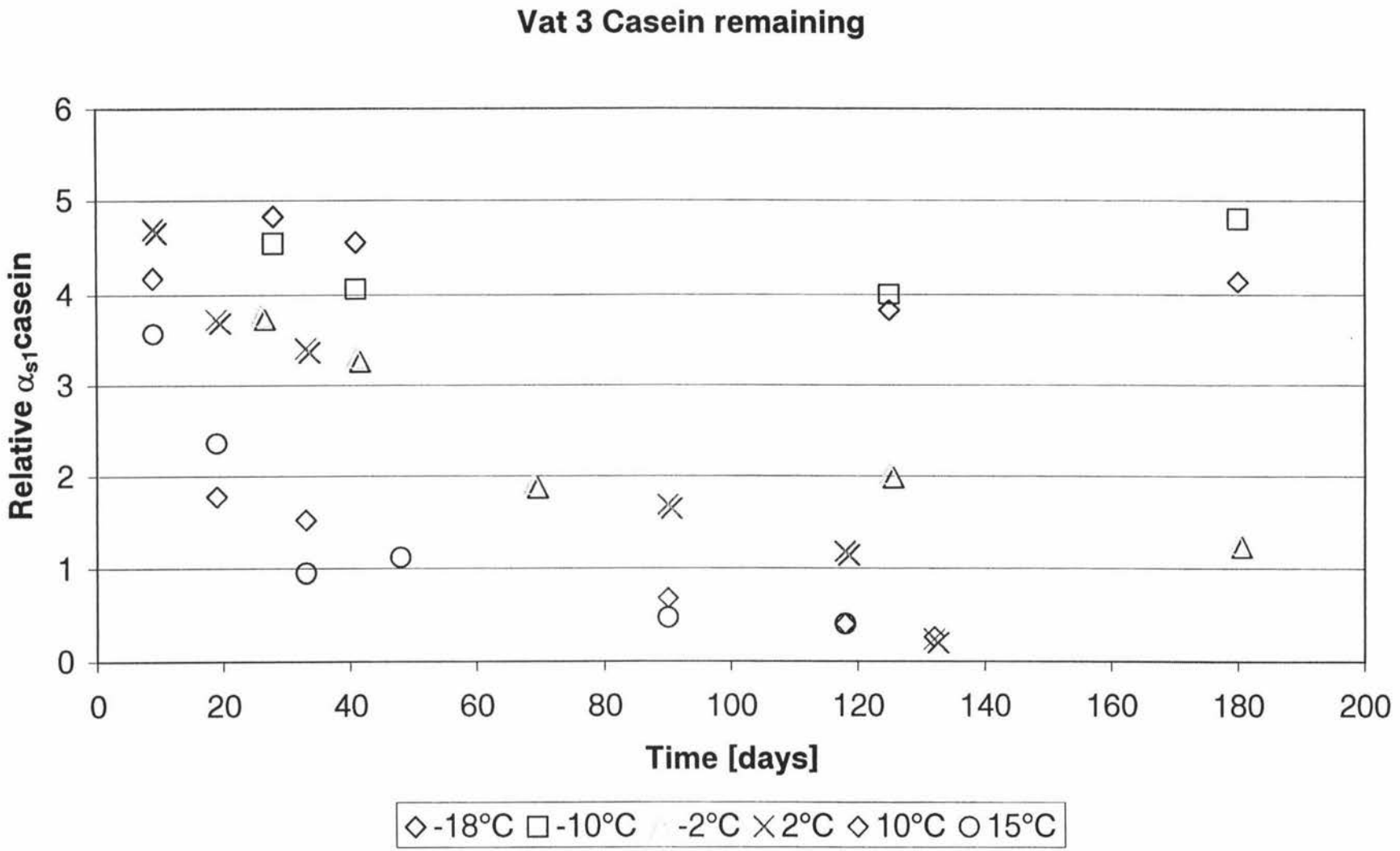
Vat 3 Casein remaining
Relative α_{s1}casein
0
1
2
3
4
5
6
0
20
40
60
80
100
120
140
160
180
200
Time [days]
◇-18°C □-10°C △-2°C ×2°C ◇10°C ○15°C

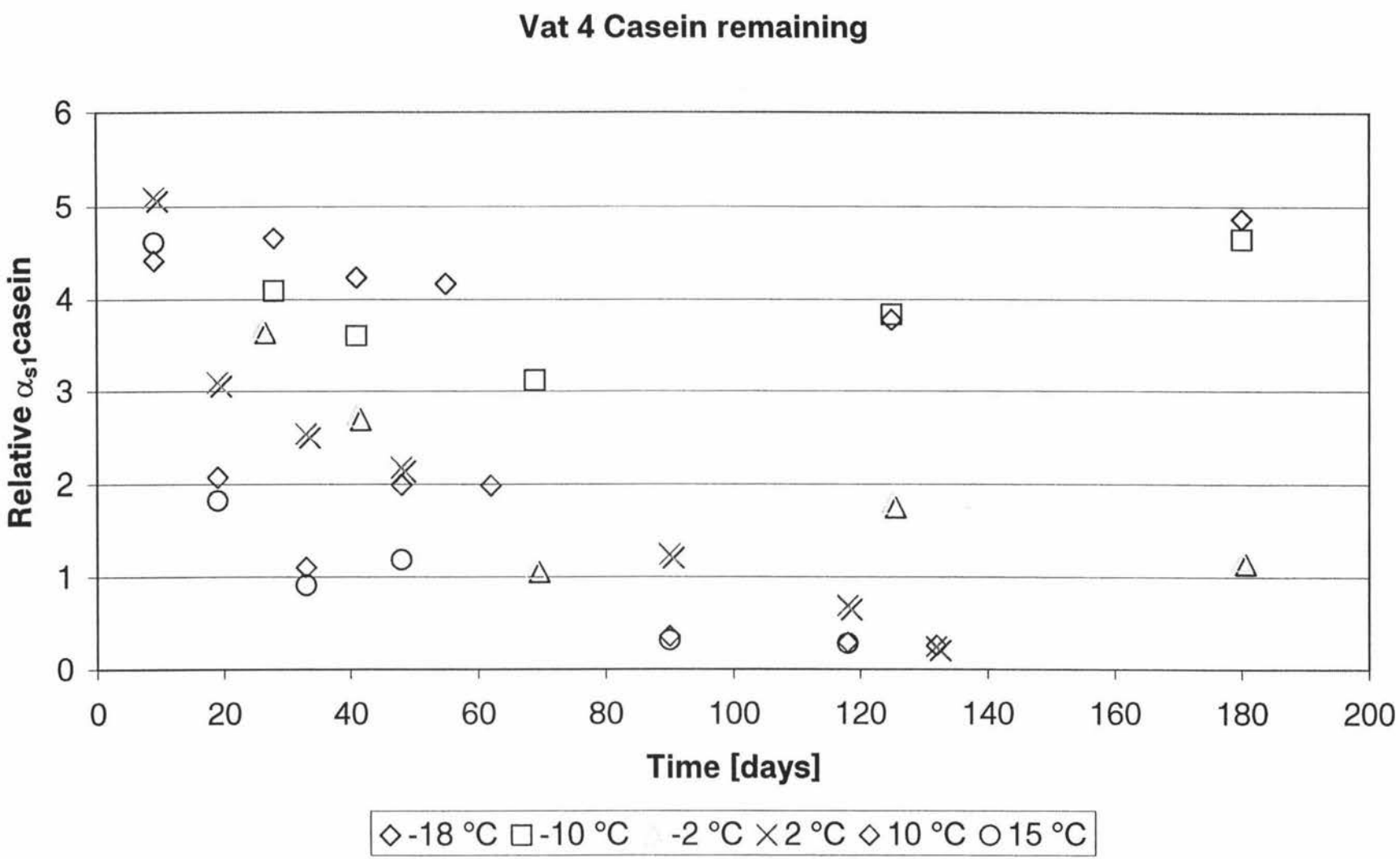
Vat 4 Casein remaining
Relative α_{s1}casein
0
1
2
3
4
5
6
0
20
40
60
80
100
120
140
160
180
200
Time [days]
-18 °C
-10 °C
-2 °C
2 °C
10 °C
15 °C

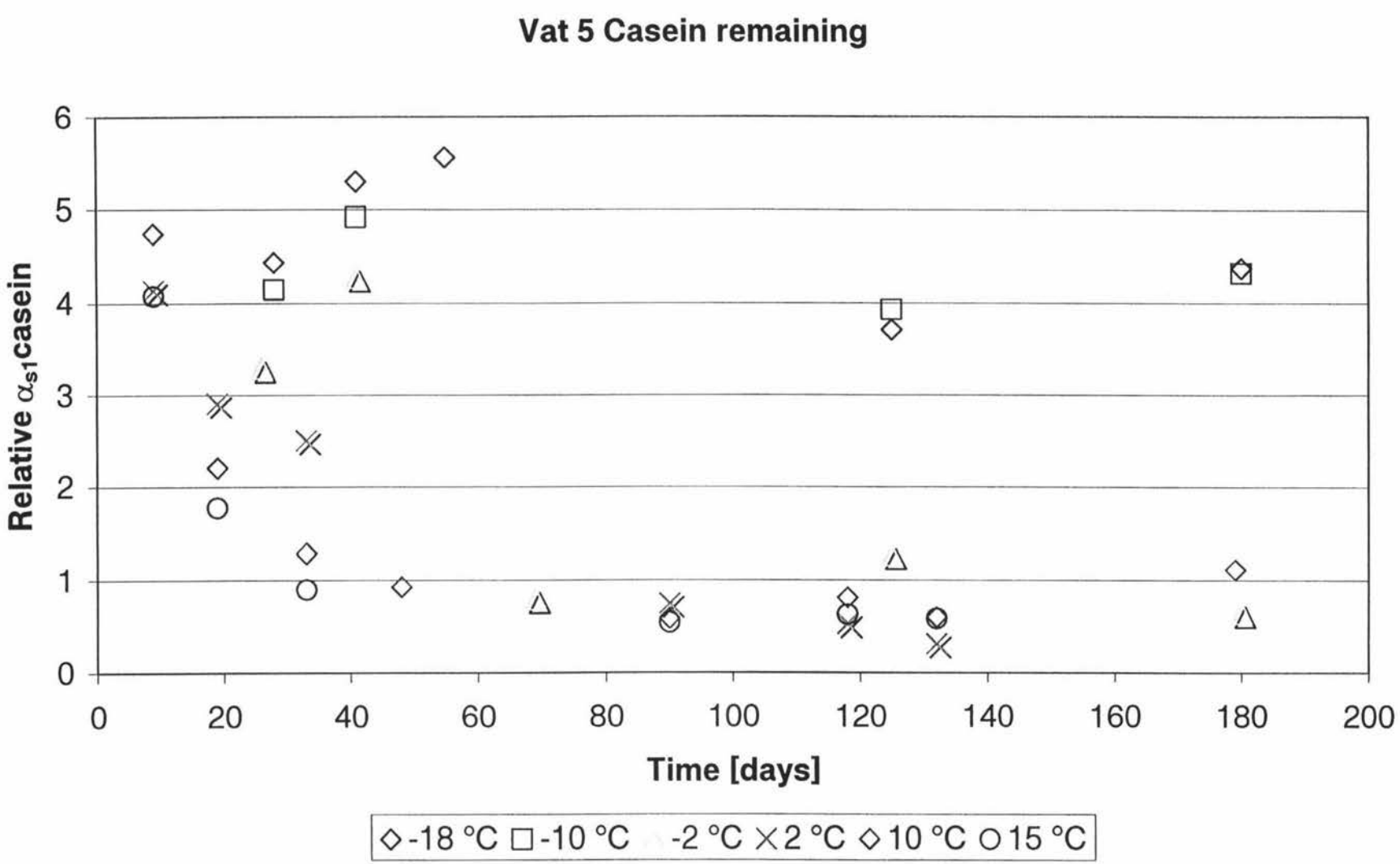
Vat 5 Casein remaining
Relative α_{s1}casein
0
1
2
3
4
5
6
0
20
40
60
80
100
120
140
160
180
200
Time [days]
-18 °C
-10 °C
-2 °C
2 °C
10 °C
15 °C

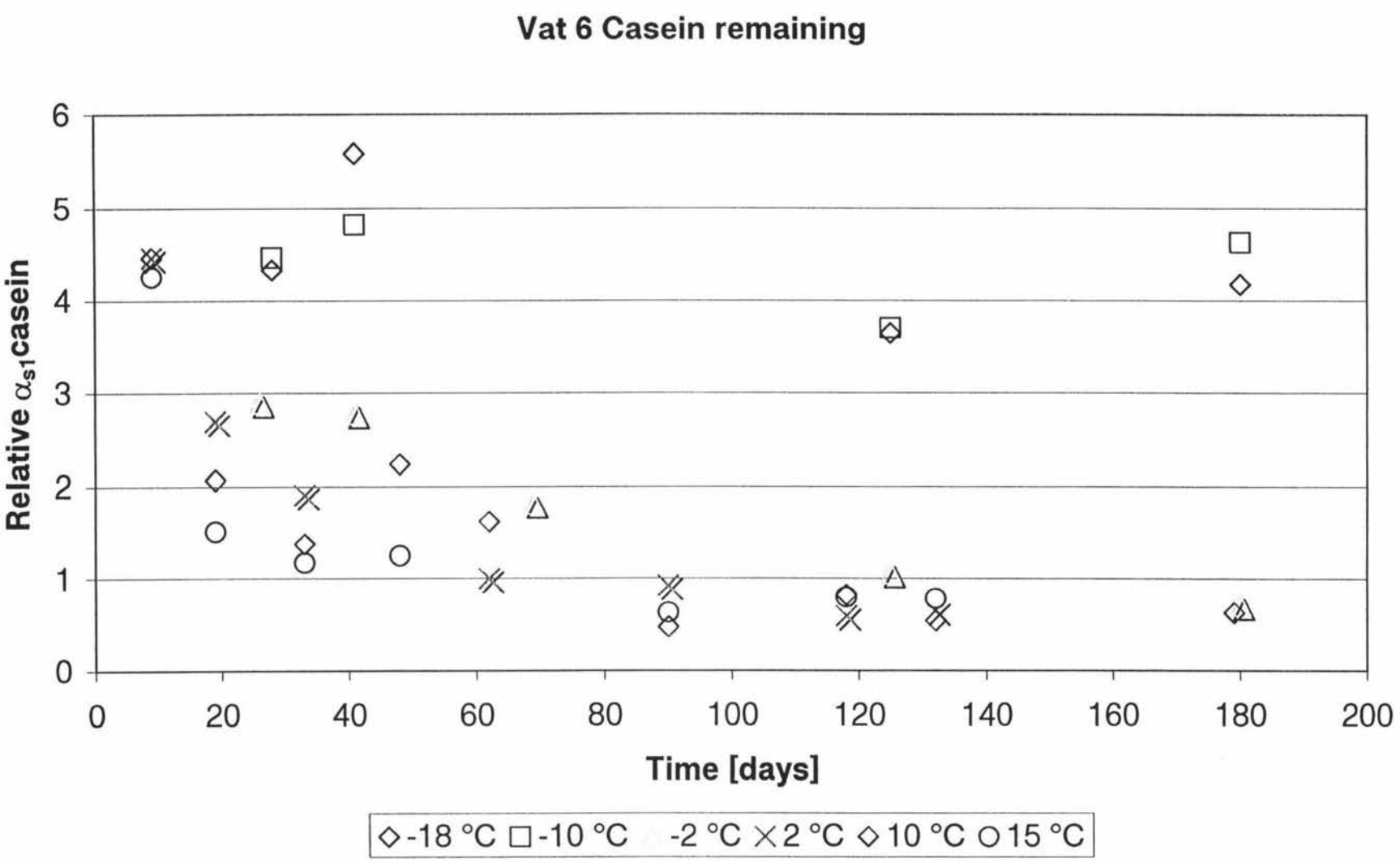
Vat 6 Casein remaining
Relative α_{s1}casein
0
1
2
3
4
5
6
0
20
40
60
80
100
120
140
160
180
200
Time [days]
-18 °C
-10 °C
-2 °C
2 °C
10 °C
15 °C

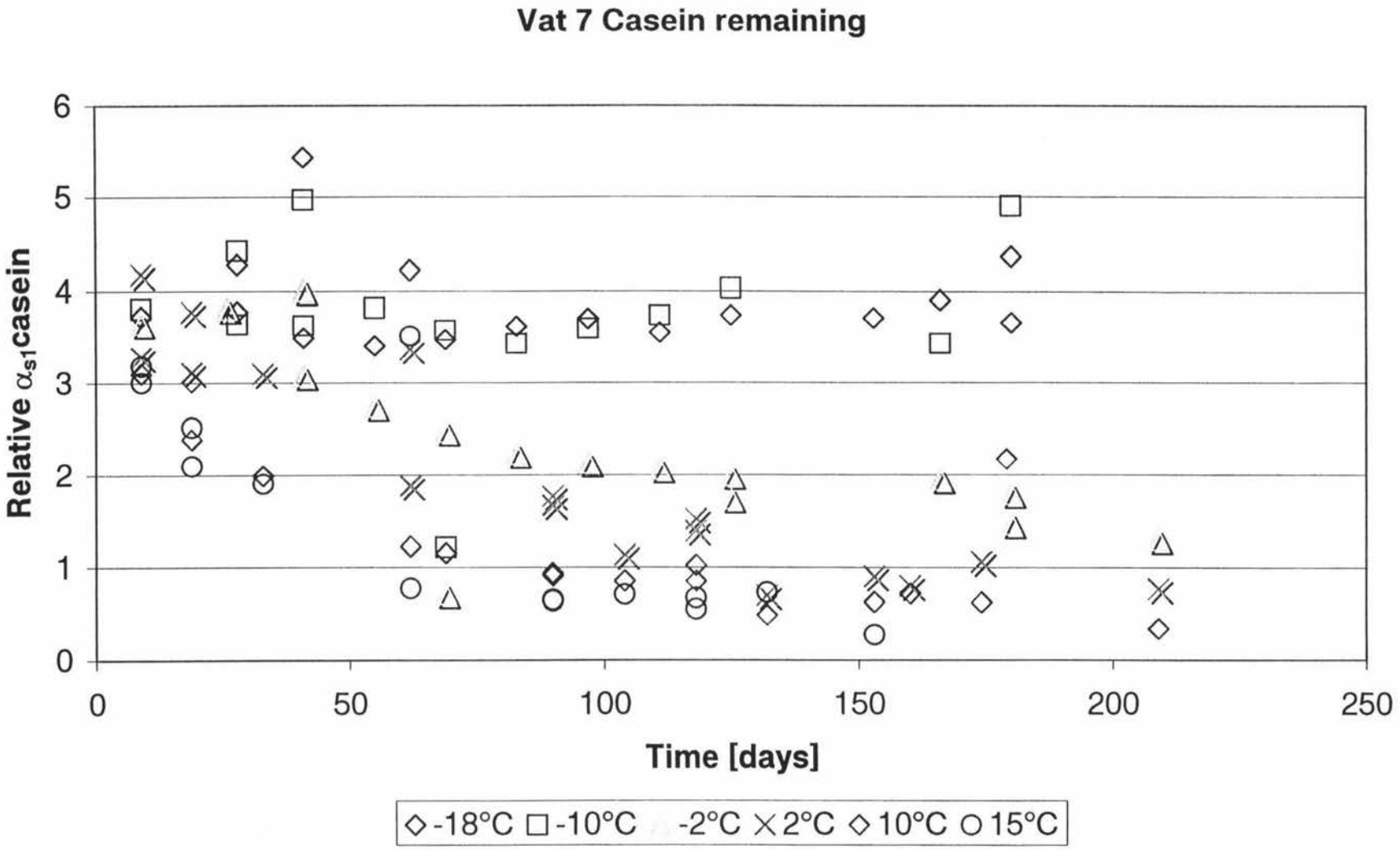
Vat 7 Casein remaining
Relative α_{s1}casein
0
1
2
3
4
5
6
0
50
100
150
200
250
Time [days]
-18°C
-10°C
-2°C
2°C
10°C
15°C

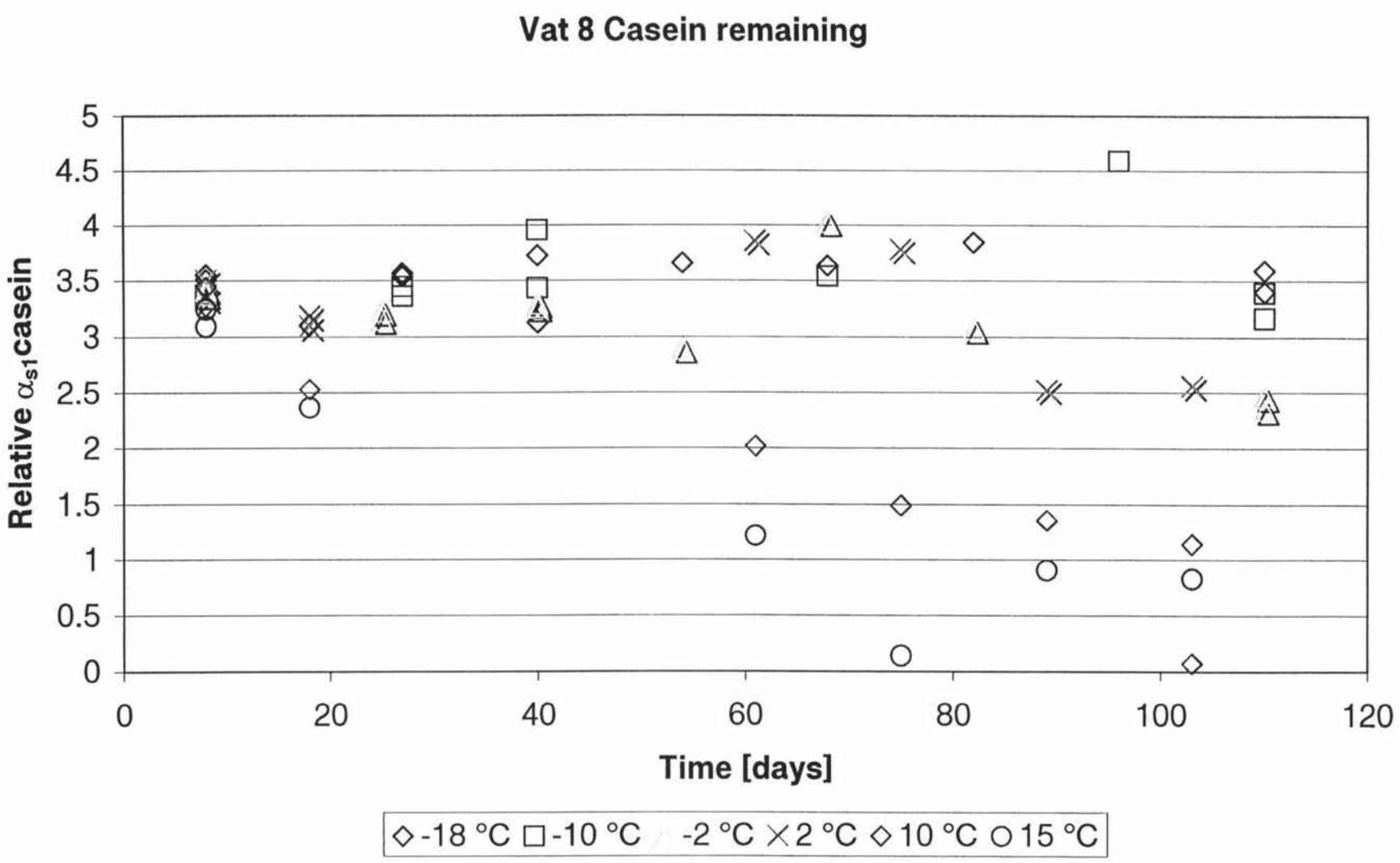
Vat 8 Casein remaining
Relative α_{s1}casein
5
4.5
4
3.5
3
2.5
2
1.5
1
0.5
0
0
20
40
60
80
100
120
Time [days]
◇ -18 °C □ -10 °C -2 °C × 2 °C ◇ 10 °C ○ 15 °C

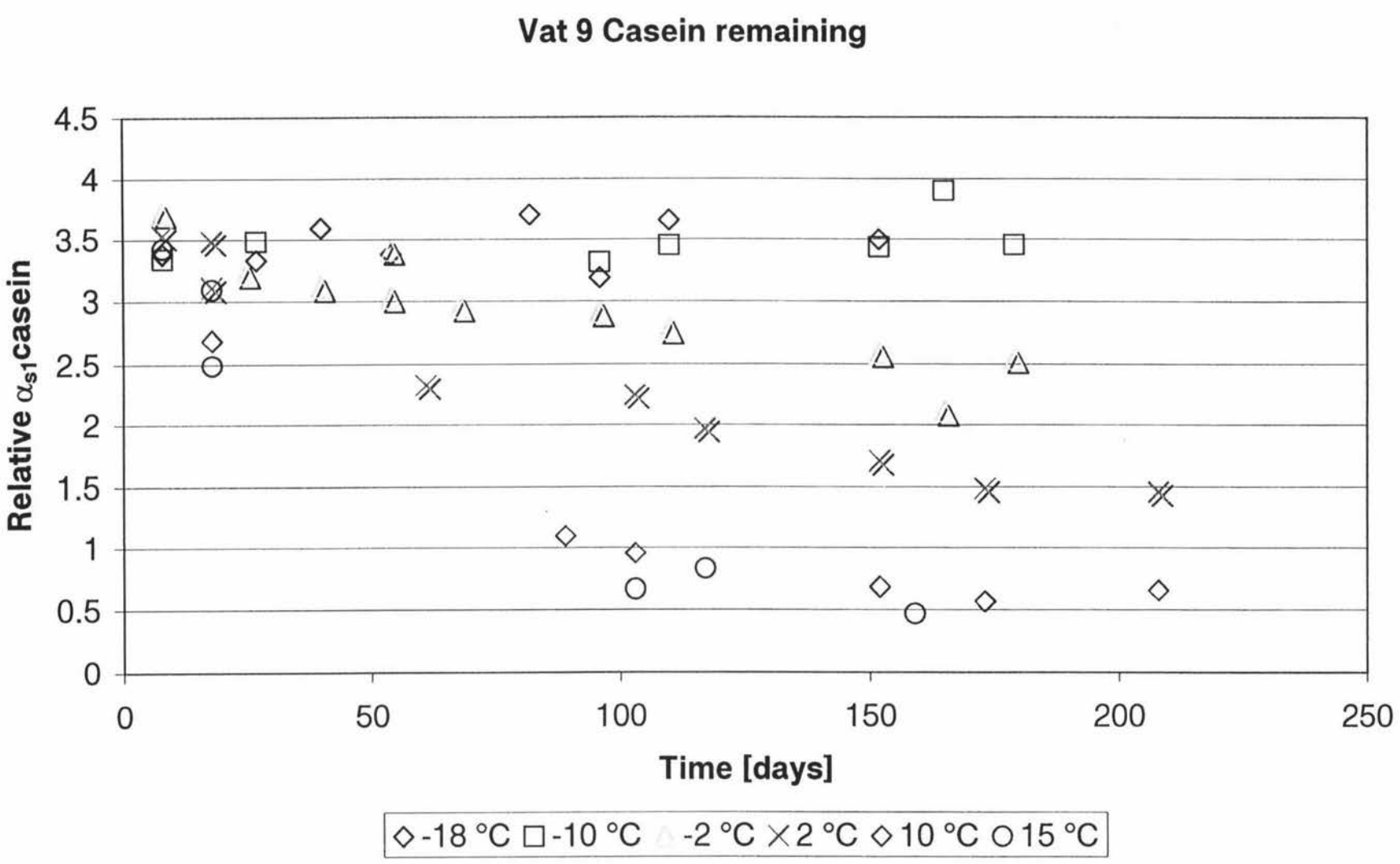
Vat 9 Casein remaining
Relative α_{s1}casein
4.5
4
3.5
3
2.5
2
1.5
1
0.5
0
0
50
100
150
200
250
Time [days]
◇ -18 °C □ -10 °C △ -2 °C × 2 °C ◇ 10 °C ○ 15 °C

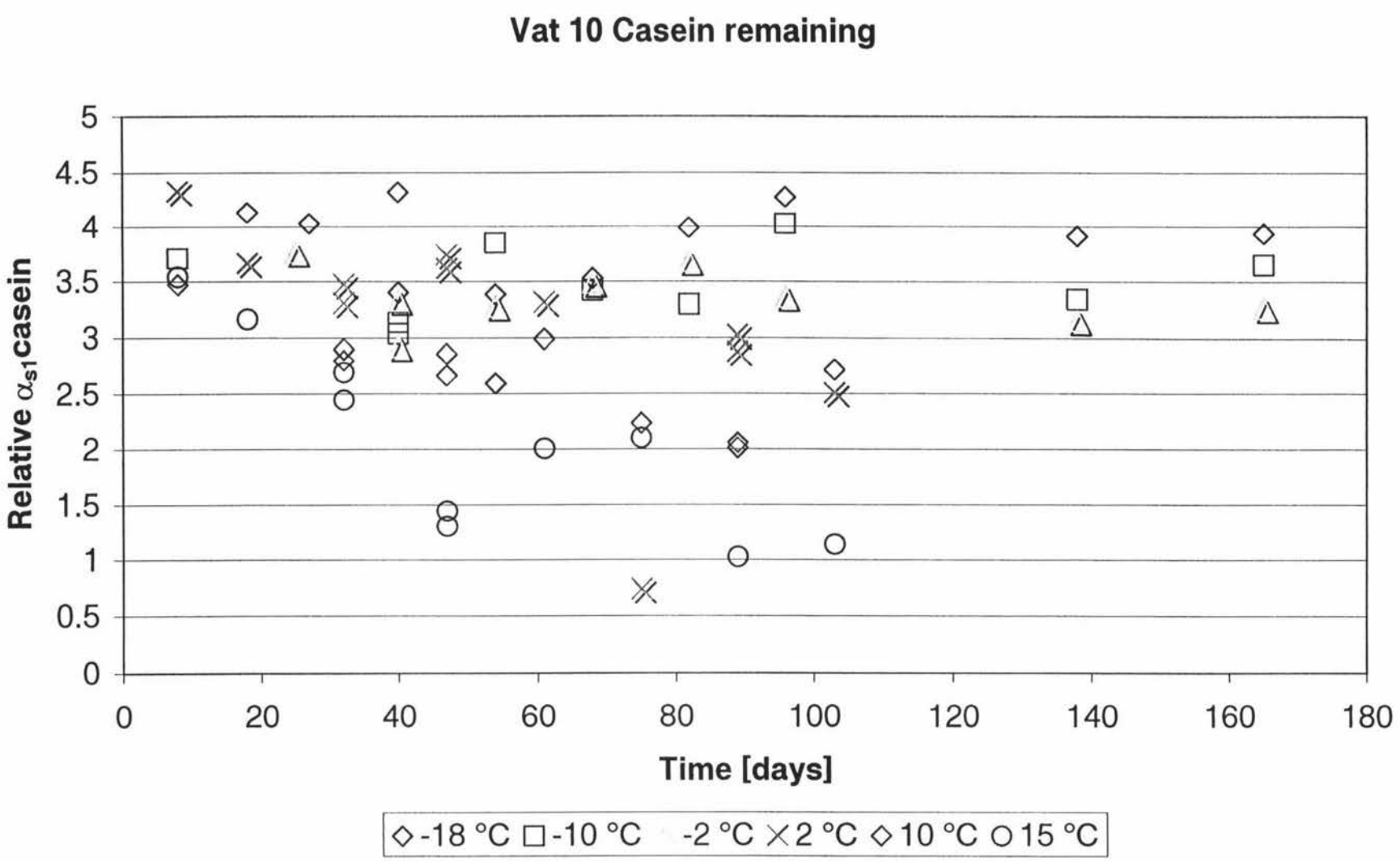
Vat 10 Casein remaining
Relative α_{s1}casein
5
4.5
4
3.5
3
2.5
2
1.5
1
0.5
0
0
20
40
60
80
100
120
140
160
180
Time [days]
◇-18 °C □-10 °C -2 °C ×2 °C ◇10 °C ○15 °C

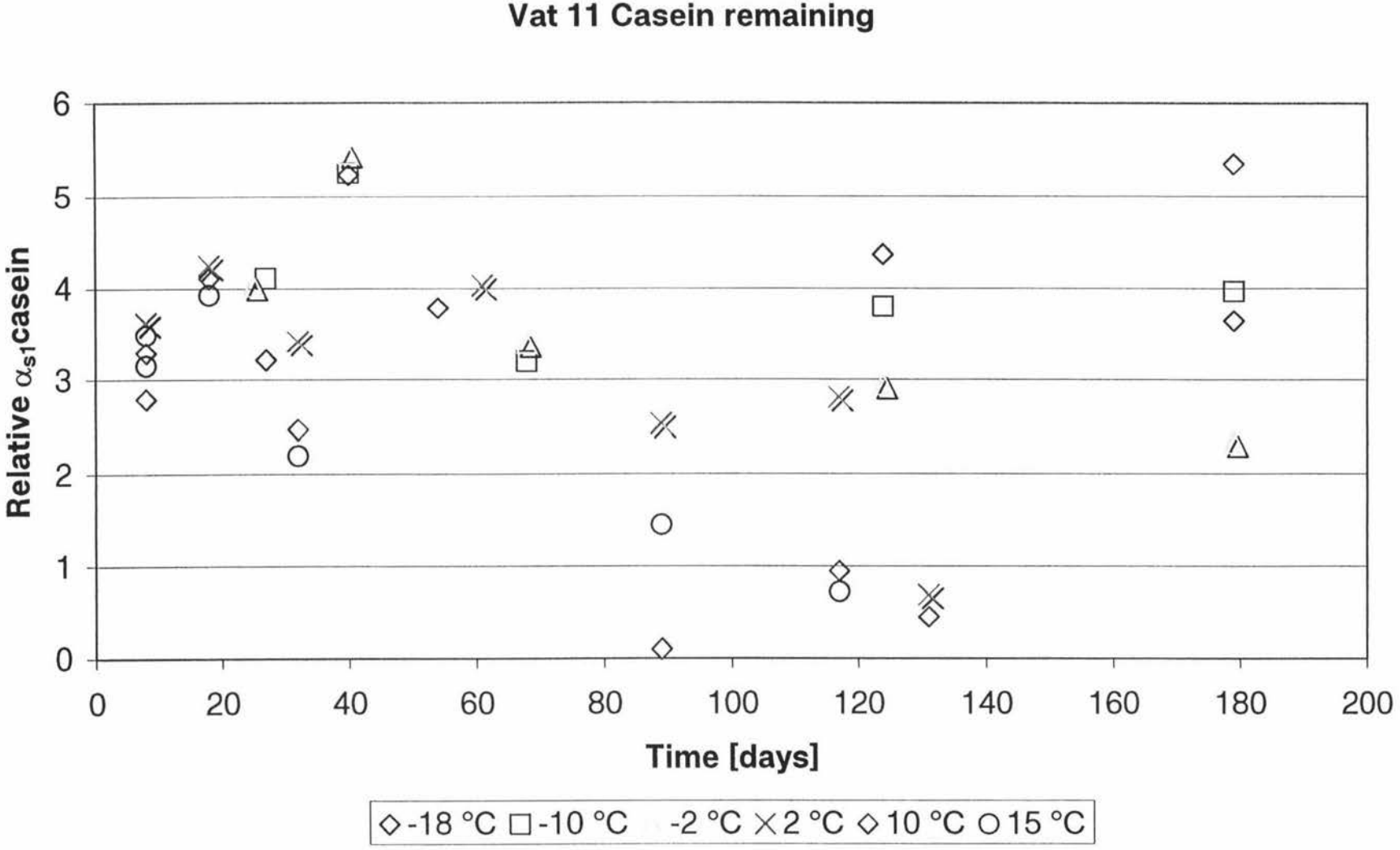
Vat 11 Casein remaining
Relative α_{s1}casein
0
1
2
3
4
5
6
0
20
40
60
80
100
120
140
160
180
200
Time [days]
◇-18 °C □-10 °C -2 °C ×2 °C ◇10 °C ○15 °C

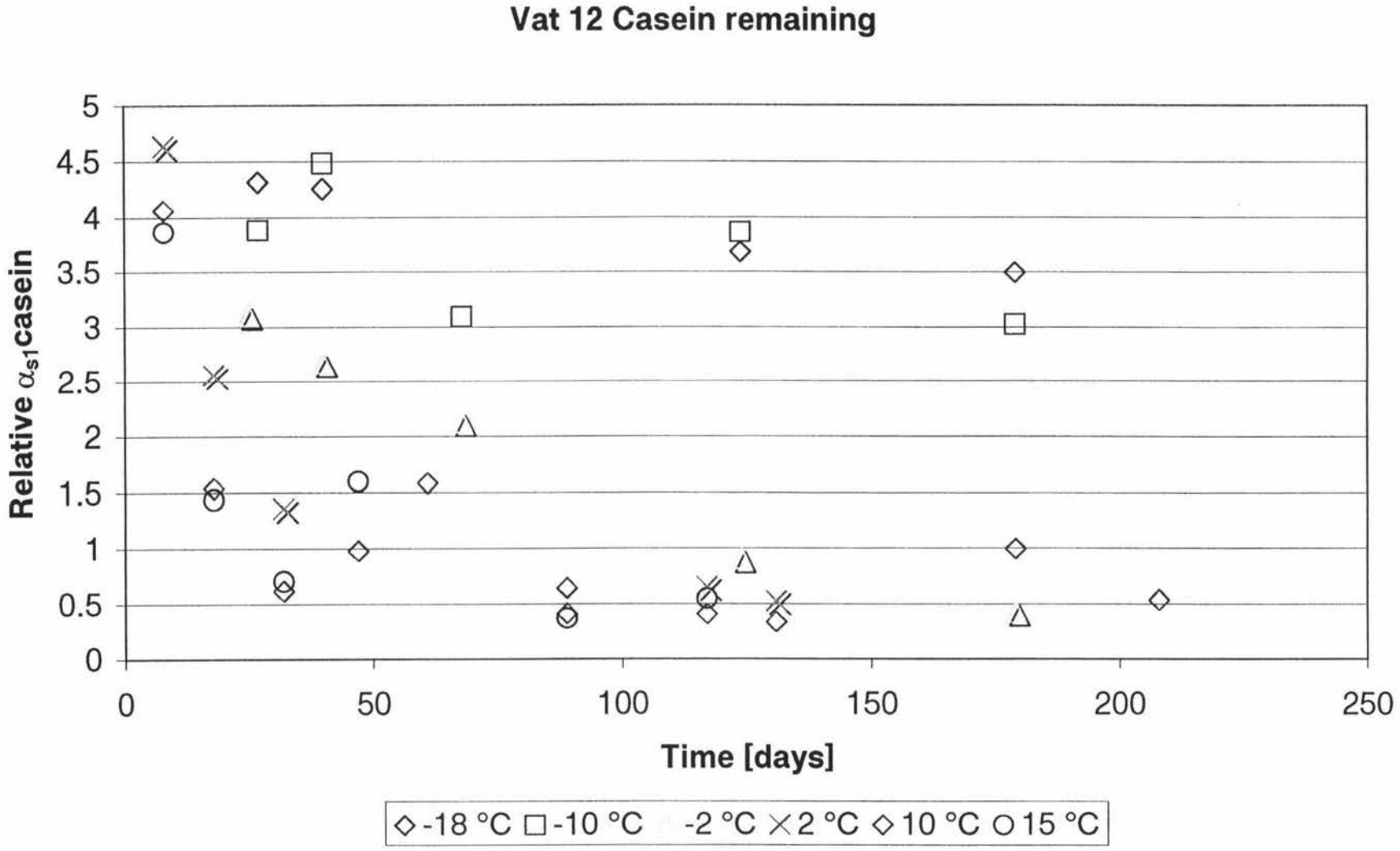
Vat 12 Casein remaining
Relative α_{s1}casein
5
4.5
4
3.5
3
2.5
2
1.5
1
0.5
0
0
50
100
150
200
250
Time [days]
-18 °C
-10 °C
-2 °C
2 °C
10 °C
15 °C

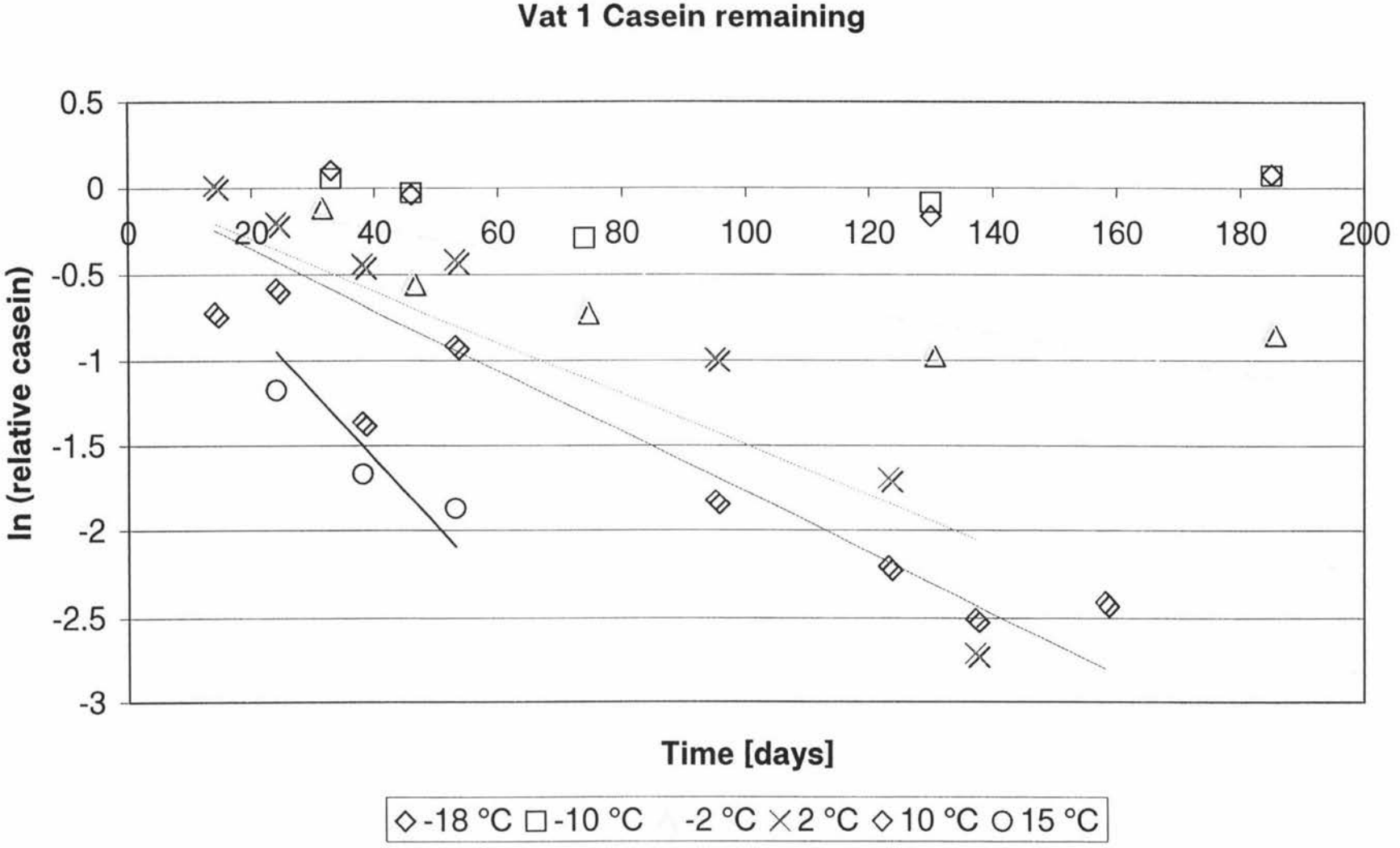
Vat 1 Casein remaining
0.5
0
-0.5
-1
-1.5
-2
-2.5
-3
0
20
40
60
80
100
120
140
160
180
200
ln (relative casein)
Time [days]
-18 °C
-10 °C
-2 °C
2 °C
10 °C
15 °C

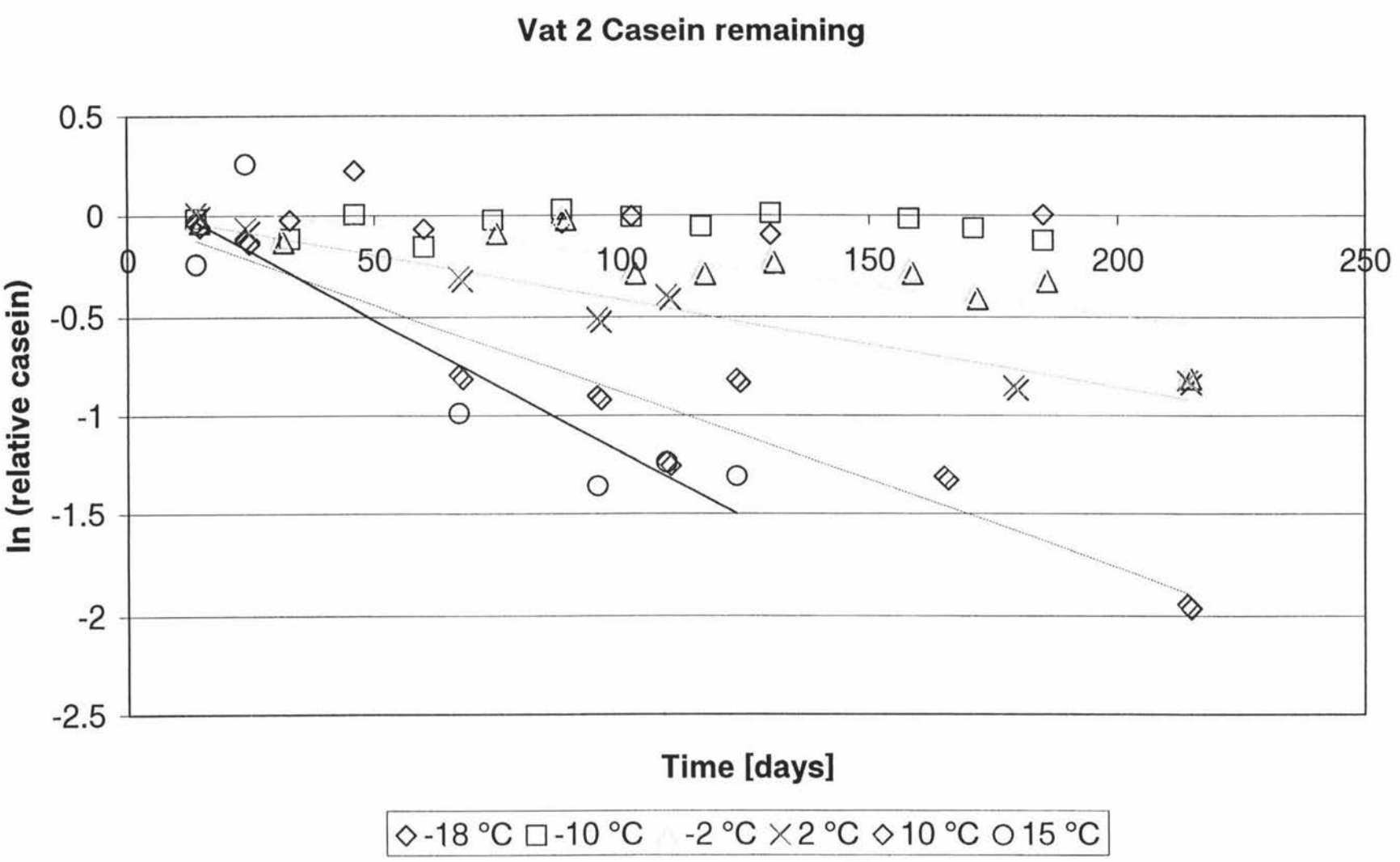
Vat 2 Casein remaining
0.5
0
-0.5
-1
-1.5
-2
-2.5
0
50
100
150
200
250
ln (relative casein)
Time [days]
-18 °C
-10 °C
-2 °C
2 °C
10 °C
15 °C

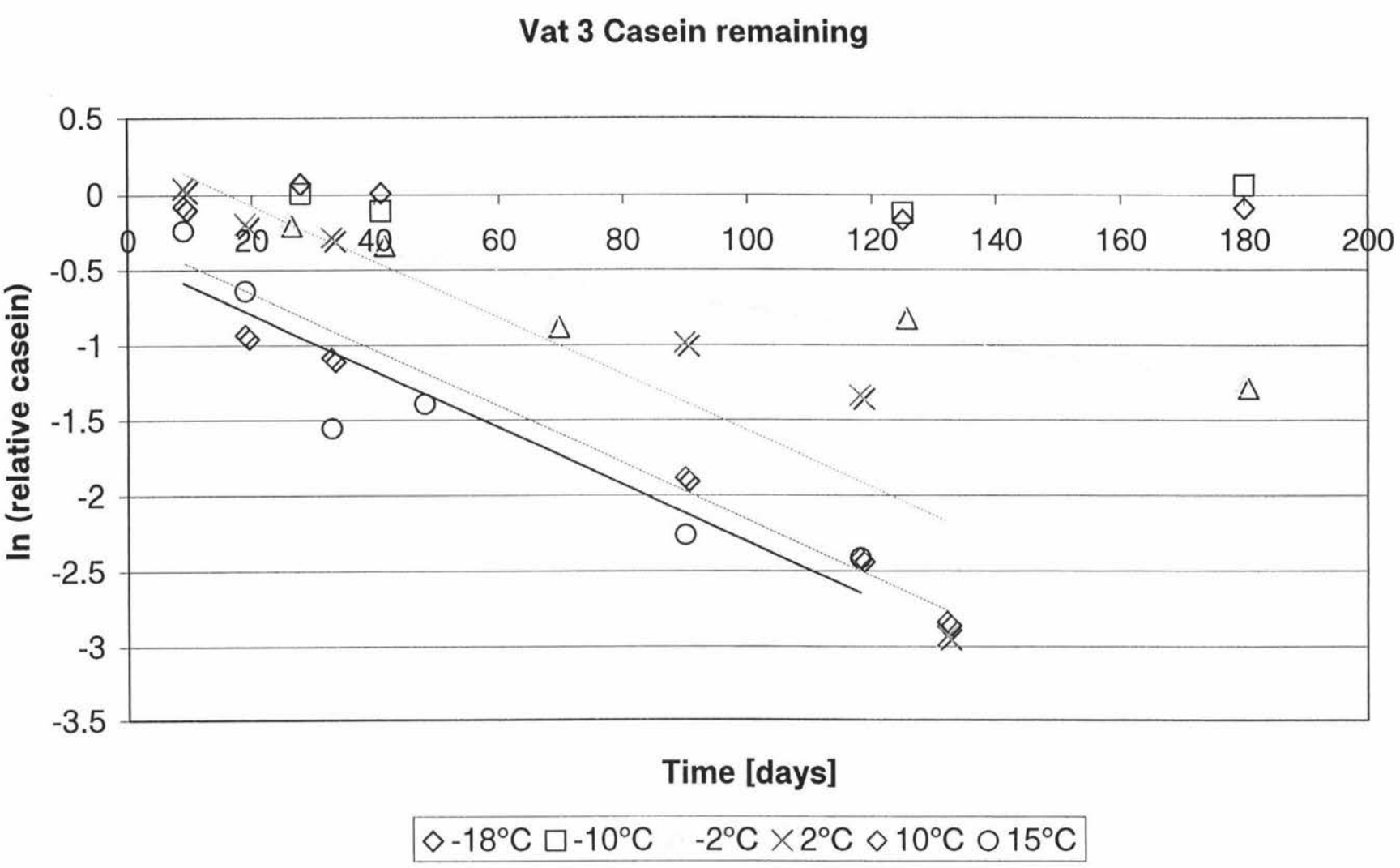
Vat 3 Casein remaining
0.5
0
-0.5
-1
-1.5
-2
-2.5
-3
-3.5
0
20
40
60
80
100
120
140
160
180
200
ln (relative casein)
Time [days]
◇-18°C □-10°C -2°C ×2°C ◇10°C ○15°C

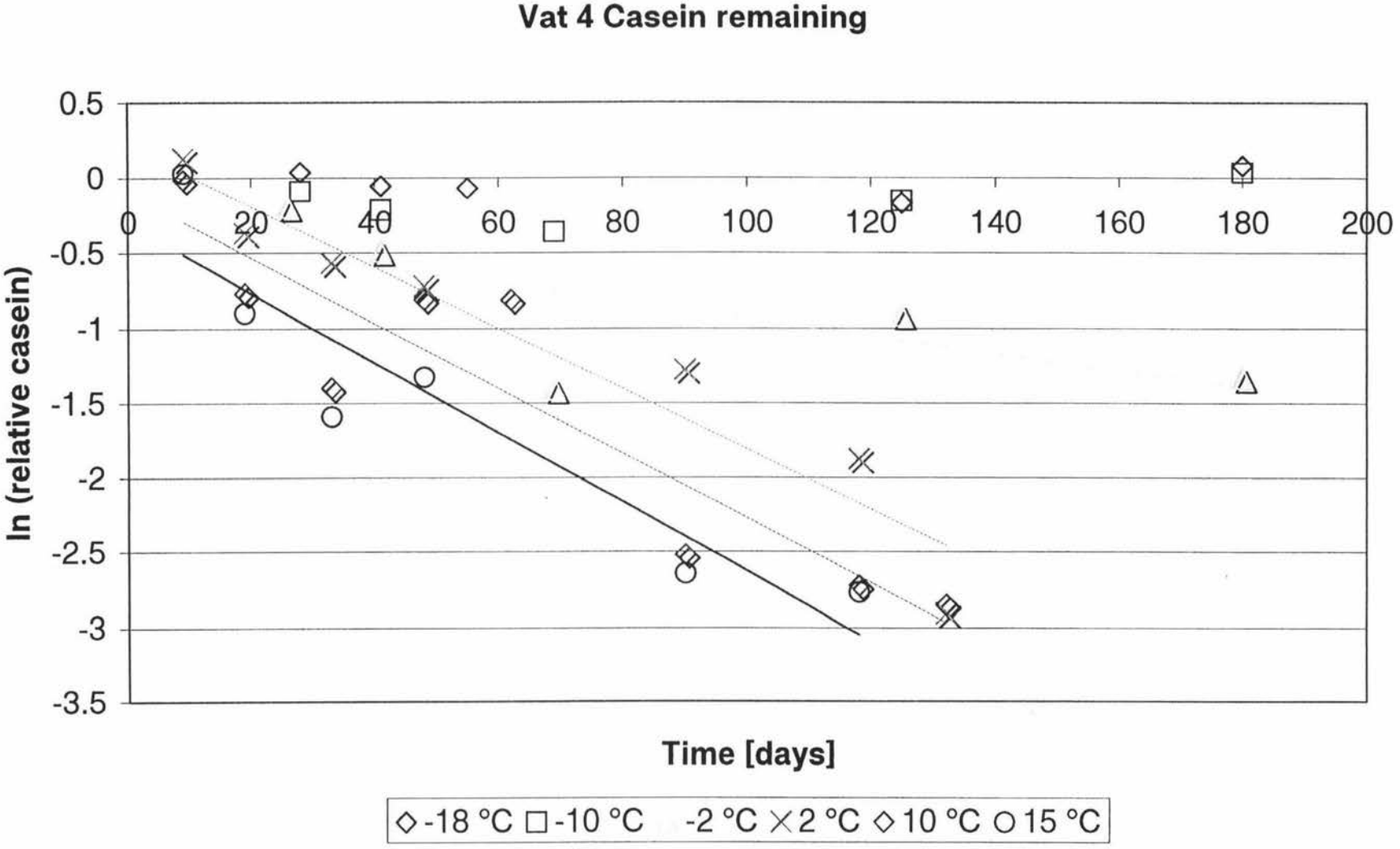
Vat 4 Casein remaining
0.5
0
-0.5
-1
-1.5
-2
-2.5
-3
-3.5
0
20
40
60
80
100
120
140
160
180
200
ln (relative casein)
Time [days]
◇ -18 °C □ -10 °C -2 °C × 2 °C ◇ 10 °C ○ 15 °C

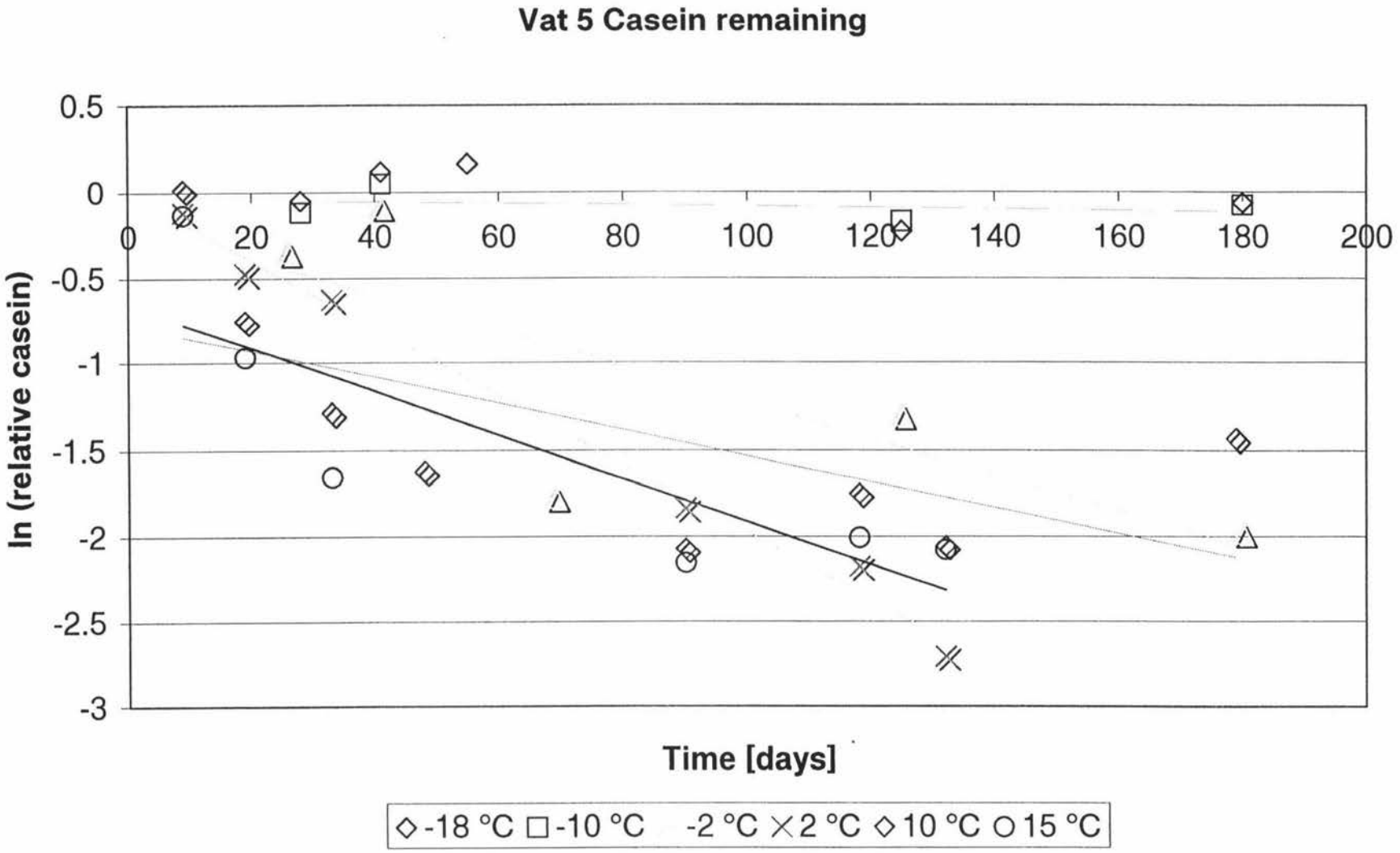
Vat 5 Casein remaining
0.5
0
-0.5
-1
-1.5
-2
-2.5
-3
0
20
40
60
80
100
120
140
160
180
200
ln (relative casein)
Time [days]
◇-18 °C □-10 °C -2 °C ×2 °C ◇10 °C ○15 °C

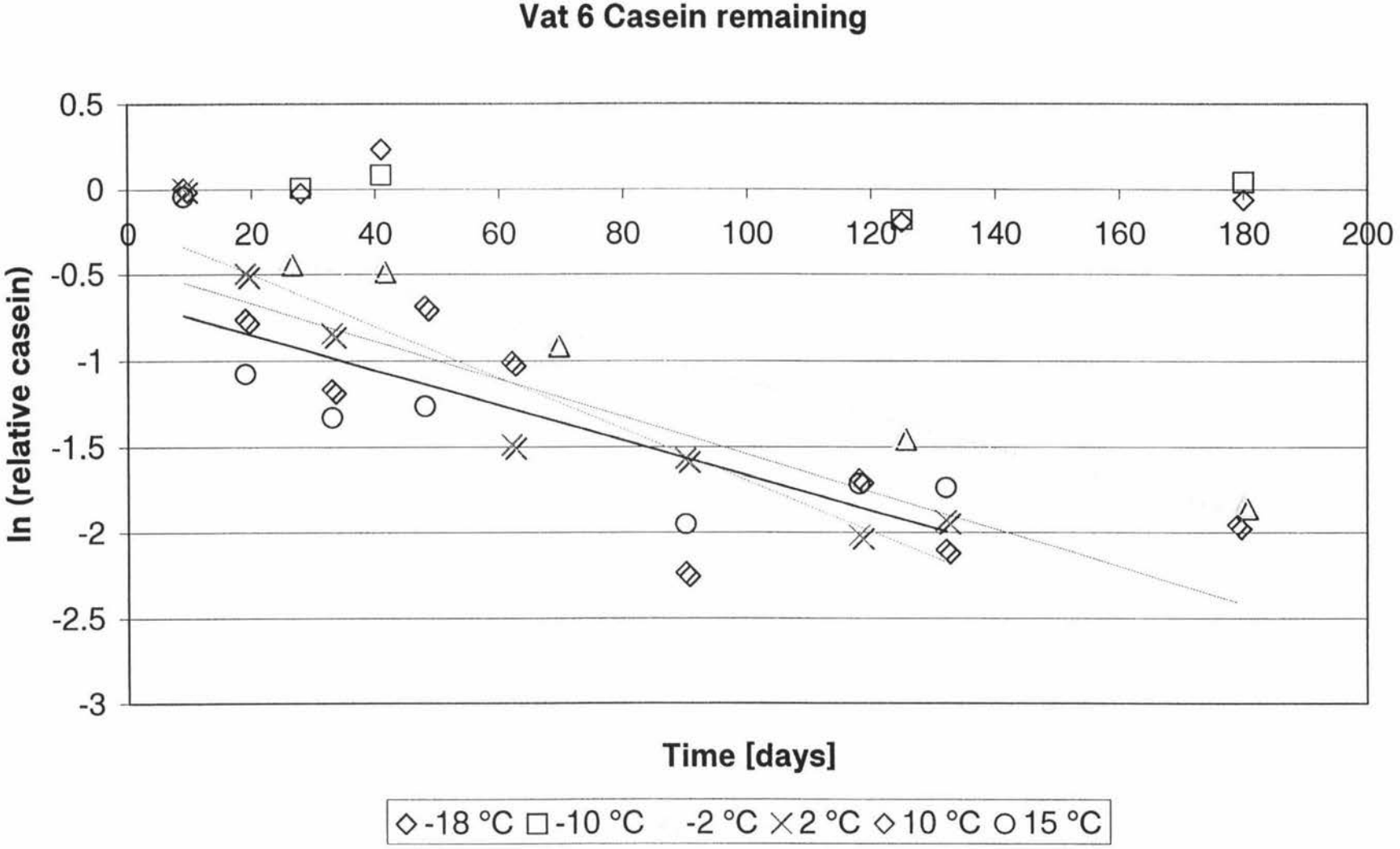
Vat 6 Casein remaining
0.5
0
-0.5
-1
-1.5
-2
-2.5
-3
0
20
40
60
80
100
120
140
160
180
200
ln (relative casein)
Time [days]
◇-18 °C □-10 °C -2 °C ×2 °C ◇10 °C ○15 °C

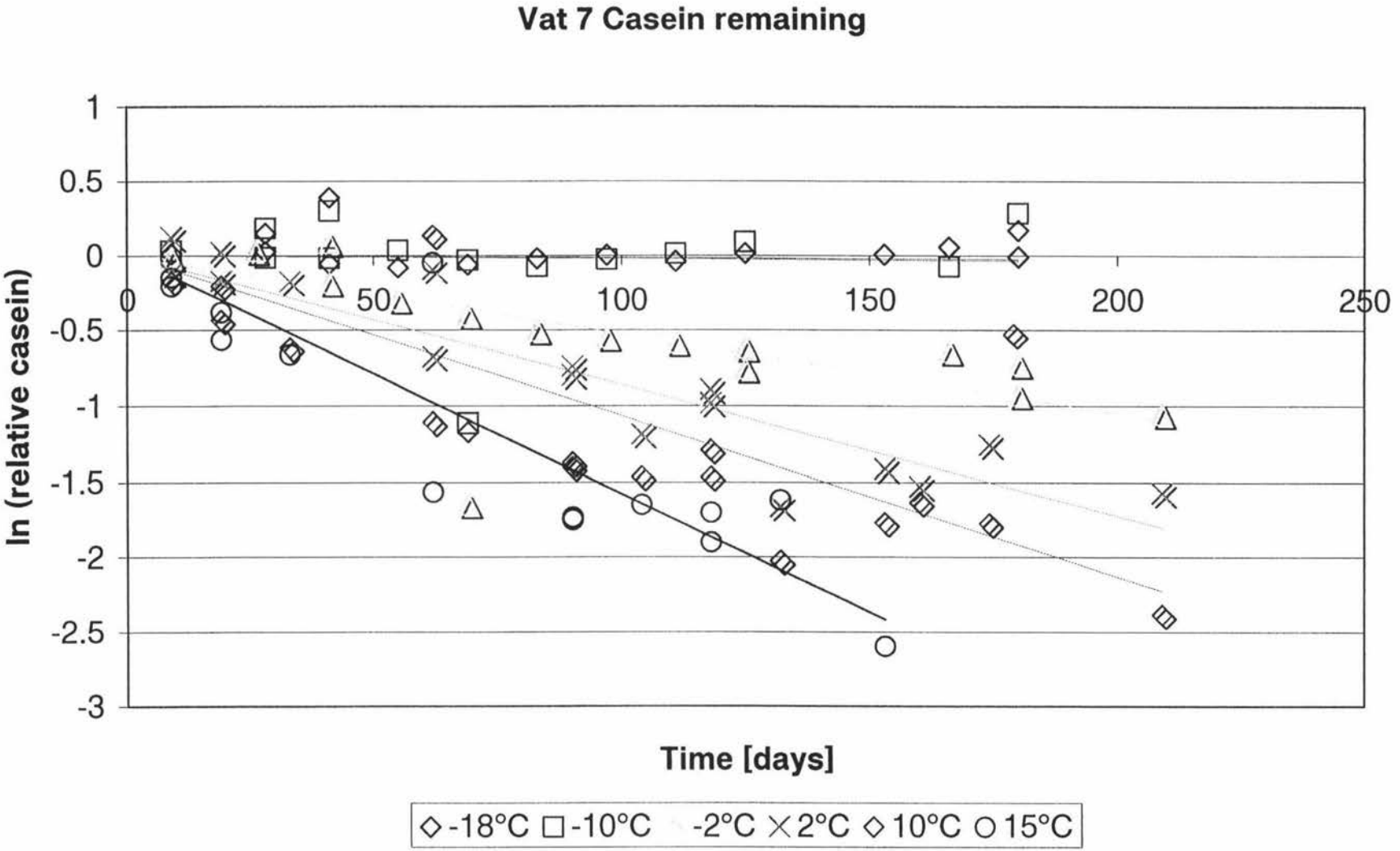
Vat 7 Casein remaining
ln (relative casein)
1
0.5
0
-0.5
-1
-1.5
-2
-2.5
-3
0
50
100
150
200
250
Time [days]
◇-18°C □-10°C -2°C ×2°C ◇10°C ○15°C

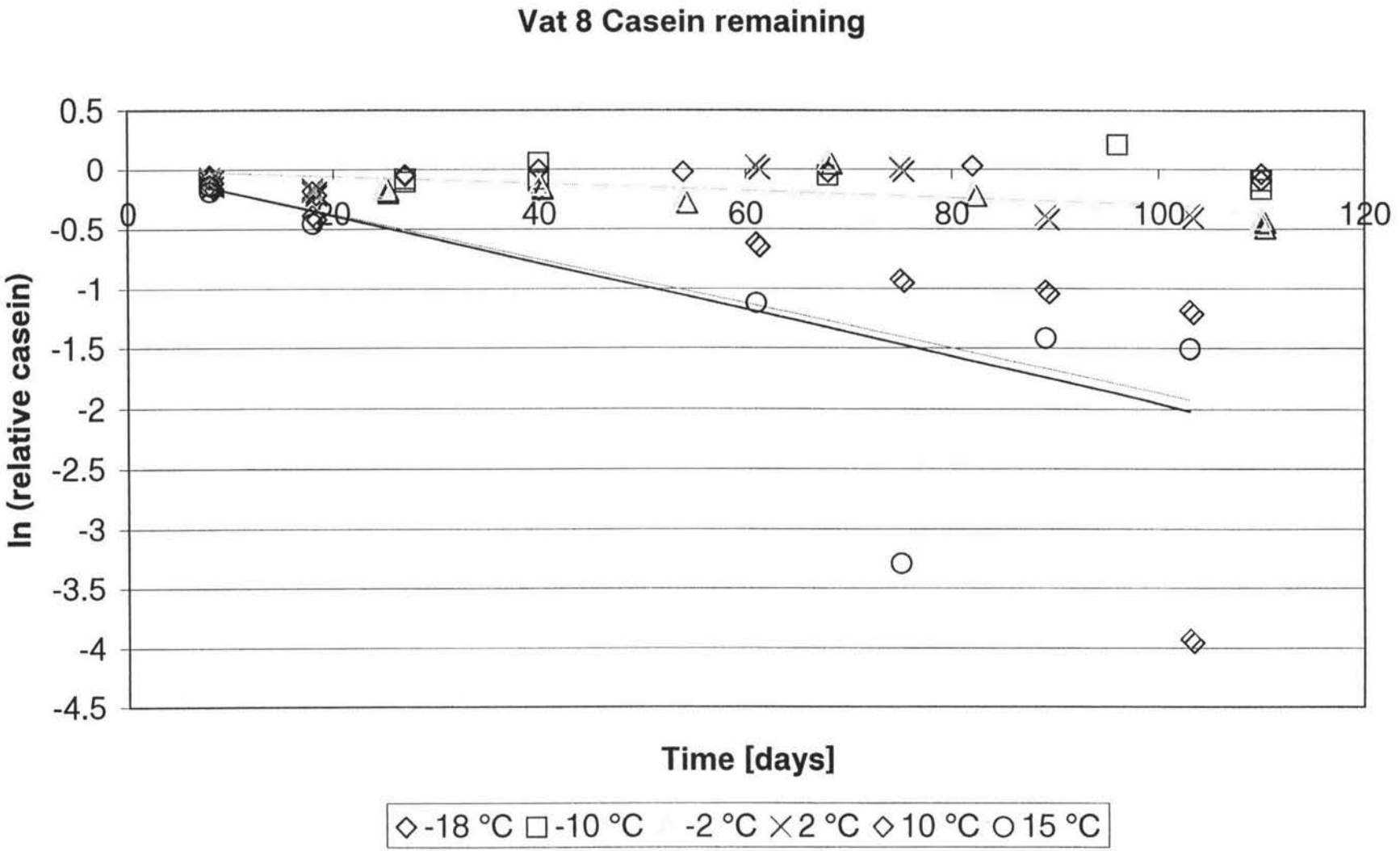
Vat 8 Casein remaining
0.5
0
-0.5
-1
-1.5
-2
-2.5
-3
-3.5
-4
-4.5
ln (relative casein)
0
20
40
60
80
100
120
Time [days]
◇-18 °C □-10 °C -2 °C ×2 °C ◇10 °C ○15 °C

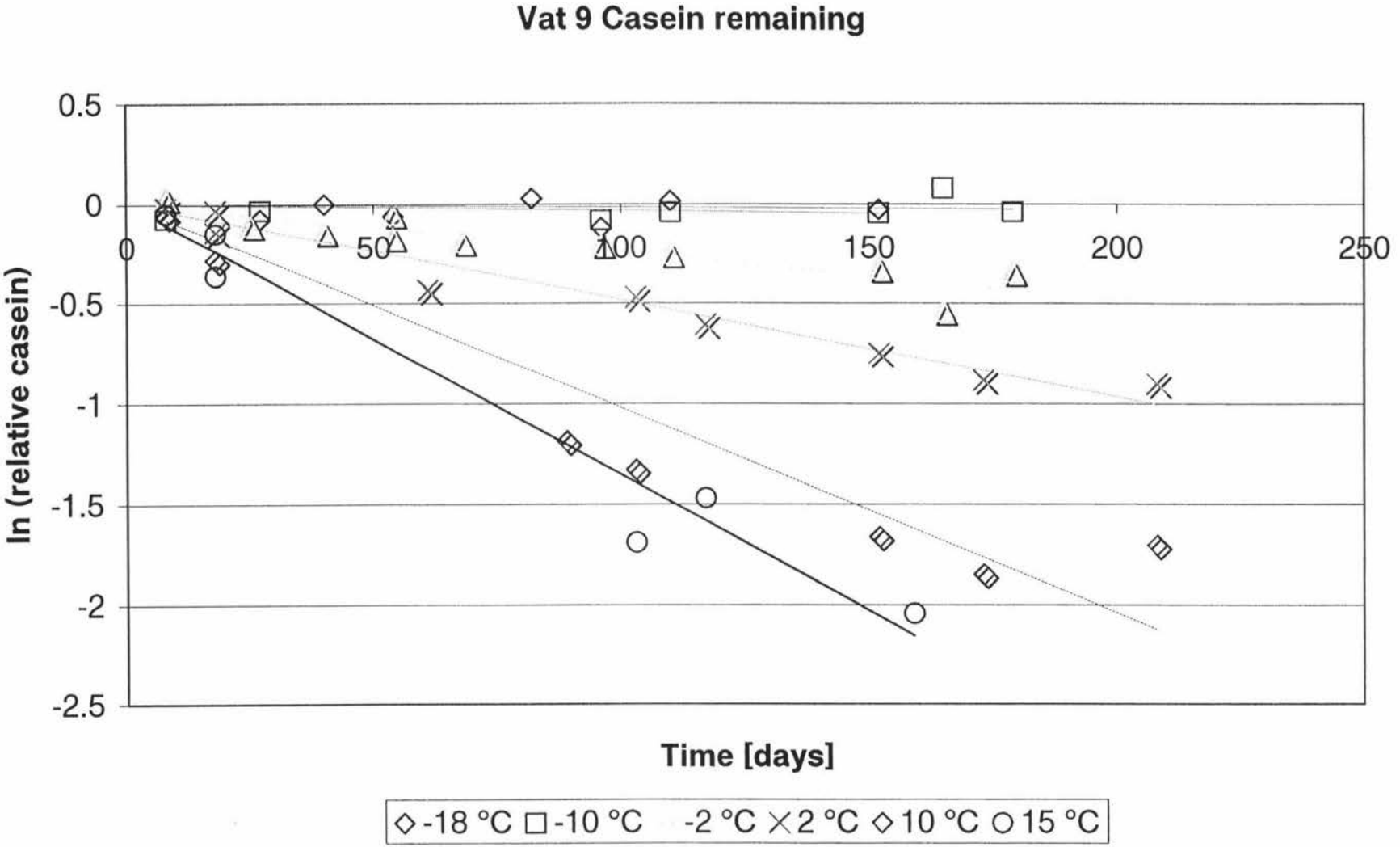
Vat 9 Casein remaining
0.5
0
-0.5
-1
-1.5
-2
-2.5
0
50
100
150
200
250
ln (relative casein)
Time [days]
◇ -18 °C □ -10 °C -2 °C × 2 °C ◇ 10 °C ○ 15 °C

7.3 MATLAB SCRIPTS

7.3.1 MODEL INPUT FILE

```
%modelinput.m

%open RADS output
filename='c:\rads3\default.RES';
fid=fopen(filename);

%create variables
global temp;
global TIMENODES;

%Input data from RADS outputs
for n=1:26
   fgets(fid);
end
TIMENODES=1000;
TIMESTEP=1;
temp=zeros(TIMENODES,11,11,11);
for t=1:TIMENODES
   for x=1:11

      for y=1:10

       fscanf(fid,'%s',3);
       temp(t,x,y,:)=fscanf(fid,'%g',11);
       fgets(fid);
       fgets(fid);
    end
    fscanf(fid,'%s',2);
```

```
        temp(t,x,11,:)=fscanf(fid,'%g',11);
        for n=1:5
            fgets(fid);
        end
    end
    for n=1:7
        fgets(fid);
    end
end

%create time dimension
time=zeros(TIMENODES,1);
for timenode=1:TIMENODES
    time(timenode,1)=timenode*TIMESTEP;
end

%create variable for graphing purposes
for n=1:10
    for i=1:11
        data(:,n)=(temp(:,i,i,11));
    end
end
```

7.3.2 MODEL OUTPUT FILE

```
%Temp-out
%output 4dimensional data for graphing

%create output variable
output=zeros(1000,11);
for i=2:11
    output(:,i)=temp(:,i,i,11);
end
```

```
output(:,1)=time;

%create output file
save 'c:\data\output.txt' output -ascii
```

7.3.3 PROTEOLYSIS SCRIPT FILE

```
%script file for chzft.m

%start calculation timer
a=clock;

%list variables required elsewhere
global temp;
global tempt;
global tempft;
global TIMENODES;
global ko;
global E;
global R;
global kout;
global p;

%prepare freeze thaw temp array from individual temp
arrays
% --- dont forget to run modelinput and thawinput first! -
--

tempft=zeros(2000,11,11,11);
tempft(1:1000,:,:,:)=temp;
tempft(1001:2000,:,:,:)=tempt;

'freeze-thaw temerature array complete'
```

```
%Set cheese type/composistion

%slow
%MNFS=0.511;
%rennet=3.3;

%fast
MNFS=0.579;
rennet=10.4;

%set Arrhenius constants
ko=exp(16.1)*MNFS^3.38*rennet^0.654*(1/24);
E=46000;
R=8.314;

%set time step for proteolysis reaction
tspan=1;
tstop=1995;
options=odeset('RelTol',1e-4);

%Set reaction initial conditions
Initialconditions=zeros(1,1331);

%solve
[t,X]=ode45('chzft',[0:tspan:tstop],Initialconditions,opti
ons);

'Integration complete'

%Reshape X into 4d output
Xsum=zeros(tstop+1,1);
```

```
    X4d=reshape(X,(tstop+1),11,11,11);
    %k4d=reshape(kout,(tstop+1),11,11,11);

    %calculated weighted average of extent of reaction in
cheese pallet
    for x=1:11
       for y=1:11
          for z=1:11
             weight=1;
             if x==1|x==11
                weight=weight/2;
             end;
             if y==1|y==11
                weight=weight/2;
             end;
             if z==1|z==11
                weight=weight/2;
             end;
             Xsum=Xsum+squeeze(X4d(:,x,y,z))*weight;
          end
       end
    end
    Xav=Xsum/(1000);

    %calculate variation in cheese pallet of extent of
reaction
    stdev=(mean((X.^2),2)-mean(X,2).^2).^0.5;

    %stop calculation timer
    b=clock;

    %outputs
```

```
    %calculation time output
    calctime=b-a;
    'calculation time'
    minutes=calctime(5)
    seconds=calctime(6)

    %plot extent of reaction at thermocouple positions from
chapter 4
    figure
    hold on
    plot(t,Xav,'go')
    for i=1:11
       plot(t,X4d(:,i,i,i),'r')
    end
    title('Extent of reaction (fraction of alpha-s1-casein
degraded)');
    xlabel('time [hrs]');
    ylabel('Extent');

    %plot temperature time profile for point equivilent to
thermocouple
    %position from chapter 4
    figure
    hold on
    for i=1:11
       plot(t,tempft((1:(tstop+1)),i,i,i),'r')
    end
    xlabel('time [hrs]');
    ylabel('temperature [°C]');

    %plot Variation in the extent of the proteolysis reaction
with time
```

```
figure
hold on
plot(t,stdev,'r')
title('Variation in the extent of the proteolysis
reaction');
xlabel('time [hrs]');
ylabel('Standard deviation');

%output file for graphing
outputx=[t,X(:,1),X(:,1331),Xav,stdev];
save 'c:\data\outputx.txt' outputx -ascii

%analytical k at ttest°C
%ttest=-10
%kttest=ko*exp(-E/R/(273.15+ttest));
%plot(t,(1-exp(-kttest.*t)))
```

7.3.4 THAW DATA INPUT FILE

```
filename='c:\rads3\thaw.RES';
fid=fopen(filename);

global tempt;
global TIMENODES;

for n=1:26
   fgets(fid);
end
TIMENODES=1000;
TIMESTEP=1;
tempt=zeros(TIMENODES,11,11,11);
for t=1:TIMENODES
   for x=1:11
```

```
        for y=1:10

          fscanf(fid,'%s',3);
          tempt(t,x,y,:)=fscanf(fid,'%g',11);
          fgets(fid);
          fgets(fid);
       end
       fscanf(fid,'%s',2);
       tempt(t,x,11,:)=fscanf(fid,'%g',11);
       for n=1:5
          fgets(fid);
       end
    end
    for n=1:7
       fgets(fid);
    end
end
time=zeros(TIMENODES,1);
for timenode=1:TIMENODES
   time(timenode,1)=timenode*TIMESTEP;
end
for n=1:10
   for i=1:11
      datat(:,n)=(tempt(:,i,i,11));
   end
end
```

7.3.5 PROTEOLYSIS INTEGRATION FILE

```
%Integration file chzft.m

function odes=chzft(t,X)
```

```
    global temp;
    global tempt;
    global tempft;
    global TIMENODES;
    global ko;
    global E;
    global R;
    global kout;

    timenode=fix(t)+1;

    %X=1dimentional array of xtent of reaction at different
positions

    Treal=zeros(1331,1);

    %Reshape 3dtemperature array in current time period to 1d
for ODE45 function
    Tt=reshape(squeeze(tempft(timenode,:,:,:)),(11*11*11),1);
    Tth=reshape(squeeze(tempft(timenode,:,:,:)),(11*11*11),1);
    Treal=mod(t,1).*(Tth-Tt)+Tt;
    clear Tt
    clear Tth

    %calc CV's
    k=zeros(1331,1);
    k=ko.*exp(-E./R./(273.15+Treal));

    %stop reation at below -10°C
    for i=1:1331
       if Treal(i)<-10
```

```
        k(i)=0;
    end
end

odes=zeros(1331,1);

%calc odes
odes=k.*(1-X);
```

7.4 RADS INPUT FILE

```
RRRRR
RICHARD
  50                    (Number of thermal conductivity data points)
   -40.000000     .200125     (Thermal conductivity; temp[°C]vs conductivity
[W.m.°C]
   -30.000000     .198740
   -28.000000     .198490
   -26.000000     .198170
   -24.000000     .197790
   -22.000000     .197280
   -20.000000     .196550
   -19.000000     .196070
   -18.000000     .195470
   -17.000000     .194790
   -16.000000     .193990
   -15.000000     .193060
   -14.000000     .192030
   -13.000000     .190850
   -12.500000     .190170
   -12.000000     .189420
   -11.500000     .188680
   -11.000000     .187830
   -10.500000     .186880
   -10.000000     .185910
    -9.750000     .185337
    -9.500000     .184808
    -9.250000     .184235
    -9.000000     .183572
    -8.750000     .182961
    -8.500000     .182295
```

-8.250000	.181522
-8.000000	.180809
-7.800000	.180130
-7.600000	.179545
-7.400000	.178833
-7.200000	.178067
-7.000000	.177390
-6.800000	.176577
-6.600000	.175708
-6.400000	.174946
-6.200000	.174025
-6.000000	.173062
-5.800000	.172259
-5.500000	.171673
-5.000000	.171673
-4.000000	.171673
-2.000000	.171673
.000000	.171674
2.000000	.171674
4.000000	.171674
6.000000	.171674
7.000000	.171674
8.000000	.171674
10.000000	.171673
50	*(number of thermal conductivity data points)*
-39.000000	1.127586 *(heat capacity; temp[°C] vs heat capacity [kJ.kg.°C]*
-29.000000	1.127586
-27.000000	1.178296
-25.000000	1.244219
-23.000000	1.413226
-21.000000	1.672718
-19.000000	1.947749
-18.000000	2.179878
-17.000000	2.449220
-16.000000	2.672344
-15.000000	2.963129
-14.000000	3.225083
-13.000000	3.625357
-12.000000	3.921047
-11.500000	4.208088
-11.000000	4.490936
-10.500000	4.830693
-10.000000	5.213835
-9.500000	5.616140
-9.000000	6.035695
-8.750000	6.236845
-8.500000	6.600829

```
      -8.250000      6.966730
      -8.000000      7.290485
      -7.750000      7.729624
      -7.500000      8.120008
      -7.250000      8.648743
      -7.000000      9.180352
      -6.800000      9.591290
      -6.600000     10.062080
      -6.400000     10.643970
      -6.200000     11.118110
      -6.000000     11.333160
      -5.800000     10.320940
      -5.600000      5.925399
      -5.400000      2.053363
      -5.200000      1.774138
      -5.000000      1.570936
      -4.800000      1.572414
      -4.500000      1.472414
      -4.000000      1.472414
      -3.000000      1.540872
      -1.000000      1.665111
       1.000000      1.783788
       3.000000      1.879932
       5.000000      2.025821
       7.000000      2.155103
       9.000000      2.261594
      10.000000      2.375692
      13.000000      2.375692
   5
   1
RRRRR
   1150.000000    1060.000000 (Size dimensions [mm])
    931.000000
  10   10                     (Number of nodes in each dimension)
  10
   5
   2    1                     (Number of ambient temperature data points)
      .000000    -15.000000          (Ambient temperature; time[hrs] vs
temperature [°C])
   1000.000000    -15.000000
      .000000      6.000000  (Surface heat transfer coefficient; time [hr] vs htc
[W.m-2.°C-1])
   1
    12.000000                (Initial temperature [°C])
   600.000000      1.000000  (Time step [s]              output time step [hr])

   1000.000000   1666.667000 (Simulation length [hr] )
```

3 1
N

7.5 ICE FRACTION DATA

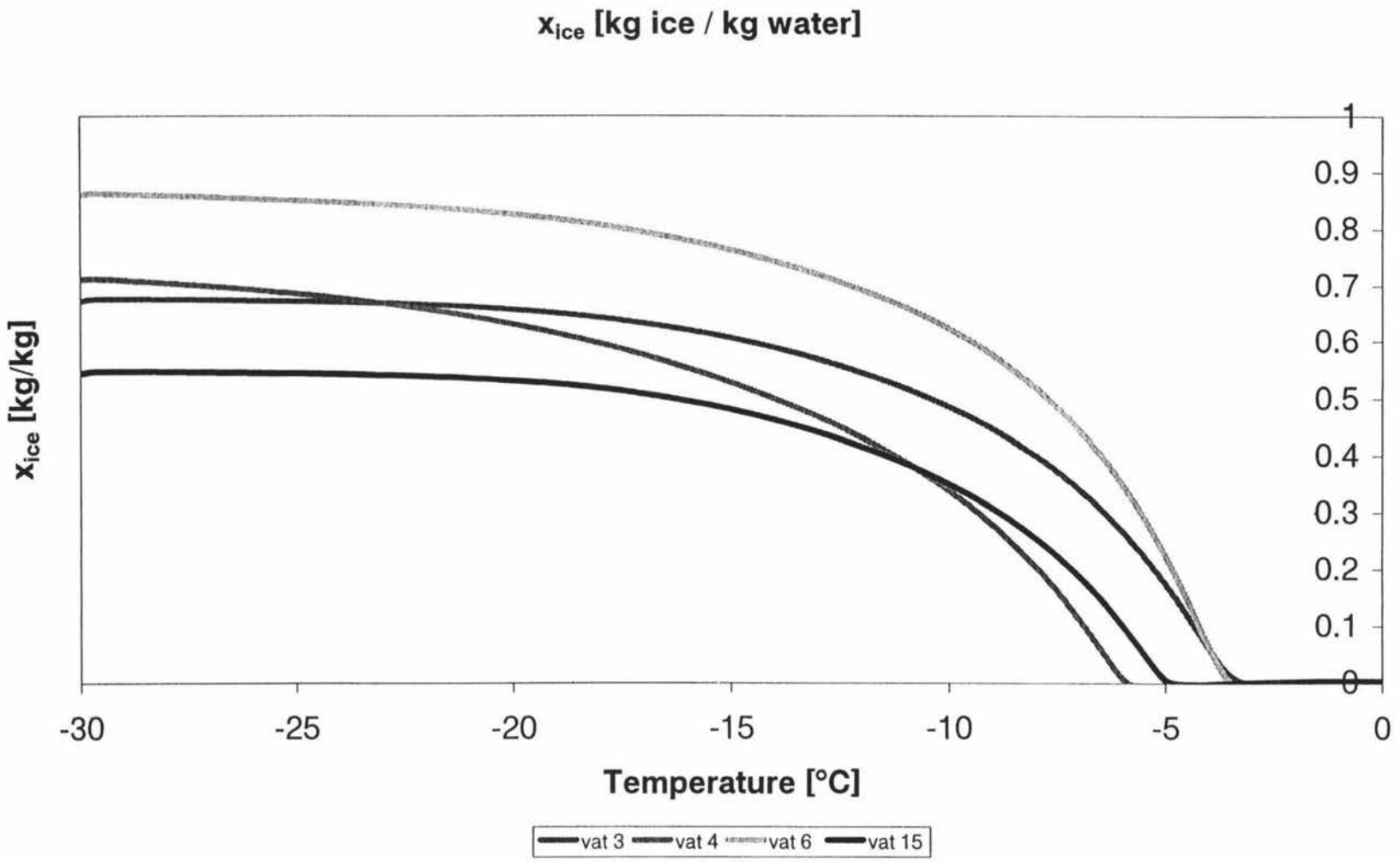
x_{ice} [kg ice / kg water]
x_{ice} [kg/kg]
1
0.9
0.8
0.7
0.6
0.5
0.4
0.3
0.2
0.1
0
-30
-25
-20
-15
-10
-5
0
Temperature [°C]
vat 3
vat 4
vat 6
vat 15

7.6 HEAT CAPACITY DATA

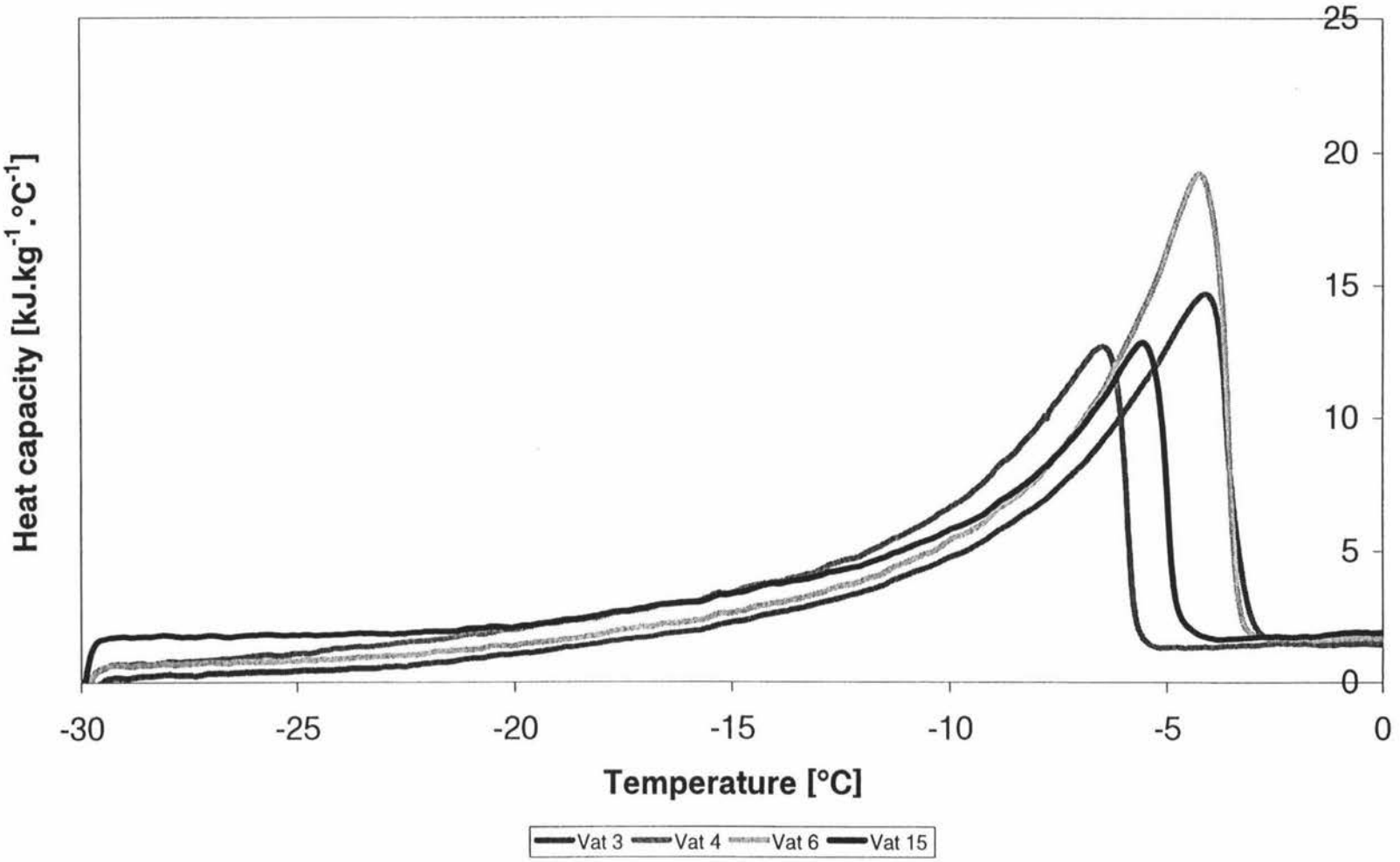

NOMENCLATURE

t	Time	[s]
x_i	Mass fraction of component i	[kg i.kg cheese^{-1}]
x_w	Mass fraction of water in cheese	[kg water.kg cheese^{-1}]
X_{ice}	Mass fraction of ice in cheese	[kg ice.kg cheese^{-1}]
x_{ice}	Mass fraction of ice in water	[kg ice.kg water^{-1}]
x_{ice}'	Mass fraction of ice in freezable water	[kg ice.kg freezable water^{-1}]
x_w'	Mass fraction of freezable water in cheese	[kg freezable water.kg cheese^{-1}]
Co	Initial concentration of αs1-Casein	[mol.kg^{-1}]
C	Concentration of αs1-Casein	[mol.kg^{-1}]
k_m	Michaelis-Menten constant	[mol.kg^{-1}]
$[E_o]$	Enzyme concentration	[mol.kg^{-1}]
k_3	Rate constant (Enzyme reaction)	[day^{-1}]
[R]	Level of rennet added	[ml.100l^{-1}]
[Rennet (normalised)]	Normalised rennet level	[ml.100l^{-1}.wt%MNFS]
[s]	Salt concentration	[kg/kg]
[m]	Moisture concentration	[kg/kg]
[MNFS]	Moisture in non fatty substance	[kg/kg]
k	Reaction rate	[hr^{-1}]
E	Arrhenius activation energy	[J.mol^{-1}]
k_o	Arrhenius pre-exponential function	[hr^{-1}]
k_r	Rennet proportionality constant	[-]
k_{wg}	Moisture proportionality constant	[-]
k_{3o}	Arrhenius pre-exponential constant	[ml.100l^{-1}.wt%MNFS.hr^{-1}]
k_c	Empirical pre-exponential constant term	[day^{-1}]

Xc	Extent of reaction	[-]
θ	Temperature	[°C]
T	Temperature	[K]
H	Enthalpy of sample at any given temperature	[$kJ.kg^{-1}$]
H_o	Datum enthalpy	[$kJ.kg^{-1}$]
A	Empirical constant	[$kJ.kg^{-1}$]
B	Empirical constant	[$kJ.kg^{-1}.K$]
C_f	Datum heat capacity	[$kJ.kg^{-1}.K$]
λ	Thermal conductivity of material	[$W.m^{-1}.°C$-1]
λ_c	Thermal conductivity of continuous phase	[$W.m^{-1}.°C$-1]
λ_d	Thermal conductivity of discontinuous phase	[$W.m^{-1}.°C$-1]
λ_i	Thermal conductivity of component i	[W.m-1.°C-1]
V_c	Volume fraction of continuous component	[m^3/m^3]
V_d	Volume fraction of discontinuous component	[m^3/m^3]
V_i	Volume fraction of continuous component	[m^3/m^3]
Φ	Heat flow	[W]
A_{ou}	Outside area	[m^2]
T_{ou}	Outside temperature	[°C]
T_{in}	Inside temperature	[°C]
r_{ou}	Outside radius	[m]
r_{in}	Inside radius	[m]
q	Heat input per unit length	[$W.m^{-1}$]
ϱ_t	Density of whole composite material	[$kg.m^{-3}$]
ϱ_i	Density of component i	[$kg.m^{-3}$]
Δ	Density of immersion liquid	[$kg.m^{-3}$]
w	Weight of material in air	[N]
w_l	Weight of material in liquid	[N]
σ	Density of air	[$kg.m^{-3}$]
c	Heat capacity	[$J.kg^{-1}.K^{-1}$]
C	Volumetric heat capacity	[$J.m^{-3}.K^{-1}$]

θ_{if}	Initial freezing point	[°C]
L_i	Heat required to achieve a change in ice content	[J.kg^{-1}]
L	Latent heat of melting	[J.kg^{-1}]
h_{ice}	Enthalpy of ice	[J.kg^{-1}]
h_w	Enthalpy of pure water	[J.kg^{-1}]
T_1	Sensible heat capacity	[J.kg^{-1}.K^{-1}]
T_2	Effect of ice content on specific heat	[J.kg^{-1}.K^{-1}]
T_3	Latent heat effect on apparent heat capacity	[J.kg^{-1}.K^{-1}]
$c_{ice(T)}$	Heat capacity of ice as a function of temperature	[J.kg^{-1}.K^{-1}]
$c_{w(T)}$	Heat water of ice as a function of temperature	[J.kg^{-1}.K^{-1}]
k_1	Empirical constant from Bartlets method	[K^{-1}]
k_2	Empirical constant from Bartlets method	[K^{-2}]
θ_{wf}	Freezing point of pure water	[°C]
Mw	Molecular weight of water	[kg.mol-1]
R	Gas constant	[J.mol^{-1}.K^{-1}]
H_{if}	Enthalpy of sample at initial freezing point	[J.kg^{-1}]
H_{fb}	Enthalpy of solid at initial freezing point assuming 100% frozen Extrapolation of 100% frozen data up to θif	[J.kg^{-1}]
H_b	Enthalpy of solid at any given temp point assuming 100% frozen Extrapolation of 100% frozen data up to θ	[J.kg^{-1}]
$L_{(\theta)}$	Latent heat of ice at some given temperature	[J.kg^{-1}]

REFERENCES

Abdalla, H., & Singh, R. P. (1985). Simulation of thawing of foods using finite element method. Journal of Food Process Engineering, 7, 273-286.

Adams, J. A., & Rogers, D. F. (1973). Computer aided heat transfer analysis. New York: McGraw-Hill, inc.

Aston, J. W., Durward, I. G., & Dulley, J. R. (1983a). Proteolysis and flavour developement in cheddar cheese. The Australian Journal of Dairy Technology, 38, 55-59.

Aston, J. W., Grieve, P. A., Durward, I. G., & Dulley, J. R. (1983b). Proteolysis and flavour developement in cheddar cheese subjected tio accelerated ripening treatments. The Australian Journal of Dairy Technology, 38, 59-65.

Bouzas, J., Kantt, F. W., Bodyfelt, F. W., & Torres, J. A. (1993). Time and temperature influence on chemical aging indicators for a commercial cheddar cheese. Journal of Food Science, 58(6), 1307-1312.

Brown, M. E. (1988) Introduction to thermal analysis: Techniques and Applications. Chapman and hall, London

Cleland, D. J. (1985). Prediction of freezing and thawing time for foods. Unpublished doctoral dissertation, Massey University.

Cleland, D. J., & Cleland, A. C. (1991). RADS.release.3.1 Palmerston North: Massey University.

Cooper, J. R., & Le Fervre, E. J. (1969). Thermophysical properties of water substance. London: Edward Arnold.

Fennema, O. (1975). Reaction Kenetics in Partially Frozen Aqueous Systems. R. B. Duckworth (Editor), Water relations of foods: Preceedings of an international symposium held in Glasgow, September 1974 (pp. 539-555). London: Academic Press.

Folkertsma, B., Fox, P. F., & McSweeney, P. L. H. (1996). Accellerated ripening of cheddar cheese at elevated temperatures. International Dairy Journal, 6, 1117-1134.

Fox, P. F. (1989). Proteolysis in cheese manufacture and ripening. Journal of Dairy Science, 72(6), 1379-1400.

Grappin, R., Rank, T. C., & Olson, N. F. (1985). Primary proteolysis of cheese proteins during ripening a review. Journal of Dairy Science, 68(3), 531-540.

Heldman, D. R., & Gorby, D. P. (1975). Computer simulation of individual quick freezing of foods. St Joseph, MI: ASAE.

Hynes, E., Delacroix-Buchet, A., Meinardi, C. A., & Zalazar, C. A. (1999). Relation between pH, degree of proteolysis and consistency in soft cheeses. The Australian Journal of Dairy Technology, 54, 24-27.

Jamieson, D. J., Cleland, D. J., & Falconer, R. M. (1993) Modelling of bulk-stacked cheese cooling in coolstores. Refrigeration science and technology proceedings International Institute of Refrigeration. Palmerston North

Johnston, K. A. (1987). Variation in the moisture content of cheddar cheese curd prior to salting. Unpublished doctoral dissertation, Massey University, Palmerton North.

Johnston, K. A., Luckman, M. S., Lilley, H. G., & Smale, B. M. (1998). Effect of various cutiing and stirring conditions on curd particle size and losses of fat to the whey during cheddar cheese manufacture in Ost vats. International Dairy Journal, 8, 281-288.

Kelly, M., Fox, P. F., & McSweeney, P. L. H. (1996). Effect of salt-in-moisture on proteolysis in cheddar type cheeses. Milchwissenschaft, 51(9), 498-501.

Kopelman, I. J. (1966). Transient heat transfer and thermal properties in food systems. Unpublished doctoral dissertation, Michigan State University, East Lansing.

Kosikowski, F. W., & Mistry, V. V. (1997). Cheese and fermented milk foods: Vol I:

Origins and principles Third addition. Conneticut: F.V.Kosikowski,L.L.C.

Law, B. A., Hosking, Z. D., & Chapman, H. R. (1979). The effect of some manufacturing conditions on the developement of flavour in Cheddar cheese. Journal of the Society of Dairy Technology, 32(2), 87-90.

Levenspiel, O. (1999). Chemical Reaction Engineering Third edition. New York: John Wiley & Sons.

Lindsay, D. T., & Lovatt, S. J. (1994). Further Enthalpy Values of Foods Measured by an Adiabatic Calorimeter. Journal of Food Engineering, 23, 609-620.

Mayes, J. J., & Radford, D. R. (1983). Density of Cheddar cheese. The Australian Journal of Dairy Technology, 3, 34.

McSweeney, P. L. H., Olson, N. F., Fox, P. F., Healy, A., & Hojrup, P. (1993). Proteolytic specificity of chymosin of bovine alpha - Casein. Journal of Dairy Research, 60(3), 401-412.

Miles, C. A., Van Beek, G., & Veerkamp, C. H. (1983). Calculation of thermal properties of food. R. Jowitt (editor), Physical Properties of food (pp. 269-313). London: Applied science publishers.

Miyawaki, O., Liu, L., & Nakamura, K. (1998). Effective Partition Constant of Solute Between Ice and liquid Phases in Progressive Freeze-concentration. Journal of Food Science, 63(5), 756-758.

Mulvihill, D. M., & Fox, P. F. Proteolytic specificity of chymosin on α_{s1}-casein. Journal of Dairy Research, 46, 641-651.

O'Keeffe, R. B., Fox, P. F., & Daly, C. (1976). Contribution of rennet and starter proteases to proteolysis in Cheddar cheese. Journal of Dairy Research, 43, 97-107.

Ohlsson, T. (1983). The measurement of thermal properties. R. Jowitt (editor), Physical Properties of food (pp. 269-313). London: Applied science publishers.

Peralta Rodríguez, R. D., M. Rodrigo, E., & Kelly, P. (1995). A Calrometric Method to

Determine Specific Heats of Prepared Foods. Journal of Food Engineering, 26, 81-96.

Pham, A., & Naki, S. (1984). Application of stepwise descriminant analysis to high pressure liquid chromatography of water extract for judging ripening of cheddar cheese. Journal of Dairy Science, 67(7), 1390-1396.

Pham, Q. T., Wee, H. K., Kemp, R. M., & Lindsay, D. T. (1994). Determination of the enthalpy of the foods by an adiabatic calorimeter. Journal of Food Engineering, 21, 137-156.

Pham, Q. T., & Willix, J. (1989). Thermal conductivity of fresh lamb meat, offals and fat in the range -40 to +30°C: Measurements and correlations. 54(3), 508-515.

Polley, S. L., Snyder, O. P., & Kotnour, P. (1980). A compilation of thermal properties of foods. Food Technolgy, 34(11), 76-94.

Rahman., S. (1995). Food properties handbook. Boca Raton: CRC press.

Ramanauskas, R., & Alencikiene. (1999). Regulation of cheese quality during refrigerated storage. 20th International Congress of refrigeration, IIR/IIF .

Saad, Z., & Scott, E. P. (1996). Estimation of temperature dependent thermal properties of basic food solutions during freezing. Journal of Food Engineering, 28, 1-19.

Sakai, S., & Hosokawa, A. (1984). Comparison of several methods for calculation of the ice content of foods. Journal of Food Engineering, 3, 13-26.

Santa-Maria, G., & Ramos, M. (1986). Application of Linear discriminant analysis to different proteolysis parameters for assessing the ripening of manchego cheese. Food Chemistry, 19, 225-234.

Schwartzberg, H. G. (1976). Effective heat capacities for the freezing and thawing of foods. Journal of Food Science, 41, 152-156.

Thomareis, A. S., & Hardy, J. (1985). Evolution de la Chaleur Specifique Apparente des Fromages Fondus Entre 40 et 100°C. Influence de Leur Composition. Journal of Food Engineering, 4, 117-134.

Wilkinson, M. G., Guinee, T. P., & Fox, P. F. (1994). Factors which may influence the determination of autolysis of starter bacteria during cheddar cheese ripening. International Dairy Journal, 4, 141-160.

Willix, J., & Amos, N. D. (1995). Thermal Properties of foods. MIRINZ Meat Research.